(1)

DYNAMICS OF THE POLAR MESOPAUSE AND LOWER THERMOSPHERE REGION AS OBSERVED IN THE NIGHT AIRGLOW EMISSIONS

BY

HANS KRISTIAN MYRABØ

NDRE PUBL-88/1001

ISSN 0800-4412

FORSVARETS FORSKNINGSINSTITUTT

NORWEGIAN DEFENCE RESEARCH ESTABLISHMENT

P O Box 25 – N-2007 Kjeller, Norway

DYNAMICS OF THE POLAR MESOPAUSE AND LOWER THERMOSPHERE REGION AS OBSERVED IN THE NIGHT AIRGLOW EMISSIONS

by

HANS KRISTIAN MYRABØ

NDRE PUBL–88/1001

ISSN 0800–4412

FORSVARETS FORSKNINGSINSTITUTT

NORWEGIAN DEFENCE RESEARCH ESTABLISHMENT

P O Box 25 – N-2007 Kjeller, Norway

February 1988

To

OH, O_2 and Na

without whom

this work would

not have been

possible

NORWEGIAN DEFENCE RESEARCH ESTABLISHMENT (NDRE)
FORSVARETS FORSKNINGSINSTITUTT (FFI)

POST OFFICE BOX 25
N-2007 KJELLER, NORWAY

UNCLASSIFIED
SECURITY CLASSIFICATION OF THIS PAGE
(when data entered)

REPORT DOCUMENTATION PAGE

1) PUBL/REPORT NUMBER	2) SECURITY CLASSIFICATION	3) NUMBER OF PAGES
NDRE PUBL-88/1001	UNCLASSIFIED	100
1a) JOB REFERENCE	2a) DECLASSIFICATION/DOWNGRADING SCHEDULE	
FFIVM/119	-	

4) TITLE

DYNAMICS OF THE POLAR MESOPAUSE AND LOWER THERMOSPHERE REGION AS OBSERVED IN THE NIGHT AIRGLOW EMISSIONS
(DYNAMIKK OG TRANSPORTFENOMENER I DEN POLARE MESOPAUSE)

5) NAMES OF AUTHOR(S) IN FULL (surname first)

MYRABØ Hans Kristian

6) DISTRIBUTION STATEMENT

Approved for public release. Distribution unlimited
(Offentlig tilgjengelig)

7) INDEXING TERMS

IN ENGLISH:	IN NORWEGIAN:
a) Nightglow	a) Nightglow
b) Polar cap	b) Polarområdet
c) Atmosphere	c) Atmosfæren
d) Mesopause	d) Mesopausen
e) Transport phenomena	e) Transport og dynamikk

THESAURUS REFERENCE: -

8) ABSTRACT (continue on reverse side if necessary)

This work utilizes night airglow emissions to deduce temperatures, dynamics, energetics, transport and photochemistry of the polar 80-110 km atmospheric region. The morphological behaviour of ~~the polar~~ 80-110 km region as seen in the night airglow emissions is best described by quasi regular to regular variations in the temperature and in the intensities of the emissions with periods ranging from minutes to a few days. Temperature amplitudes are seen from a few degrees up to ±50 K. Intensity changes up to several hundred percent may occur. Gravity waves from below are generally found to be present in the region, being responsible for much of the short period variations. The long period variations are seen to be related to circulation changes in the lower atmosphere. Stratospheric warmings are generally associated by a cooling of the 80-110 km region by a ratio approximately twice as large in

9) DATE	AUTHORIZED BY This page only	POSITION
26 Feb 88	Erik Klippenberg	Director

UNCLASSIFIED
SECURITY CLASSIFICATION OF THIS PAGE
(when data entered)

ABSTRACT (continued)

amplitude as the heating at the 10 mbar level. The semidiurnal tide is found to be dominant with a peak to peak amplitude of about 5 K, in contrast to model calculations. Effects from geomagnetic phenomena on the energetics and dynamics of the region are not seen, and if present, have to be small or rare as compared to the influence from below. There is a mesopause temperature maximum at winter solstice. Pronounced differences in the day to day and seasonal behaviour of the odd oxygen associated nightglows at the North and South Pole are found. This may indicate fundamental differences at the two poles in the winter mesopause region circulation and energetics.

PREFACE WITH ACKNOWLEDGEMENTS

The work reported here were initiated by the author during 1982 while at the Norwegian Defence Research Establishment (NDRE), Division for Physics. Most of the work, however, was carried out and completed during two periods of sabbatical leave in 1982/83 and in 1985 at the Geophysical Institute of the University of Alaska. The author wishes to express his gratitude to colleagues at the Geophysical Institute for support and encouragement. Particularly appreciated is the close professional contact with Professor C S Deehr, whose advice have been of great help throughout the preparation of this work. The author is also indebted to Professor G G Sivjee for the use of spectrophotometric data from Longyearbyen and Poker Flats. Special thanks go to Mrs Sheila Finch for her expert typing of various publication manuscripts. The engineers J Baldridridge and D Osborne are acknowledged for the great effort put down to keep instruments and computers working around the clock.

The sabbatical periods at the Geophysical Institute were supported by the NDRE, by the Royal Norwegian Council for Scientific and Industrial Research through fellowship programs, and by the Geophysical Institute through grants from the National Science Foundation. Thanks also to Mr T Hvinden, formerly Head of the Division for Physics and to the Head of the Division for Weapons and Equipment, Dr philos B Haugstad and to his Chief Scientist Dr philos P Thoresen for practical support during this work.

Kjeller, February 1988

H K Myrabø

H K Myrabø

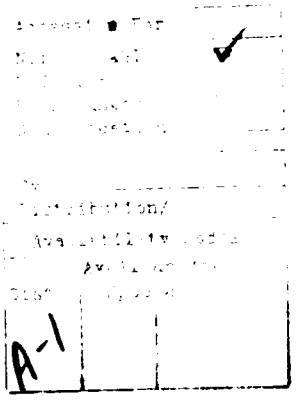

CONTENTS

DYNAMICS OF THE POLAR MESOPAUSE AND LOWER THERMOSPHERE REGION AS OBSERVED IN THE NIGHT AIRGLOW EMISSIONS

SUMMARY

This work utilizes night airglow emissions to deduce temperatures, dynamics, energetics, transport and photochemistry of the polar 80-110 km atmospheric region. The morphological behaviour of the polar 80-110 km region as seen in the night airglow emissions is best described by quasi regular to regular variations in the temperature and in the intensities of the emissions with periods ranging from minutes to a few days. Temperature amplitudes are seen from a few degrees up to ±50 K. Intensity changes up to several hundred percent may occur. Gravity waves from below are generally found to be present in the region, being responsible for much of the short period variations. The long period variations are seen to be related to circulation changes in the lower atmosphere. Stratospheric warmings are generally associated by a cooling of the 80-110 km region by a ratio approximately twice as large in amplitude as the heating at the 10 mbar level. The semidiurnal tide is found to be dominant with a peak to peak amplitude of about 5 K, in contrast to model calculations. Effects from geomagnetic phenomena on the energetics and dynamics of the region are not seen, and if present, have to be small or rare as compared to the influence from below. There is a mesopause temperature maximum at winter solstice. Pronounced differences in the day to day and seasonal behaviour of the odd oxygen associated nightglows at the North and South Pole are found. This may indicate fundamental differences at the two poles in the winter mesopause region circulation and energetics.

1 INTRODUCTION AND OUTLINE

The upper mesosphere, mesopause and lower thermosphere region (i.e. 80-110 km) hereafter abbreviated the mesopause region, has been and still is one of the least understood and investigated regions of our atmosphere. (Romick et al, 1986a; Romick et al, 1986b; Myrabø, 1987).

The main reason for this seems to have been the relative inaccessability of this part of the atmosphere to most of the common atmospheric measuring techniques. Further, the existing observations have been almost entirely restricted to low and mid latitudes.

A basic parameter, such as the temperature, has only been crudely known in the polar 80-110 km region. As an example of this, prior to 1983, knowledge of temperatures at the polar mesopause height was mainly based on a few sporadic measurements of the OH night airglow rotational temperatures, showing temperatures in the range 150-300 K (Myrabø et al, 1983). Together with a small number of rocketsonde data from Heiss Island (CIRA 1972), these constituted our observational information of the atmospheric temperature profile for the 80-110 km region in the polar cap area. Seasonal variations, amplitudes and phases of tides, possible effects of gravity waves, connection to stratospheric warmings, auroral effects and the influence of these on the energetics, small and large scale dynamics and photochemistry had barely been investigated. Particularly information about the small scale dynamical phenomena, being dependent on continuous ground based monitoring, was lacking. This composed a serious limitation in our understanding of the polar 80-110 km region and therefore also in our understanding of the polar atmosphere as a whole (Romick et al, 1986b; Myrabø, 1986; Myrabø et al, 1987).

Consequently, the first goal of this work was to gain basic knowledge of the polar 80-110 km region, starting with a study of the short and long term (seasonal) morphological behaviour of the temperatures of the region, utilizing currently available instrumentation that actually operated at the latitudes in question.

To resolve the short term dynamical phenomena and to obtain the needed temporal coverage, ground based operating instrumentation was needed. The only available ground based instrumentation operating within the polar cap, potentially capable of obtaining temperatures of the 80-110 km region, were the optical spectrometers of the Geophysical Institute of the University of Alaska. These instruments had operated at Svalbard (78^{o}N) for some years to study the high latitude and dayside aurora (Deehr et al, 1980). A spectrometric data base was present. Inspection of the data base looked promising. Using spectrometers to measure night airglow features in the polar cap, and to obtain the neutral temperature from the distribution of the rotational lines (Kvifte, 1959) of the OH and O_2 (0-1) Atm band emissions seemed thus

feasible. However, only the winter 80-110 km region could be studied by this approach, due to the limitation in the observing method, i.e. nightglow cannot be observed from the ground in the twilight and daylight atmosphere. In the polar region this excluded the summer period from equinox to equinox.

The problem with contamination by auroral emissions faced in earlier high latitude airglow experiments (Meriwether, 1975; Kvifte, 1967) was partly solved by selecting the vibrational bands, by monitoring in the same spectra, one or more auroral atomic lines directly excited by precipitating particles and by using a relatively high spectral resolution. In addition, the observing site was situated in the polar cap region where contaminations from the aurora was mainly by atomic lines and less frequent than in the auroral zone (Sivjee and Deehr, 1980; Gault et al, 1981).

Also the ability to record short period intensity variations in the emissions became greatly improved in the 1980s due to new detector development (i.e. GaAs photomultipliers). Short time period dynamics could thus readily be studied and unwanted effects by auroral emission more easily restricted to fewer spectra and thus to much shorter time intervals than had been feasible earlier. The acquisition and reduction techniques were further refined to give reliable temperatures from nightglow spectra down to a few minutes (Myrabø et al, 1987), which is comparable with the Brunt Väissällä period of the atmosphere in the 80-110 km region.

The second objective of this work was to relate the experimental data to physical phenomena in and outside the 80-110 km region, and if possible to derive connections and parameters important for the dynamical and photochemical state of the region. The presence of tides, gravity wave activity, connections to stratwarms etc were thus searched for, and different experimental setups were designed particularly to be optimal for studies of each of these phenomena.

The detailed scientific results of the research are given in ten separate papers included in this report. The general morphological behaviour of the mesopause region as seen through the night airglow

emissions is particularly, but not exclusively, depicted in papers 4.2, 4.7, 4.8 and 4.9. Evidence and effects of gravity waves are mainly discussed in papers 4.1 and 4.5. The behaviour of the polar mesopause region temperature during stratospheric warmings is reported in paper 4.4. Additional results relevant to stratospheric warming events are found in papers 4.6 and 4.7. Tidal components in the temperatures and night airglow intensities are discussed in papers 4.2, 4.7 and 4.9. In paper 4.7 results from a search for possible geomagnetic/auroral interactions with the mesopause region are reported. This is also touched upon in papers 4.9 and 4.10. Seasonal variations are mainly dealt with in paper 4.6, 4.7 and 4.10. Paper 4.10 also treats differences in the morphological behaviour of the odd oxygen associated night airglow at the North and South Polar regions. References made in the first three sections to the papers in section 4 have been underlined.

2 SUMMARY OF SCIENTIFIC ACHIEVEMENTS

As a result of this work one may conclude that the dynamics of the polar mesopause region and its interaction with other regions of the atmosphere are found to be more complex than previously believed (Gärtner and Memmesheimer, 1984; Offermann, 1985; Forbes, 1982a; Evans and Nagy, 1981; Holton, 1979). Dynamics is here mainly manifested in terms of temperature, and may indirectly be related to density, pressure, wind-velocity etc.

2.1 General morphology

At Spitsbergen (~ 78°N, geographic latitude) intensities of the night airglow emissions from different OH bands and from the O_2 (0-1) atmospheric band together with deduced temperatures from the rotational distributions of the emissions at the respective emission heights, i.e. the mesopause region, were obtained. The measurements of the night sky covered 5 winter seasons, i.e. from autumn 1979 through spring 1984. Intensities and temperatures were collected on time sca-

les from a few minutes to hours throughout this period. For part of the winter season 1976 through 1978 mesopause region temperatures were also calculated from OH night airglow data at Poker Flats, Alaska (~ 65^{o}N, geographic latitude).

Both from the Spitsbergen and Poker Flats data it is found that the morphological behaviour of the polar mesopause region, as manifested in the deduced temperatures and in the intensities of the different emissions, is best described in terms of quasi regular to irregular variations (Myrabø, 1984; Myrabø, 1986). Temperature variations ranging from a few percent to tens of percent (hundreds in the intensities) and periods lasting from minutes to several days are seen. Time intervals of several hours void of significant variations are rare (Myrabø, 1986). This is in contrast to the morphology of the temperature variations at mid and low latitudes (Takahashi and Batista, 1981; Wiens, 1974; Shefov 1969; Takeuchi et al, 1979; Tarrago and Chanin, 1982). Consequently, the local dynamics and the larger scale circulation patterns of the polar mesopause region have to be very different from those at lower latitudes (Myrabø, 1984; Myrabø et al, 1984a; Myrabø, 1986). Temperatures at the mesopause height have been measured from 298 K to 158 K during the winter season. This is up to ~90 K in deviation from the CIRA 1972 model atmospheric mean.

2.2 Gravity waves

Measurements of one or more night airglow emissions situated at different heights in the atmosphere were obtained during clear weather situations. Sampling time scales from 30 minutes down to 5 minutes (the latest being close to the Brunt-Väissällä frequency at the mesopause region) were employed. From the simultaneously obtained emission intensities and temperatures at the different heights evidence of gravity wave activity could be searched for (see Fritts et al, 1984; Fritts, 1984; Hatfield et al, 1981; Fredrerick 1979; Noxon, 1978; Krassovsky, 1972).

It was found that in a large fraction of cases, short period variations in temperature and intensities displayed similar behaviour,

i.e. when strong variations in the temperature occurred, the same was seen in the intensity, and with approximately equal periods of variations (Myrabø et al, 1983; Myrabø, 1984). In cases where several emissions at slightly different heights were measured, similar variations, i e same periods, were often seen both in temperature and intensities at the different heights (Myrabø et al, 1987). Most frequently, in phase variations were observed between intensity and temperature. From analysis of the power spectra of the temperature variations, an approximately $k^{-5/3}$ dependence on the temperature variations with wave number was found in a large number of cases, implying the presence of a quasi saturated or saturated gravity wave field with breaking gravity waves (Myrabø et al, 1987).

The bulk of the temperature and intensity variations, with periods in the time domain ~ 5 minutes to 3-4 hours, may therefore be explained in terms of gravity waves penetrating or breaking in the 80-110 km region (Fritts et al, 1984). Both examples of simple cases with monochromatic waves and more complex cases, with combinations of several modes including breaking waves were found (Myrabø et al, 1983; Myrabø et al, *1987*). *Even a case of standing waves near the Brunt* Väissällä frequency, probably excited by longer period gravity waves (Tuan et al, 1979), was observed (Myrabø et al, 1987).

Upper levels of gravity wave induced vertical eddy diffusion coefficient in the range ~ 10^6-10^7 cm^2/s were deduced from the intensity variations of the emissions (Myrabø et al, 1987). This is a pronouncedly larger eddy diffusion coefficient than normally seen at lower latitudes (Thrane et al, 1985; US Standard Atmosphere, 1976) and is possibly in disagreement with the predictions by Lindzen (1981) quoting a minimum in the eddy diffusion coefficient near the mesopause at high latitudes. The large eddy diffusion coefficient may also be taken as an additional indication of very strong gravity wave activity in the polar winter atmosphere. Heights of the sodium emissions and the OH(6-2) emission were found to be separated by about 1 km, indicating the OH(6-2) emission to be situated approximately at 90 km in the polar winter atmosphere (Myrabø et al, 1987). This is ~ 5 km higher than average quotations for lower latitudes (Taylor et al,

1987). It also places the polar winter mesopause at ~ 90 km (Myrabø and Deehr, 1984).

Finally the occurence of gravity waves, penetrating or breaking, is found to be an almost omni-present feature of the polar 80-110 km region (Myrabø et al, 1986), in contrast to mid and low latitudes (Tarrago and Chanin, 1982). The sources of the waves are in no cases found to be associated with geomagnetic or auroral phenomena, thus implying that the sources of the waves are generally the lower and middle atmosphere, i.e. the mesosphere, stratosphere or troposphere (Myrabø et al, 1987; Myrabø, 1984; Myrabø and Deehr, 1984).

2.3 Stratospheric warming events

In the northern hemisphere the stratosphere and lower mesopause is known to undergo a circulation reversal once or more during mid-winter before the final circulation reversal takes place in spring (Labitzke, 1977). In connection with the mid-winter reversal there is found to be a heating of the stratosphere (stratospheric warming) with a corresponding cooling of the mesosphere up to at least ~ 60 km height (Labitzke and Barnett, 1985).

To study possible effects of the stratospheric warmings on the polar mesopause region (i.e. 80-110 km), 12-24 hours averaged mesopause temperatures were compared to temperatures of the stratosphere and mesosphere (i.e. up to ~ 60 km height). The stratospheric/mesospheric temperatures were available from the Nimbus satellite radiometers and covered the polar cap area (Drummond et al, 1980).

It was found that the polar 80-110 km region cooled considerably (at least up to the 90-95 km region), during mid-winter stratospheric warming events (Myrabø et al, 1984a; Myrabø et al, 1986). The amplitude of the cooling at the mesopause was found to be approximately twice as large as the amplitude of the associated warming in the stratosphere at the 10 mbar level (Myrabø et al, 1984a). Daily mean temperature as low as 170 K were observed at the mesopause during a stratospheric warming at solstice. After the stratospheric warming vanished, the cooling of the mesopause was followed by a heating above

the "average" temperature by nearly the same amplitude as the cooling (Myrabø, 1986).

Outside periods of major and minor stratospheric warmings, the long period (day by day) variations of the temperature at the mesopause height were found to have similar or equivalent periods of variations as the day to day variations of the temperature in the mesosphere and in the stratosphere (Myrabø, 1984; Myrabø, 1986). This seems to imply a common origin and that the long term variations in the temperatures at the mesopause are somehow connected to the circulation and temperature changes in the underlying atmosphere.

2.4 Tides

Both emission intensities and temperatures deduced from the emissions at different heights have been analysed for tidal components (Myrabø, 1984; Myrabø and Deehr, 1984; Myrabø et al, 1986). Fourier analysis and superimposed epoch methods have been employed. The diurnal tide component at the mesopause, that according to the latest tidal models should dominate in polar region (Forbes, 1982b), is not found to be present above the noise level, i.e. 1 K. On time scales from a few days to about 20 days the semidiurnal tide component is seen to dominate with peak to peak temperature amplitudes in the range 4 to 8 K. The absence of the diurnal component may be explained by strong interactions of this mode with gravity waves (Beer, 1975). However, the observed amplitude of the semidiurnal mode is far larger than predicted by the current tidal models. Even higher semidiurnal amplitudes are currently reported to exist over short time intervals (Waterscheid et al, 1986). Tidal models should therefore be revised to match the observations better.

2.5 Geomagnetic/auroral effects

Including more than one month with almost continuous temperature data and a good coverage in the intensity data, correlation studies of OH temperatures and intensity variations with geomagnetic Kp, Ap index,

with sudden storm commencement and with the interplanetary magnetic field (Bz) showed no significant correlation (Myrabø and Deehr, 1984). However, for truncated data set taken from the same period (i e case studies) both positive, negative or insignificant correlation could be produced.

The long disputed geomagnetic/auroral influence on the temperature and dynamics in the 80-110 km region (Krassovsky, 1956; Saito, 1962; Shefov, 1969; Maeda and Aikin, 1968; Brekke, 1977; Takahashi and Batista, 1981; Baker et al, 1985) may thus be settled (Myrabø, 1984). In view of the results above and from corresponding analysis of the total amount of temperature and intensity data for the other seasons, it may be concluded that the atmospheric temperature and the dynamics of the polar mesopause region, at least up to the ~ 90 km level, are dominated from below (Myrabø, 1986; Myrabø et al, 1987). Influence from the aurora, if present, have to be rare or too small to be detected as compared to the competing interactions from the atmosphere below. This limits the amplitudes of the perturbations from auroral sources to be generally one order of magnitude or more smaller than the perturbations originating in the underlying atmosphere.

2.6 Seasonal variations

Daily averaged temperatures together with 5 or 10 days running averages were calculated from individual 30 minutes and 1 hour temperatures in order to study the seasonal variations of the mesopause region temperatures (Myrabø, 1984). Tidal components were removed. Forming 5 and 10 days running averages also removed the day to day variations mainly connected to the larger scale variations in the circulation (Myrabø, 1984; Myrabø et al, 1984a). In the polar cap area, (i e Spitsbergen, 78^{o}N geographic) temperatures for 5 seasons were used, covering ~ 4 months around winter solstice. Also temperature data obtained from Poker Flats, 65^{o}N geographic, for the seasons 1976 through 1978 have been analysed with respect to seasonal variations (Myrabø et al, 1984c). Mainly OH emissions have been used in obtaining the temperatures. At 78^{o}N a relatively low temperature in late December followed by a very warm mesopause in January is found to be consistent

for all four winter periods (Myrabø, 1986). A hypothesis is that this is associated with changes in the transmission of gravity waves to the upper mesosphere in connection with stratospheric and lower mesospheric circulation changes.

The average temperature maximum in January was found to be 223 K, data from five winter seasons being used. This is about 15 K higher than the CIRA 1972, 70°N, January model atmoshpere at 90 km. The temperature variation from November through March is best described by a standing wave with a period of about 50 days, peaking in early December and in mid January (Myrabø, 1986). The peak to peak amplitude is about 20-30 K. The corresponding local minimum around solstice is found to be present both during winters with and without major stratospheric warmings. There is, however, both at the 78°N and at the 65°N site an average winter solstice maximum, pointing clearly to lower temperatures both in the autumn and in the spring (Myrabø, 1986; Myrabø et al, 1984c). At the 65°N site there is no clear local minimum around solstice (Myrabø et al, 1984c).

The intensities of the O_2(0-1) Atm band have been used to deduce oxygen concentration at the 95 km level (Myrabø et al, 1984b; Myrabø et al, 1986; Myrabø, 1987). No clear minimum in the deduced oxygen concentration is found at winter solstice. The 2-3 months of data around winter solstice for the two winters of the O_2(0-1) band observations is best described as consisting of strong enhancements in the intensity lasting for days and being superimposed on a constant background level. This is contrary to model calculations estimating that a very clear minimum in the oxygen concentration should occur around winter solstice (mainly due to the lack of production of odd oxygen through dissociation of O_2 by solar ultraviolet radiation in the polar night) (Elphinstone et al, 1984). The lack of a clear minimum indicates that the origin of the oxygen is outside the terminator. Consequently, a more effective transport from outside the solar terminator into the dark polar cap than previously thought has to be awoked. Calculations should therefore be reconsidered.

2.7 Differences in winter solstice conditions at the north/south pole

Differences in the variations of the emission intensities of the odd oxygen associated nightglows at the two poles might be used to indicate differences in the dynamics.

To study this, absolute intensities of the O_2(0-1) Atm band emission were obtained from measurements at Spitsbergen (78°N) (Myrabø, 1987). Two winters, i e 1982/83 and 1983/84, of measurements covering ~2½ months around winter solstice have been analysed. Contamination by aurora was removed, securing that the obtained O_2(0-1) band intensities only reflected the variations in the night airglow component of the O_2(0-1) band.

The O_2(0-1) band absolute intensitites from 78°N were compared with night airglow absolute intensities of the OI5577 emissions over the South Pole, reported by Ismail and Cogger (1982), utilizing satellite data from the ISIS 2 limb scanner. As the O_2 Atm band emission and the OI5577 emission co-varies, a comparison reveals any differences in the odd oxygen variations at the two poles.

Comparing the two sets of data shows striking differences both in the seasonal and in the day to day variations (Myrabø, 1987).

While the intensities at the South Pole show a relatively smooth decline towards a minimum around winter solstice, the emission intensities in the northern polar region reveals variations with very strong emission enhancements lasting for days up to a week or more. The seasonal trend at the North Pole does not show any clear minimum in the emission intensities and thus no minimum in the odd oxygen concentration.

In the south polar region there are no major stratospheric warmings during the mid-winter and thus a more consistent circulation pattern in the stratosphere and in the mesosphere (Shoebend, 1977; Labitzke, 1981). If it is assumed that the enhanced levels of emissions are connected to changes in the circulation and transport within and into the

upper mesoshpere and lower thermosphere, the observed differences in the emission intensities reflect differences in the circulation and transport in the two hemispheres (Myrabø, 1987). Whether this is further connected to differences in gravity wave activity caused by differences in the topography (i.e.land masses) in the two polar regions or of other origin is open to question.

3 FURTHER RESEARCH

This work has illuminated a polar mesopause region with a dynamical complexity; involving strong tidal forcing, almost ever present gravity wave activity, and longer period variations (i e a day or more) in temperature, density and circulation connected to variations in the atmospheric regions below. One of the surprises was to find the atmosphere at mesopause height not particularly affected by geomagnetic or auroraly related activity, but with the variations in temperature and density rather controlled by interactions with the atmospheric regions below, all the way down to the stratosphere.

In order to understand the circulation, transport, energetics and chemistry of the entire polar winter atmosphere, it is crucial to identify the transition region in the atmosphere where the atmosphere changes from mainly being governed by interactions from below, to regions where interactions caused by geomagnetic activities dominates. This region is certainly above ~ 90 km. Monitoring the penetration and breaking of gravity waves from below and through the 90 km region and upwards in addition to monitoring geomagnetic activity should therefore be given priority to identify this transition region. It is also urgent to get a better measure of the amount of energy deposited by the almost ever present gravity waves in the polar winter atmosphere.

Further, efforts should be made to identify if a coupling between gravity waves and tides exists in the polar mesopause region (Walterscheid et al, 1986), and eventually be able to estimate the

amount of energy transferred from the gravity waves to the tides.

Monitoring the presence of gravity waves over large spatial scales, - before, during and after stratospheric warmings, to see if gravity waves might play a part in the stratospheric warming events is another important item that should be pointed out.

Monitoring of a restricted number of nightglow emissions using ground-based spectrometric equipment is scarcely likely to answer the questions outlined above. However, a combination of spectrometric observations from a number of ground stations with the additional use of Rayleigh lidars and monochromatic imagers reinforced possibly by in-situ measurements might provide the information needed. Programs aimed in this direction seem now to be in progress (Romick et al, 1986a).

References

Baker D F, A F Steed, G A Ware, D Offermann, G Lang and H Lauche, Ground-based atmospheric infrared and visible emission measurements, J Atm Terr Phys, 47, 133 (1985)

Beer T, Atmospheric waves, A Hilger, London (1975)

Brekke A, Auroral effects on neutral dynamics, in Dynamical and Chemical Couping Between the Neutral and Ionized Atmoshpere, edited by Grandal B and Holtet J A, p 313, Reidel, Dordrecht (1977)

CIRA, COSPAR Working Group 4, COSPAR International Reference Atmosphere, Pergamon Press, Oxford (1972)

Deehr C S, G G Sivjee, A Egeland, K Henriksen, P E Sandholt, R Smith, P Sweeney, C D Duncan and J Gilmer, Ground-based observations of F Region associated with the magnetospheric cusp, J Geophys Res, 85, 2185 (1980)

Drummond F R, F T Houghton, G D Peskett, C D Rodgers, M F Wale, F Whitney and E J Williamson, The stratospheric and mesospheric sounder on Nimbus 7, Phil Trans R Soc Lond , A 296, 219 (1980)

Elphinstone R D, J S Murphree and L L Cogger, Dynamics of the lower thermosphere consistent with satellite observations of 5577Å airglow: II., Atomic oxygen, local, turbulence and global circulation results, Can J Phys, 62, 382 (1984)

Evans J V and A F Nagy, Solar-Terrestrial Research for the 1980's, National Academy Press, Washington DC (1981)

Forbes F M, Atmospheric tides; the solar and lunar semidiurnal components, J Geophys Res, 87, 5241 (1982a)

Forbes F M, Atmospheric Tides 1., Model Description and results for solar diurnal component, J Geophys Res, 87, 5222 (1982b)

Frederick J E, Influence of gravity wave activiy on lower thermospheric photochemistry and composition, Planet Space Sci, 27, 1469 (1979)

Fritts D C, Gravity wave saturation in the middle atmosphere: A review of theory and observations, Rev Geophys Space Phys 22, 275 (1984)

Fritts D C, M A Geller, B B Balsley, M L Chanin, I Hirota, J R Holton, S Kato, R S Lindzen, M R Schoebend, R A Vincent and R F Noodman, Research status and recommendations from the Alaska Workshop on Gravity Waves and Turbulence in the middle atmosphere, Fairbanks, Alaska, 18-22 July 1983, Bull Am Met Soc, 65, 149 (1984)

Gault W A, R A Koehler, R Link and G G Shepherd, Observations of the optical spectrum of the dayside magnetospheric cleft aurora, Planet Space Sci, 29, 321, (1981)

Gärtner V and M Memmesheimer, Computation of the zonally-averaged circulation driven by heating due to radiation and turbulence, J Atm Terr Phys, 46, 755 (1984)

Hatfield R, T F Tuan and S M Silverman, On the effects of atmospheric gravity waves on profiles of H, O_3 and OH emissions, J Geophys Res, 86, 2429 (1981)

Holton F R, An Introduction to dynamical meteorology, Academic Press, Orlando, Fla (1979)

Ismail S and L L Cogger, Temporal variations of polar cap OI5577Å airglow, Planet Space Sci, 9, 865 (1982)

Krassovsky V I, Infrared night airglow as a manifestation of the process of oxygen recombination, in Airglow and Aurora, edited by E B Armstrong and A Dalgarno, p 195, Pergammon Press, New York (1956)

Krassovsky, V I, Infrasonic variations of the OH emissions in the upper atmosphere, Ann Geophys, 28, 739 (1972)

Kvifte G, Nightglow observations at Ås during the IGY, Geophys Publ, 20, 1 (1959)

Kvifte G J, Hydroxyl rotational temperatures and intensities in the nightglow, Planet Space Sci, 15, 1515 (1967)

Labitzke K, Stratospheric - mesospheric mid-winter warmings, in Dynamical and Chemical Coupling Between Neutral and Ionized Atmosphere, edited by Grandal B and Holter J A, p 17, Reidel, Dordrecht (1977)

Labitzke K, Stratospheric-mesospheric mid-winter disturbances; A summary of observed characteristics, J Geophys Res, 86, 9665 (1981)

Labitzke K and J J Barnett, Stratospheric and mesospheric large-scale height and temperature field during the November/December 1980 Energy Budget Campaign, J Atm Terr Phys, 47, 173 (1985)

Lindzen, R S, Turbulence and stress due to gravity wave and tidal breakdown, J Geophys Res, 86, 9707 (1981)

Maeda K and Aikin A C, Variations of polar mesopheric oxygen and ozone during events, Planet Space Sci, 16, 371 (1968)

Meriwether J W, High latitude airglow observations of correlated short term fluctuations in the hydroxyl Meinel 8-3 band intensity and rotational temperature, Planet Space Sci, 23, 1211, (1975)

Myrabø, H K, C S Deehr and G G Sivjee, Large-Amplitude Nightglow OH(8-3) band intensity and rotational temperature variations during a 24 hour period at 78^{o}N, J Geophys Res, 88, 9255, (1983)

Myrabø H K, C S Deehr and B Lybekk, Polar cap OH airglow rotational tempreatures at the mesopause during a stratospheric warming event, Planet Space Sci, 32, 853 (1984a)

Myrabø H K, K Henriksen, C S Deehr and G J Romick, $O_2(b^1 \Sigma^+ g - X^3 \Sigma^- g)$ atmospheric band night airglow measurements in the northern polar cap region, J Geophys Res, 89, 9148 (1984b)

Myrabø H K, G J Romick, G G Sivjee and C S Deehr, Night airglow OH(8-3) band rotational temperatures at Poker Flats, Alaska, J Geophys Res, 89, 9153 (1984c)

Myrabø H K, Temperature variations at mesopause levels during winter solstice at 78^{o}N, Planet Space Sci, 32, 249 (1984)

Myrabø H K, and C S Deehr, Mid winter hydroxyl night airglow emissions intensities in the northern polar region, Planet Space Sci, 32, 263 (1984)

Myrabø H K, C S Deehr, G J Romick and K Henriksen, Mid-winter intensities of the night airglow O_2(0-1) atmospheric band emissions at high latitudes, J Geophys Res, 91, 1684 (1986)

Myrabø H K, Winter-season mesopause and lower thermosphere temperatures in the polar region, Planet Space Sci, 34, 1023 (1986)

Myrabø H K, C S Deehr, R Viereck and K Henriksen, Polar mesopause gravity wave activity in the sodium and hydroxyl night airglow, J Geophys Res, 92, 2527 (1987)

Myrabø H K, Night airglow O_2(0-1) atmospheric band emission during the northern polar winter, Planet Space Sci (in press) (1987)

Noxon, J F, Effects of internal gravity waves upon night airglow temperatures, Geophys Res Letters, 5, 25 (1978)

Offermann D, The Energy Budget Campaign 1980; Introductory review, J Atm Terr Phys, 47, 1 (1985)

Romick G J, C S Deehr, M A Bondi, J C Foster, T L Killeen, R W Schunk, C F Sechrist Jr, B A Tinsley and D G Torr, Coupling, Energetics, and Dynamics of Atmospheric Regions "CEDAR", Vol I: Overview, Report to the Aeronomy Program of the National Science Foundation (1986a)

Romick G J, C S Deehr, M A Bondi, J C Foster, T L Killeen, R W Schunk, C F Sechrist Jr, B A Tinsley and D G Torr, Coupling, Energetics and Dynamics of Atmospheric Regions "CEDAR", Vol II, Report to the Aeronomy Program of the National Science Foundation, p 18 (1986b)

Saito B, Unusual enhancement of night airglow intensity at low latitudes on November 13, 1960, Antarctic Rec, 14, 8 (1962)

Schoebend M R, Stratospheric warmings, observations and theory, Rev Geophys, Space Phys, 16, 521 (1977)

Shefov N N, Hydroxyl emissions of the upper atmosphere - I. The behaviour during solar cycle, seasons and geomagnetic disturbances, Planet Space Sci, 17, 797 (1969)

Sivjee G G and C S Deehr, Differences in polar atmospheric optical emissions between mid-day cusp and night-time auroras, in Exploration of the Polar Upper Atmosphere, edited by C S Deehr and J A Holtet, p 199, Reidel, Hingham, Mass (1980)

Takahashi H and P P Batista, Simultaneous measurements of OH(9.4), (8.3), (7.2), (6.2) and (5.1) bands in the airglow, J Geophys Res, 86, 5632 (1981)

Takeuchi I, K Misawa, Y Kato and I Aoyama, Rotational temperatures and intensities of OH(6-2) and OH(8-3) bands in the nightglow, J Atm Terr Phys, 41, 387 (1979)

Tarrago A and M L Chanin, Interpretation in terms of gravity waves of structures observed at the mesopause level by photogrametry and lidar, Planet Space Sci, 30, 611 (1982)

Taylor M, M A Hapgood and P Rothwell, Observations of gravity wave propagation in the OI (557.7 nm), Na (589.2 nm) and the near infrared OH nightglow emissions, Planet Space Sci, 35, 413 (1987)

Thrane E V, Ø Andreassen, T Blix, B Grandal, A Brekke, C R Philbrick, F J Schmidlin, H U Widdel, U Von Zahn and F J Lübken, Neutral air turbulence in the upper atmosphere observed during the Energy Budget Campaign, J Atm Terr Phys, 47, 243 (1985)

Tuan T F, R Hedinger, S Silverman and M Okuda, On gravity wave induced Brunt-Väissällä oscillations, J Geophys Res, 84, 393, (1979)

U S Standard Atmosphere, 1976, NOAA-S/T76-1562, Washington D C (1976)

Walterscheid R L, G G Sivjee, G Schubert and R M Hamwey, Large-amplitude semidurnal temperature variations in the polar mesopause; evidence of a pseudotide, Nature, 324, 347 (1986)

Wiens R H, Diurnal variations of the (8-3)/(5-0) intensity ratio of nightglow OH at Agi Udri, Planet Space Sci, 22, 1059 (1974)

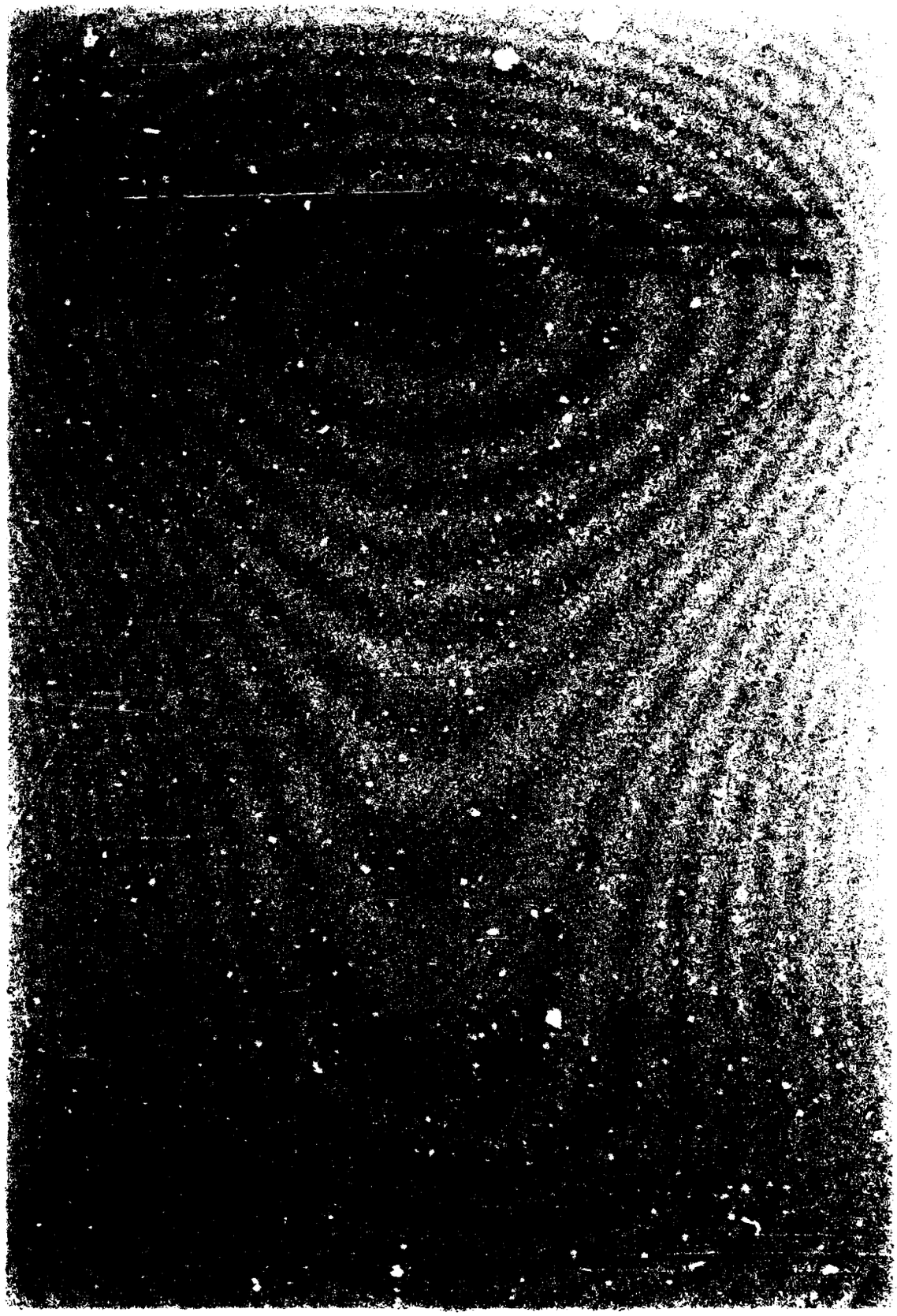

JOURNAL OF GEOPHYSICAL RESEARCH, VOL. 88, NO. A11, PAGES 9255–9259, NOVEMBER 1, 1983

Large-Amplitude Nightglow OH (8–3) Band Intensity and Rotational Temperature Variations During a 24-Hour Period at 78°N

H. K. MYRABØ,[1] C. S. DEEHR, AND G. G. SIVJEE[2]

Geophysical Institute, University of Alaska

We report results from a continuous 24-hour measurement of the OH (8–3) band emission in the nightglow at 78.4°N. A mean temperature of 273 K and a mean band intensity of 596 R were observed. Extreme temperature variations were seen with amplitudes up to ±70 K from the mean. It is suggested that these variations are related to the passage of internal gravity waves. If so, the extreme amplitudes of the variations might imply that the OH emitting layer is situated above 90 km at this latitude in January. The deduced η values ($\Delta I / \Delta T$, T) favor the ozone mechanism to be responsible for the OH emission with the possibility of an additional mechanism contributing up to 5%.

1. INTRODUCTION

Since *Meinel* [1950] identified the OH band system in the night airflow, a large number of investigators have tried to elucidate the physics and chemistry behind the different patterns of behavior of the OH nightglow.

The study of OH emissions alone or together with other nightglow emissions provides important information on temperature, density, composition, and behavior of the upper mesosphere. OH emission measurements may also be used as an important tool for observing the effects of propagating gravity waves through the atmosphere [*Krassovsky*, 1972; *Krassovsky and Shagaev*, 1974; *Noxon*, 1978; *Frederick*, 1979; *Hatfield et al.*, 1981].

Almost all of the observations of OH have previously been made at latitudes less than approximately 70°. Measurements above latitude 55° are sparse compared to lower latitudes.

The only measurements at high (i.e., above 70°) latitudes seem to be those of *Chamberlain and Oliver* [1953] in Thule, the flights by the U.S. Air Force KC-135 jet aircraft in March 1963 and 1964 reported by *Noxon* [1964], and the 1968 NASA auroral airborne expedition [*Sivjee et al.*, 1972].

Chamberlain and Oliver's data consited only of a few spectra with relatively coarse spectral and temporal resolution. They found an OH rotational temperature ranging from 300 to 350 K which is believed to be approximately 30–40 K too high due to erroneous molecular constants used in the reduction of the data [*Krefte*, 1959].

Noxon's results, which are based mainly on two spectra averaged in time and space over latitudinal ranges 77°–85°N and 69°–85°N gave temperatures 160 and 185 K, respectively. He also reported a significant decrease in intensity and temperature with increasing latitudes.

The NASA airborne observations performed between January and March 1968 consisted of a larger number of flights and thus provided more data pertinent to the picture of the latitudinal dependence of the temperaure. Latitudes 70°–78°N gave temperatures in the range 190–245 K with a mean close to 225 K [*Sivjee et al.*, 1972].

These measurements, although providing valuable data on temperature and intensity with latitude only gave a snapshot (and therefore a very limited understanding) of OH morphology at high latitudes. For this purpose continuous measurements from the ground and if possible linked with satellite measurements from above will provide the best data.

Satellite measurements alone have been utilized. *Reed* [1976] reported indications of strong polar enhanced OH emissions. Further, *Walker and Reed* [1976] found the effects from an early major stratospheric warming in December 1967 on the OH emission intensity to be largest between 70° and 80°N. Unfortunately, the measurements were broadband optical measurements, and contamination by aurora, as was pointed out in both these works, cannot be ruled out.

The lack of observations at high latitudes is due, in part, to the problem of contamination by auroral emissions. In the auroral zone this is caused by auroral molecular bands which cover almost the entire visible and near infrared [*Vallance-Jones*, 1974; *Meriwether*, 1975].

However, at higher latitudes (i.e., into the polar cap region), auroral molecular emissions diminish and the aurora emits mainly atomic lines [*Sivjee and Deehr*, 1980]. Thus a normal, high-responsivity auroral spectrophotometer operated at a resolution of 2000 (4-Å bandwidth) may be used to measure most of the OH bands and lines clearly resolved from the auroral emissions. Because of the high geographic latitude of the station, observations may be carried out continuously for 24 hours per day for 2 months around each winter solstice. The auroral observatory at Longyearbyen may therefore be regarded as a suitable site for high latitude OH observations from the ground.

2. INSTRUMENTATION, OBSERVATIONS, AND REDUCTION

The OH emission data employed in this work were part of the measurements undertaken during the multinational Svalbard auroral expedition beginning in 1978 at an observatory [*Deehr et al.*, 1980] close to Longyearbyen on West Spitsbergen (geographic latitude 78.4°N).

The 1-m and ½-m high-throughput Ebert-Fastie spectrophotometers are coupled to a minicomputer and record in the photon-counting mode. The 1-m instrument, used for these measurements reported here, is further described by *Dick et al.* [1970] and *Sivjee et al.* [1972].

From three seasons of data, i.e., 1979/1980, 1980/1981, and 1981/1982, we have been able to utilize limited periods during

[1] On leave from Norwegian Defense Research Establishment.
[2] Now at National Science Foundation

Paper number 3A0690
0148-0227/83/003A-0690$05.00

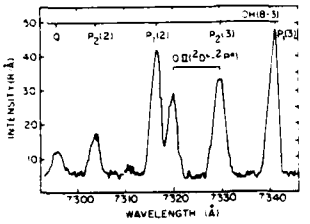

Fig. 1. An example of the spectra used for deducing temperature and intensity. Each spectrum is acquired during a 10-min period summing 75 individual 8-s scans. In addition to the OH (8–3) lines, also the forbidden oxygen doublet at 7320/7330 Å originating in the aurora is indicated.

clear weather where the instruments were run in a suitable manner for OH measurements. Of particular interest are observations from a single 24-hour period of continuous measurement of the OH (8–3) band where the OH intensity and temperature were observed to change considerably. Unfortunately, none of the other usable periods in the data collection contained a full 24-hour period with as high a time resolution. How often this behavior occurs is therefore not yet known.

The spectrophotometer was pointing toward zenith and the λ 7285-Å–7350-Å region was scanned in 8 s by using the spectrophotometer in the second order with a 1-mm slit corresponding to a bandwidth of 1.5 Å and a resolution of 4900. Each scan was recorded on magnetic tape. In most cases, an adequate signal-to-noise ratio was acquired by integrating 75 individual scans over 10 min. An example of the quality of the data may be seen in Figure 1.

Rotational temperature was calculated by Kvifte's method, using the intensity ratio of the $P_1(2)$ and $P_1(3)$ lines [*Kvifte*, 1959]. The band intensity was then based on the measured intensity of the $P_1(2)$ line together with the calculated temperature. Absolute intensity calibration was performed in the field by using a standard lamp and a diffusing screen.

Probable error in the calculated temperature is estimated to be ± 5 K caused by the uncertainty in defining the $P_1(2)$ and $P_1(3)$ background levels, while the possible error in the absolute intensity is approximately 20%, mainly caused by the calibration uncertainty.

The aurora could easily be monitored through the 7320/7330-Å OII lines. Additional care was taken to assure that there was no contamination of the data from the N_2 1*P* and other auroral molecular emissions.

3 Results and Discussion

3.1. *Intensities and Rotational Temperatures*

Intensities and rotational temperatures as derived from the measured OH (8–3) band lines between January 6 and 7, 1981, 0600–0550 UT are presented in Figure 2. They are given respectively as broken and solid lines. The mean 24-hour rotational temperature is 237 K and the mean intensity of the OH (8–3) band is 596 R. For comparison we may mention that the average temperature and band intensity found by *Takahashi et al.* [1977] at 23°S for the period July 1972 to October 1974 was 179 K and 408 R, respectively.

No obvious diurnal or semidiurnal trend is visible in the 24-hour record presented here.

Previous temperature measurements at latitudes 70°–85°N cover the range 160 to approximately 300 K. However, such a large variation in temperature as seen here (± 70 K), has not been reported from a single station and a limited time span. *Krassovsky and Shagaev* [1977] report extremes of ± 50 K during the propagation of internal gravity waves through the mesosphere.

There is no way of ascertaining that the variations seen here are due to the propagation of internal gravity waves. To do that would have required simultaneous determination of temperatures at least at two altitudes [*Noxon*, 1978] or measurements taken simultaneously at three places in the sky [*Krassovsky*, 1972; *Krassovsky and Shagaev*, 1974].

However, it is difficult to find another mechanism that could lead to such extreme variation in the temperature and intensity. An indication that at least part of the variations seen here are due to the propagation of gravity waves is the correlation between temperature and intensity. A correlation between temperature and intensity was found by *Shagaev* [1974] and *Krassovsky and Shagaev* [1977] during the propagation of gravity waves, while under conditions where gravity waves were not likely, poor or not correlation was found [*Harrison et al.*, 1971; *Takahashi et al.*, 1974; *Takeuchi et al.*, 1979]. Figure 3 shows the intensity-temperature plot. The correlation coefficient found is 0.56 using $N = 286$ points. The best fit curve with a slope $\Delta I/\Delta T = 1.93$ R/K is indicated.

It has been shown theoretically by *Weinstock* [1978] that the relation between temperature and intensity during gravity wave passage is complex. It might show phase shifts and depend upon the scale height of the respective minor component (e.g., H) relative to total scale height at the particular

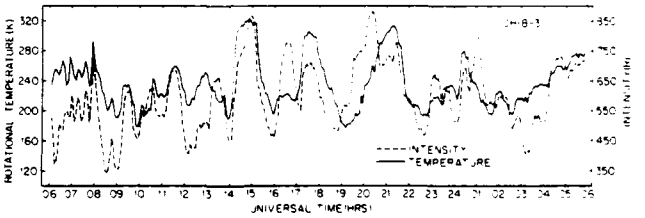

Fig. 2. Intensity and rotational temperatures as derived from measured OH (8–3) bands during January 6–7, 1981, at Longyearbyen, Svalbard. The intensity and rotational temperature as obtained each 5 min from 10 min of scans (50% overlapping) are plotted as points. Straight lines are drawn between successive points.

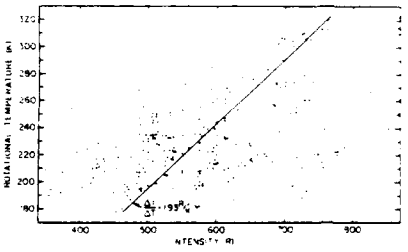

Fig. 3. Correlation between OH (8–3) rotational temperature and intensity during the 24-hour period as obtained employing each point (5-min interval) in Figure 1 directly. The correlation analysis was performed by using $N = 286$ points, giving a correlation coefficient $r = 0.56$.

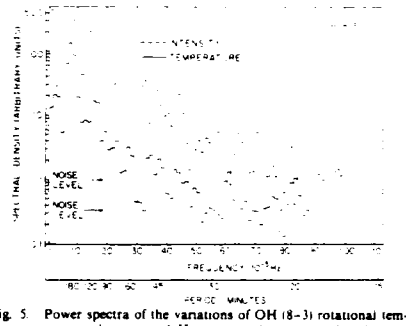

Fig. 5. Power spectra of the variations of OH (8–3) rotational temperature and intensity. A Hanning window was employed.

altitude. The coherent motion of the emitting particles (i.e., OH) moving in and out of the field of view may also influence the observed relation. According to Weinstock, nonlinear corrections to the oscillations may be neglected at OH height, i.e, 85–90 km.

An attempt to improve the correlation between temperature and intensity waves was made by phase shifting the temperature with regard to the intensity. The maximum obtained was 0.59, i.e., not significantly different from that with no phase shift. Slight phase shifts between temperature and intensity and/or changes in the intensity-temperature amplitude ratio during the observation period as might be inferred from Figure 2 may help explain the relatively low correlation found.

This does not eliminate gravity waves as the source because correlation coefficients in the same range (i.e., 0.5–0.9, *Krassovksy and Shagaev* [1977]) are typical of gravity wave data. A higher coefficient (i.e, up to 0.8) might be obtained from our data by selecting only part of the observed period.

The relationship between amplitude and periods as shown in Figure 4 also strongly points to gravity waves as the source. It shows the same linear relationship as found by *Krassovsky and Shagaev* [1977] during gravity wave propagation. It differs, however, in the striking manner, that for the same period of oscillation our results show about twice as high an amplitude. This may be interpreted to mean that the OH-emitting layer over Longyearbyen, i.e, at extreme high latitudes, is situated at a slightly higher altitude than at middle to moderately high latitudes [*Frederick*, 1979]. From simultaneous measurements of different vibrational levels of OH bands during December 1980 and January 1981, a positive temperature gradient was found for the OH emitting region [*Myrabø*, 1983]. This may be interpreted to mean that the emission region is situated at or slightly above the mesopause. Owing to the polar jet, the mesopause is believed to be at a higher altitude of midwinter above the polar regions than elsewhere [*Rodgers*, 1977]. In view of the above, a reasonable interpretation is that all or part of the larger amplitude found is due to the higher altitude of OH emitting layer. This contradicts the suggestion of *Sivjee et al.* [1972], who suggested that the height of the OH-emitting layer is independent of latitude. The latter results are, however, based on a comparison of a very limited amount of temperature data with temperatures taken from a model.

Figure 5 shows a Fourier analysis of the temperature and intensity variations, which exhibit a decreasing energy in the higher frequencies. This is also in agreement with *Krassovsky and Shagaev* [1977], who find the same characteristic feature during gravity wave propagation conditions. Periods in the range 3 hours to approximately 20 min are clearly recognizable in the power spectra of both intensity and temperature shown in Figures 5 and 1. They are all within the domain of internal gravity waves [*Hines*, 1960].

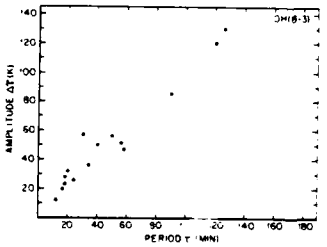

Fig. 4. Amplitude of the rotational temperature, ΔT in degrees Kelvin plotted against period τ in minutes for the most well-defined oscillations in Figure 1.

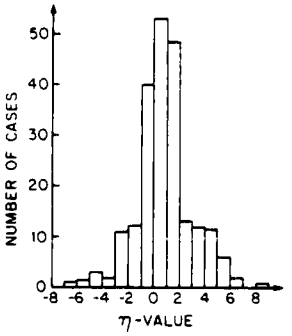

Fig. 6. Distribution of the η value ($\Delta I / I \; \Delta T / T$) for the measurements on January 6–7. Cases with $\eta > 8$ not included here were in the range 0–2 for a single interval.

All of these indications seem to support the hypothesis that a large part of the variations in OH temperature and intensity reported here have been due to the passing of internal gravity waves.

A closer inspection of Figure 2 reveals a tendency of a fine structure of the order of 10–15 min superimposed on the longer period waves. Fine structure might be seen both in the intensity and in the temperature. Similar fine structure in the 5577-Å and 6300-Å night airglow intensity is known to exist [*Okuda*, 1962; *Silverman*, 1962] and is in some cases believed to be associated with local instability in gravity waves having amplitudes greater than approximately 20% [*Hodges*, 1967]. According to *Tuan et al.* [1979], the ripple frequency should be close to the buoyancy period, (i.e. the Brunt-Väisällä period), which in our case is of the order of 5–7 min. Our integration time and sampling rate might, however, modulate and obscure the real frequency pattern, i.e. the real oscillations might be considerably smaller than 10–15 min. A further investigation and discussion of this is therefore advisable to leave until data with a much higher sampling rate (i.e. the order of 1 min) is obtained.

Babakov [1975], *Kuzmin* [1975], and *Shagaev* [1974] report the occurrence of gravity waves to be correlated to geomagnetic activity as measured by the geomagnetic K index. *Shagaev* [1974] reports southward travelling waves, indicating an origin in polar regions. *Krassovsky and Shagaev* [1974, 1977] report the sources to be connected with active meteorological phenomena in the troposphere in connection with jet streams, weather fronts, cyclones, anticyclones, etc. But they do not exclude a dependence on geomagnetic activity.

Svalbard is indeed closely surrounded by both geomagnetic and meteorological phenomena. Not enough data have yet been accumulated to establish how common this behavior of the OH emission is, and how it connects to the overall mesospheric temperature, density, composition, wind velocities, etc.

3.2. *The Observed η Value and the OH Emission Mechanism*

The η value was first introduced by *Krassovsky* [1972] and is defined as follows:

$$\eta = \Delta I/I/\Delta T/T = 2(\gamma - 1) - A_s$$

where $\Delta I/I$ and $\Delta T/T$ are relative increments in the intensity and temperature, γ is the ratio of the specific heats, and A_s is the exponent in the temperature dependent rate coefficient (i.e., $k = k_0 T - A_s$, k and k_0 being the respective reaction coefficients at temperatures T and T_0). The theoretical justification of the η value and its relation to the emission process in the case of an adiabatic oscillation of the atmosphere is also dealt with by *Krassovsky* [1972]. It is an important parameter to evaluate and may be used as a means of identifying the emission process. *Krassovsky* [1971] introduced the perhydroxyl process and suggested that other processes may be important in addition to the ozone mechanism suggested by *Bates and Nicolet* [1950] and *Herzberg* [1951]:

$$O_3 + H \rightarrow OH^*(v \leq 9) + O_2(+3.34\ eV) \qquad (1)$$

Takahashi and Batista [1981] find evidence in their data for the mechanism

$$HO_2 + O \rightarrow OH^*(v \leq 6) + O_2(+2.4\ eV) \qquad (2)$$

proposed by *Nicolet* [1970] in addition to the ozone mechanism. *Takeuchi et al.* [1981], however, report strong evidence for the ozone mechanism to be the only emission mechanism operative, since they find η values confined to the range -0.5 to $+1.5$. (The theoretical η value for the process (1) is $\eta = 1$, while for the perhydroxyl mechanism and process (2), η is 3.7.)

Weinstock [1978] has reviewed Krassovsky's η value, introducing a more complex relation between temperature and intensity which is dependent upon the scale height of the minor component (i.e., H or O) with respect to the total scale height. Thus phase shifts and amplitude ratio variations may be introduced. However, the main effects of phase shift and variation in the scale height of the minor component during the passage is most likely to broaden the η distribution (i.e., smear out the relation to A_s). Thus the η values derived here by using Krassovsky's relation should be able to distinguish between processes with values as different as 1 and 3.7.

Figure 6 presents a histogram showing the occurrence frequency distribution for the values of η calculated from the 24 hours of observations reported here. The mean η value is 1.08, which implies the ozone mechanism to be responsible for the OH emission. Other emission mechanisms with η close to 1 can, however, not be ruled out, but mechanisms with $\eta > 1.5$, such as, for example, the perhydroxyl mechanism, if operative at all, seem not to contribute significantly to the OH emissions. An upper level of 5% may be estimated to be the largest possible contribution.

4. Summary

From continuous 24-hour measurements of the OH (8–3) band nightglow emission at 78.4°N, a mean temperature of 237 K, and a mean band intensity of 596 R is found. Temperature variations are very large, showing oscillations with extremes up to ±70 K from the mean. The large variation between previous temperature measurements [*Chamberlain and Oliver*, 1953; *Noxon*, 1964; *Sivjee et al.*, 1972] at latitudes 70°–85°N cover the range 160 K to approximately 300 K and was previously thought to be too large when compared to measurements at lower latitudes. The observation of this variation in a single 24-hour period from a single station lends credence to the validity of all the previous observations. In addition, there are indications that these large variations were due to the passage of internal gravity waves through the mesosphere. If so, the extreme amplitudes of the variations imply that the OH-emitting layer at high latitudes is slightly higher in the atmosphere than at middle and low latitudes in January [*Frederick*, 1979]. The deduced η values ($\Delta I/I/\Delta T/T$) favor the ozone mechanism to be responsible for the OH emission with the possibility of an additional mechanism contributing up to 5% of the emission.

Acknowledgments. Financial support for this research was provided by National Science Foundation through grants ATM77-20837, ATM77-24838, ATM80-12718, and ATM82-00114 to the Geophysical Institute of the University of Alaska. One of us (H. K. M.) is supported by a fellowship grant from Royal Norwegian Council for Scientific and Industrial Research.

The Editor thanks T. F. Tuan and another referee for their assistance in evaluating this paper.

References

Babakov, N. A., On the influence of the planetary state of magnetosphere on the parameters of the hydroxyl emission, *Izv. Akad. Nauk Turkm. SSR*, *5*, 67, 1975.

Bates, D. R., and M. Nicolet, The photochemistry of atmospheric water vapor, *J. Geophys. Res.*, *55*, 301, 1950.

Chamberlain, J. W., and N. J. Oliver, OH in the airglow at high latitudes, *Phys. Rev.*, *90*, 1118, 1953.

Deehr, C. S., G. G. Sivjee, A. Egeland, K. Henriksen, P. E. Sandholt,

R. Smith, P. Sweeney, C. Duncan, and J. Gilmer, Ground-based observations of F region associated with the magnetospheric cusp, *J. Geophys. Res.*, *85*, 2185, 1980.

Dick, K. A., G. G. Sivjee, and H. M. Crosswhite, Aircraft airglow intensity measurements: Variations in OH and OI (5577), *Planet. Space Sci.*, *18*, 687, 1970.

Frederick, J. E., Influence of gravity waves activity on lower thermospheric photochemistry and composition, *Planet. Space Sci.*, *27*, 1469, 1979.

Harrison, A. W., W. F. J. Evans, and E. J. Llewellyn, Study of the (4–1) and (5–2) hydroxyl bands in the night airglow, *Can. J. Phys.*, *49*, 2509, 1971.

Hatfield, R., T. F. Tuan, and S. M. Silverman, On the effects of atmospheric gravity waves on profiles of H, O, and OH emission, *J. Geophys. Res.*, *86*, 2429, 1981.

Hertzberg, G., The atmosphere of the planets, *J. R. Astron. Soc. Can.*, *45*, 100, 1951.

Hines, C. O., Internal atmospheric gravity waves at ionospheric heights, *Can. J. Phys.*, *38*, 1441, 1960.

Hodges, R. R., Generation of turbulence in the upper atmosphere by internal gravity waves, *J. Geophys. Res.*, *72*, 3455, 1967.

Krassovsky, V. I., The hydroxyl emission problem and part of its solution, *Ann. Geophys.*, *27*, 211, 1971.

Krassovsky, V. I., Infrasonic variations of OH emission in the upper atmosphere, *Ann. Geophys.*, *28*, 739, 1972.

Krassovsky, V. I., and M. V. Shagaev, Optical method of recording acoustic or gravity waves in the upper atmosphere, *J. Atmos. Terr. Phys.*, *36*, 373, 1974.

Krassovsky, V. I., and M. V. Shagaev, On the nature of internal gravitational waves observed from hydroxyl emissions, *Planet. Space Sci.*, *25*, 200, 1977.

Kuzmin, K. I., Intensity oscillations of the 5577Å and 5893Å emissions and geomagnetic activity, *Aurorae Airglow USSR Acad. Sci.*, *23*, 28, 1975.

Kvifte, G., Nightglow observations at Ås during the I.G.Y., *Geophys. Publ.*, *20*, 1, 1959.

Meinel, A. B., OH emission bands in the spectrum of the night sky, *Astrophys. J.*, *111*, 555, 1950.

Menwether, J. W., High latitude airglow observations of correlated shortterm fluctuations in the hydroxyl Meinel 8–3 band intensity and rotational temperature, *Planet. Space Sci.*, *23*, 1211, 1975.

Myrabø, H. K., Temperature variation at mesopause levels at 78°N during winter solstice, *Planet. Space Sci.*, in press, 1983.

Nicolet, M., Ozone and hydrogen reactions, *Ann. Geophys.*, *26*, 531, 1970.

Noxon, J. F., The latitude dependence of OH rotational temperature in the night airglow, *J. Geophys. Res.*, *69*, 4087, 1964.

Noxon, J. F., Effects of internal gravity waves upon night airglow temperatures, *Geophys. Res. Lett.*, *5*, 25, 1978.

Okuda, M., A study of excitation processes in night airglow, *Sci. Rep. Tohoku Univ.*, *15*, 9, 1962.

Reed, E. I., Polar enhancements of nightglow emissions near 6230Å, *Geophys. Res. Lett.*, *3*, 5, 1976.

Rodgers, C. D., Morphology of upper atmosphere temperatures, in *Dynamical and Chemical Coupling Between the Neutral and Ionized Atmosphere*, edited by B. Grandal and J. A. Holtet, p. 3, D. Reidel, Hingham, Mass., 1977.

Shagaev, M., Fast variations of hydroxyl night airglow emission, *J. Atmos. Terr. Phys.*, *36*, 367, 1974.

Silvermann, S. M., Unusual fluctuations of 5577Å OI airglow emission intensity on October 28–29, 1961, *Nature*, *195*, 481, 1962.

Sivjee, G. G., and C. S. Deehr, Differences in polar atmospheric optical emissions between mid-day cusp and night-time auroras, in *Exploration of the Polar Upper Atmosphere*, edited by K. Deehr and K. Holter, p. 199, D. Reidel, Hingham, Mass., 1980.

Sivjee, G. G., K. A. Dick, and P. D. Feldman, Temporal variations in the night-time hydroxyl rotational temperature, *Planet. Space Sci.*, *20*, 261, 1972.

Takahashi, H., and P. P. Batista, Simultaneous measurements of OH (9, 4), (8, 3), (7, 2), (6, 2) and (5, 1) bands in the airglow, *J. Geophys. Res.*, *86*, 5632, 1981.

Takahashi, H., B. R. Clemesha, and Y. Sahai, Nightglow OH (8–3) band intensities and rotational temperatures at 23°S, *Planet. Space Sci.*, *22*, 1323, 1974.

Takahashi, H., Y. Sahai, B. R. Clemesha, P. P. Batista, and N. R. Teixeira, Diurnal and seasonal variations of the OH (8–3) airglow band and its correlation with OI 5577Å, *Planet. Space Sci.*, *25*, 541, 1977.

Takeuchi, I., K. Misawa, Y. Kato, and I. Aoyama, Rotational temperatures and intensities of OH (6–2) and OH (8–3) bands in the nightglow, *J. Atmos. Terr. Phys.*, *41*, 387, 1979.

Takeuchi, I., K. Misawa, Y. Kato, and I. Aoyama, Seasonal variations of the correlation among nightglow radiations and emission mechanism of OH nightglow emission, *J. Atmos. Terr. Phys.*, *43*, 157, 1981.

Tuan, T. F., R. Heinger, S. M. Silvermann, and M. Okuda, On gravity wave induced Brunt-Väisällä oscillations, *J. Geophys. Res.*, *84*, 393, 1979.

Vallance Jones, A., *Aurora*, D. Reidel, Hingham, Mass., 1974.

Walker, J. D., and E. I. Reed, Behavior of the sodium and hydroxyl nighttime emissions during a stratospheric warming, *J. Atmos. Sci.*, *33*, 118, 1976.

Weinstock, J., Theory of interaction of gravity waves with O_2 ($^1\Sigma$) airglow, *J. Geophys. Res.*, *83*, 5175, 1978.

C. S. Deehr and H. K. Myrabø, Geophysical Institute, University of Alaska, Fairbanks, AK 99701

G. G. Sivjee, National Science Foundation, 1800 G St., N. W., Washington, D. C. 20550.

(Received February 16, 1983,
revised April 18, 1983,
accepted May 2, 1983.)

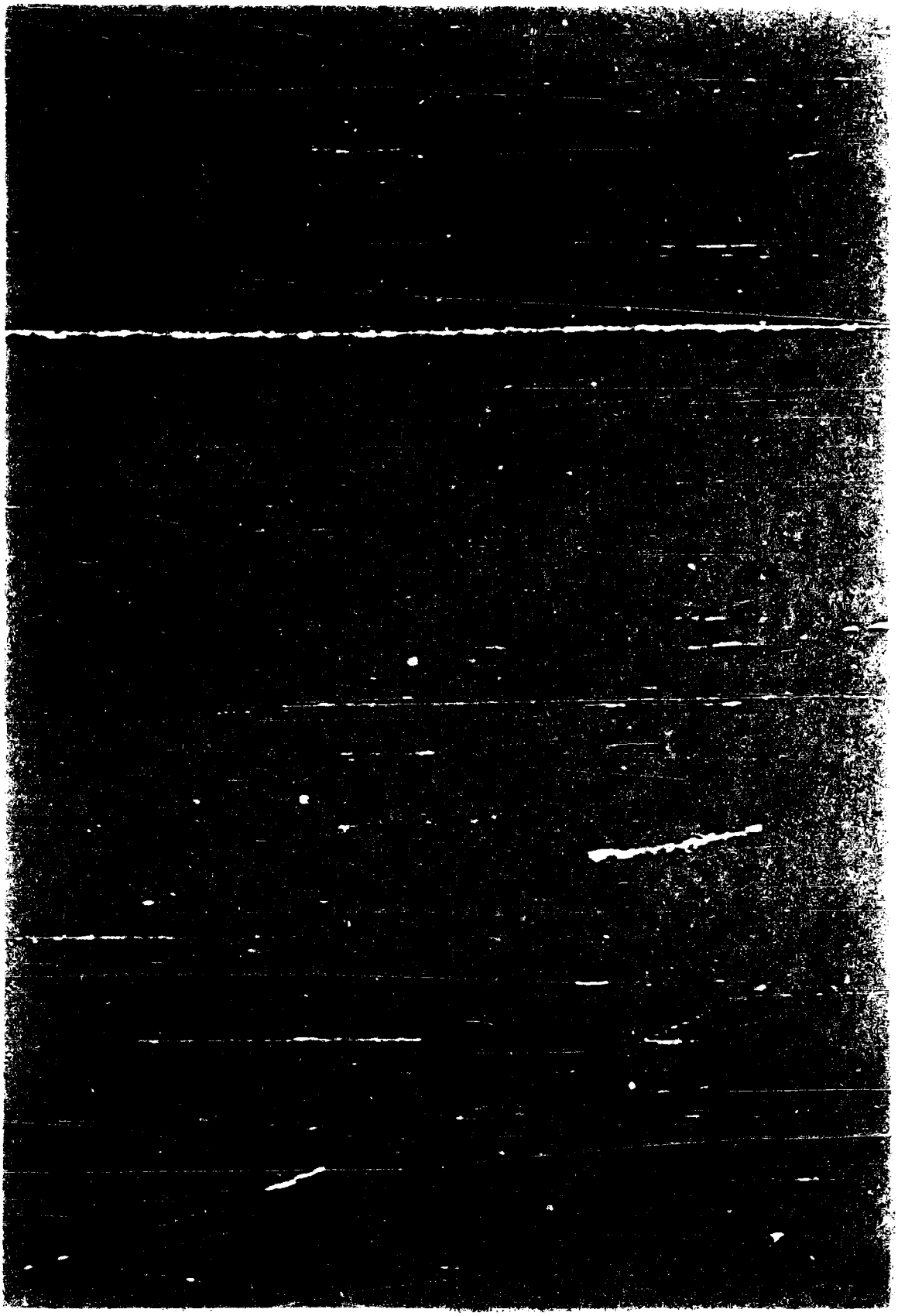

Planet. Space Sci., Vol. 32, No. 2, pp. 249–255, 1984
Printed in Great Britain

0032-0633/84 $3.00 + 0.00
Pergamon Press Ltd.

TEMPERATURE VARIATION AT MESOPAUSE LEVELS DURING WINTER SOLSTICE AT 78°N

H. K. MYRABO*
Geophysical Institute, University of Alaska, Fairbanks, AK 99701, U.S.A.

(*Received in final form* 27 *June* 1983)

Abstract—Atmospheric temperatures from the polar mesopause are deduced from spectrophotometric measurements of hydroxyl bands and lines in the night airglow made at 78°N during December and January 1980/81 and 1982/83. An overall mean temperature of 220 K is found with a range from 172 to 257 K in the daily mean values. Several warm periods lasting 3–6 days may be due to heat dissipated by gravity waves. One week of consistently low temperatures was apparently connected to a stratospheric warming. Both datasets show a warmer mean temperature later in January than for early and mid-December. The polar OH airglow seems to peak at or just above the mesopause. The data also indicate that the mesopause is situated at approx. 90 km with an upper temperature gradient of 1 K km^{-1}, indicating a very shallow mesopause. A superposed epoch analysis of 19 consecutive 24-h periods reveals a semidiurnal variation in the temperature around winter solstice with an amplitude of 5 K. No diurnal variation of amplitude greater than 1 K is apparent. Average wind velocity deduced from the amplitude of the semidiurnal temperature variation is 9 m s^{-1}.

1. INTRODUCTION

Temperature is a basic physical parameter of the atmosphere. It is involved in most of our understanding of atmospheric processes and behavior.

Common temperature-measuring techniques above the troposphere involve radiosonde balloons, grenade probes, rockets, satellites and different methods of optical, i.r. and radar remote sensing.

Temperatures in the polar mesosphere and lower thermosphere, i.e. 60–110 km, are only crudely known from sporadic measurements and only a single, all-seasons 80°N model for the altitude range 25–80 km is given in CIRA 1972. Variations assumed to be caused by phenomena such as tides, winds, gravity waves, etc. are not included.

Recently, satellite probes such as those on board the Nimbus and TIROS-N/NOAA series (Sissala, 1975; Rodgers, 1977; Schwalb, 1978; Drummond *et al.*, 1980) have provided temperature measurements of the stratosphere and mesosphere up to the 60–70 km region. Emissions from the 15 μm bands of atmospheric CO_2 are used to deduce these temperature profiles (Rodgers, 1976; Gille *et al.*, 1980). Above 80 km CO_2 is not in local thermodynamic equilibrium and thus temperatures obtained by radiance inversion from channels including this height could be largely in error (Drummond *et al.*, 1980). Above 60 km, vertical resolution is in the range 15–30 km (Rodgers, 1977; Barnett, 1980) leaving 60 km as the approximate upper height for usable temperature determination.

While rocket and gun-probe measurements give a single profile in time and space, satellites may cover the entire globe within a 24-h period (Sissala, 1975). Satellites are therefore superb for measuring the large scale spatial and temporal variations of temperature caused by the main global transport and heating processes.

Nevertheless, for continuous measurements of the dynamical behavior of temperature in local time (caused by gravity waves, tides, winds, etc.), ground-based remote-sensing techniques are the only tool. In the mesopause region (i.e. 80–95 km altitude) one ground-based technique is to extract temperatures from the measured intensity distribution among the rotational lines of particular vibration band of the hydroxyl nightglow emission (Kvifte, 1959).

Mesopause region temperatures have been obtained this way since Meinel (1950) identified the OH band system in the night airglow. Numerous investigators have reported temperatures, their different variations and connection to other atmospheric parameters and processes (Kvifte, 1960; Wallace, 1961; Noxon, 1964; Shefov, 1969; Visconti *et al.*, 1971; Sivjee *et al.*, 1972; Wiens and Weill, 1973; Takahashi *et al.*, 1974, 1977, 1981; Takeuchi *et al.*, 1979).

Due both to environmental problems and problems with auroral contamination (Meriwether, 1975) a sparse amount of OH-derived temperatures exist for high latitudes and only a few occasional measurements

*On leave from Norwegian Defense Research Establishment, N-2007, Kjeller, Norway.

are reported for latitudes greater than 70° (Myrabø *et al.*, 1983). This is also true of other ground based techniques. As a result, the effects of gravity waves, tides and winds in the polar mesosphere and mesopause region are not yet experimentally investigated.

The purpose of this paper is to report and discuss results from recent measured OH rotational temperatures at 78°N.

2. OBSERVATIONS AND DATA REDUCTION

The OH emission data employed in this work were part of measurements undertaken during the 1980/81 and 1982/83 campaigns of the Multi-National Svalbard Auroral Expedition (Deehr *et al.*, 1980) close to Longyearbyen on West Spitsbergen (78.4°N, Lat., 15°E, Long. geographic).

OH emissions are normally predominant in the near-i.r. part of the night sky spectra. Contamination by auroral molecular emission in the auroral zone (Vallance-Jones, 1974; Meriwether, 1975) is normally insignificant at Spitsbergen because auroras are generally at a high altitude and emit mainly atomic lines (Sivjee and Deehr, 1980). Thus, a normal, high-responsivity auroral spectrophotometer operated at a resolution around 4 Å or less may be used to measure most of the OH bands and lines clearly resolved from auroral emissions.

At the Longyearbyen Observatory, a 1 m and a 1/2 m high-throughput Ebert-Fastie spectrophotometer are coupled to a mini-computer recording in the photon-counting mode. The 1 m instrument, used for the measurements reported here, is further described by Dick *et al.* (1970) and Sivjee *et al.* (1972).

The spectrophotometer was normally operated for 24 h a day from December 1982 to January 1983. (During 1980/81 other spectral regions were scanned and 24-h operation was not routinely performed.) Spectra were rejected when Fraunhofer absorption lines appeared during the twilight period (i.e. 3–6 h during mid-day in the last half of January 1983) and during full moon with overcast weather. Operation ceased only during snow or storm. The sensitivity of the instrument allowed temperatures on an hourly basis to be extracted even during overcast sky conditions.

The spectrophotometer was pointed towards the zenith and the 7280–7410 Å region was scanned in 8 or 32 s using the spectrophotometer in the second order with a 1 mm slit corresponding to a bandwidth of 1.5 Å. Each scan was recorded on magnetic tape. Individual rotational temperatures were calculated from 1- and 3-h integrated scans, by employing Kvifte's method using the intensity ratio of the $P_1(2)$, $P_1(3)$, $P_1(4)$ and $P_1(5)$ lines (Kvifte, 1959).

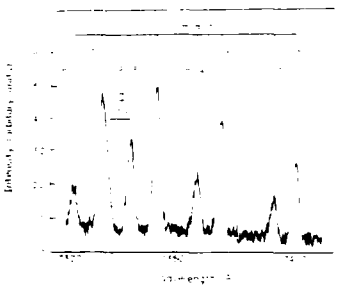

FIG. 1. AN EXAMPLE OF THE SPECTRA USED FOR DEDUCING TEMPERATURE.
Each spectrum is acquired during a 60 min (or 180 min) period summing 450 (1350) scans. In addition to the OH (8-3) P branch lines, the forbidden oxygen doublet at 7320/30 Å originating in the aurora is indicated.

The quality of the spectra used for temperature deduction may be seen in Fig. 1. Probable error in a single calculated temperature is estimated to be ±3 K caused by the uncertainty of defining the background levels.

Daily mean temperatures are based on 24-h averages of the 1- and 3-h temperatures. For diurnal variation only 1-h integration was used.

The auroral activity was monitored by the intensity of the 7320/30 Å OII lines. Additional care was taken to assure that there was no contamination from N_2 1P and other auroral molecular emissions.

3. RESULTS AND DISCUSSION

3.1. *Day-to-day variability and December–January pattern*

Temperatures for each day from 5 December to 30 January 1983 as derived from the hourly (3-h) means are plotted in Fig. 2. The daily means are indicated by filled circles and straight lines are drawn between each mean. Dashed lines indicate that the temperature for one or more days is missing. Heavier lines indicate the daily mean temperatures obtained from OH emissions during the 1980/81 campaign.

Some of the 1980/81 measurements did not cover a whole 24-h period. Missing temperatures were added where possible by interpolation before daily means were calculated. Due to a different observing program during 1980/81, a number of OH bands other than the 8-3 band were utilized to obtain the temperatures shown.

The most obvious feature in Fig. 2 is the large, week-long cold period around January 1, followed by a

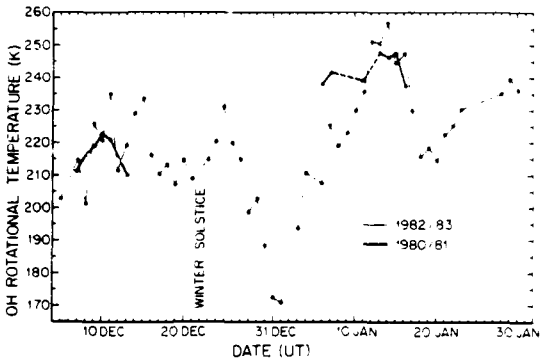

FIG. 2. MEAN DAILY TEMPERATURES FOR DECEMBER AND JANUARY.

warming to a peak in the daily mean temperature of 257 K in mid-January. The similarity between the 1980/81 and 1982/83 temperatures is also striking, i.e. a tendency to a higher mean temperature in mid-January compared to early and mid-December.

The 2–6 day warming periods previous to the cold period may be explained by heat deposition from gravity waves dissipating in the upper mesosphere, mesopause region (Hines, 1965). The energy available by dissipating gravity waves seems to be able to provide a heating rate of at least 10 K day^{-1} at 90 km (Hines, 1965; Clark and Morone, 1981) which is sufficient to explain the warming periods in Fig. 2. Since gravity wave activity is believed to be associated with tropospheric weather systems such as fronts, cyclones, jet streams, etc. (Clark and Morone, 1981; Krassovsky and Shagaev, 1977) the duration of the heating is likely to be of the order of days. This fits the observed data. It may also be noted that from the spectrum of atmospheric winds velocity fluctuations at 86 km altitude, as measured from Poker Flat, Alaska (65°N gg Lat., 147°W gg Long., Balsley and Carter, 1982), a significant peak in the power density spectrum appears at a period around 3–4 days. Time-averaged OH rotational temperature and mesospheric temperatures generally, are closely associated with wind fluctuations (Krassovsky and Shefov, 1980).

It seems less likely that gravity waves originating in connection with heating caused by ion drag or Joule heating during magnetospheric substorms contain enough energy to heat the mesopause region tens of degrees for a period of several days. For example, during the substorm of 15 February 1978 approx. 10^{22} erg was released into the ionosphere during 6–7 h (Shashun 'Kina and Yudovich, 1980). According to Brekke (1977) even if a significant part (i.e. 20%) of this energy is deposited at 80–90 km level, it could not increase the temperature by more than some tenths of a degree. This does not rule out the possibility that gravity waves originating in the ionosphere in connection with geomagnetic storms could cause significant oscillations of the mean temperature in the mesopause region. We find, however, no clear connection between these 3–7 day warming periods and geomagnetic activity or substorms.

The 1 week cold period ($\leqslant$200 K) observed at year's end and the continuous warming from 172 to 257 K (i.e. 85 K) in the daily mean temperature seemed too large to be connected with gravity waves. Its long duration could suggest that it was connected to large scale transport of cold air from low or mid-latitudes. Another means of producing such a large change in temperature is in connection with a "stratospheric warming" or "stratwarm" (Labitzke, 1980). Initial

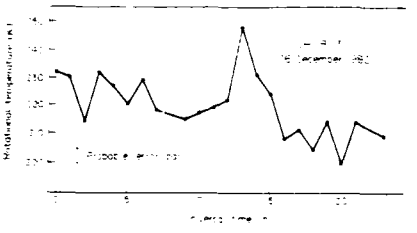

FIG. 3. HOURLY MEAN TEMPERATURES FOR 24-h PERIOD AT LONGYEARBYEN, 78°N.

warming of the polar stratosphere is expected to produce a cooling effect at the mesopause (Labitzke, 1977; Schoeberl, 1978). A stratospheric warming is seen on the 10 mbar level charts around 31 December (Najoukat *et al.*, 1983). Thus, the direct connection between these two phenomena seen here (i.e. a drop in the observed temperature of the mesopause around the stratwarm) confirms the theory (Labitzke, 1977).

As one would expect, the large-scale temperature trend is clearly visible in the data from individual 24-h periods, i.e. there is normally a longer-term trend taking place with shorter fluctuations superimposed (less than 1 day). Figure 3 illustrates this by showing a slice of the downward trend in the cold period late in December 1982. Figure 3 contains a typical, moderate fluctuation pattern, but there are also observations of very large and violent fluctuations in temperature with amplitudes in excess of ± 70 K (Myrabø *et al.*, 1983).

3.2. *The height of the* OH *emissions layer, the mesopause level and the temperature gradient*

Laboratory measurements by Charters *et al.* (1971) showed that at pressures comparable to those at 80–100 km height, an increase in the pressure leads to an increase in the OH excitation rate in inverse proportion to the number of the vibrational state. A result of this would be that emissions from lower vibrational levels of the OH molecule would correspond to a slightly lower altitude range in the atmosphere.

This interpretation was suggested by Gattinger (1971) and employed by Wiens (1974) to interpret regular changes of the OH (8–3)/(5–1) band intensity ratio during the night at Adi Ugri.

Figure 4 shows the temperatures from the different bands before averaging and interpolation. Some of the scatter may be explained by the different bands not covering the same time interval. This was the case for most of the January measurements. When different bands were acquired simultaneously, the differences in temperature between the bands were, in most cases, within the measuring uncertainty (i.e. 4 K).

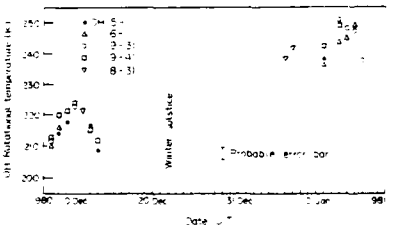

FIG. 4. TEMPERATURES AS DERIVED FROM THE DIFFERENT OH BANDS FOR THE 1980–1981 MEASUREMENTS. Symbols indicate the different bands.

Taking all the 1980/81 measurements for December together, there is a small tendency for the temperatures obtained from OH (9–4) and OH (9–3) bands to be slightly higher than those from the OH (5–1) and OH (6–2) bands (see Fig. 4). The mean temperature difference between the (9–4) and the (5–1) band temperatures is found to be 3 K which is statistically significant.

Rodgers *et al.* (1973) reported from their rocket observation at Poker Flat (65°N gg Lat.) that the emission height profile of the lower vibrational bands of OH is displaced to lower altitudes. They suggested chemical quenching by atomic oxygen to be responsible for the observed effect together with an additional excitation process. Simultaneous observations of OH (9, 4), (8, 3), (7, 2), (6, 2) and (5, 1) band intensities by Takahashi and Batista (1981) may also be interpreted as support for the hypothesis that quenching is responsible for the observed altitude distribution.

Rodgers' measurements were performed at high latitude (65°N gg Lat.) during March while Frederick *et al.* (1978) used data from satellite measurements in May–June and for low latitudes. Use of these two independent measurements covering different latitudes and seasons to deduce height difference between the OH band emissions as done by Takahashi and Batista (1981) is open to question.

Taking the height of the peak $v = 9$ level emission from Frederick *et al.* (1978) and the $v = 5$ level from Rodgers *et al.* (1973) results in a height difference of approx. 1 km. This implies a temperature gradient of 3 K km^{-1}.

From winter observations at Zvenigorod (55°N) during gravity wave propagation in the mesosphere, Krassovsky and Shagaev (1977) report a significantly larger temperature disturbance in temperatures deduced from the $v = 9$ level then from the $v = 4$ level. Average temperature differences between the two levels were found to be 12 K ranging from 3 to 26 K. On another occasion, Krassovsky *et al.* (1977) report temperature differences between the $v = 9$ and $v = 5$ level temperatures of 3–14 K with a mean close to 6 K. If this is to be interpreted as corresponding to temperatures at the respective emission heights of the different bands, the peak altitude difference as deduced from Rodgers *et al.* (1973) and Frederick *et al.* (1978) (i.e. 1 km) seems too small.

Using the temperature slope deduced from U.S. Standard Atmosphere, Supplement 1966 for 60°N, winter, for the 89–98 km level just above the mesopause (i.e. 1.8 K km^{-1}) and the temperatures derived by Krassovsky *et al.*, a mean height difference of at least

3 km would be expected between the (9–3) and (5–1) bands. Observations during gravity wave propagation conditions reported by Krassovsky and Shagaev (1977) and Shagaev (1980) give an average height difference of 4 km. Applied to our results this establishes a positive temperature slope in the range 0.8–1 K km^{-1}.

From the results by Krassovsky and Shagaev (1977), Krassovsky *et al.*, (1977) and our result presented here, it is seen that the OH emission is situated in an altitude range with a positive temperature slope. This may be interpreted to mean that the mesopause is at approx. 80 km with the OH emissions originating in the 80–85 km region. This interpretation is in agreement with the rocket observation of Rodgers *et a* . (1973) at 65°N in March.

However, the very large amplitude temperature and intensity disturbances at 78°N (probably due to the passage of gravity waves) reported here and by Myrabø *et al.* (1983) indicate a higher altitude layer. Results reported by Shagaev (1980) from Zvenigorood (55°N) also indicate a mesopause above 85 km in winter. A temperature slope of 1.8 K km^{-1} was reported.

The polar winter vortex, which has a peak westerly flow at about 50–60 km altitude (Rodgers, 1977), forces the stratopause and mesopause at extreme high latitudes in winter to be situated at higher altitudes than elsewhere. A mesopause at about 80 km in early winter at 78°N is therefore unlikely, and a more reasonable interpretation is that the mesopause is situated approx. at 90 km and the OH emissions—at least for high and extremely high latitudes in winter—peak at or just above 90 km.

From the temperature slope deduced here (i.e. 0.8–1 K km^{-1}) it seems reasonable to point out that the extreme high latitude winter atmosphere does not seem to have a very pronounced mesopause.

3.3. *Diurnal, semidiurnal and short time variations*

Data from 19 days around winter solstice from 9 December to 27 December 1982 were selected to be examined for regular variations with periods less than or equal to 24 h, originating from the solar tide (i.e. periods of the type 24/m, m being an integer 1, 2, 3, ...). Hourly mean temperatures for each of the days were superimposed resulting in hourly means for the period. The hourly means are plotted in Fig. 5 and a semidiurnal trend is clearly visible.

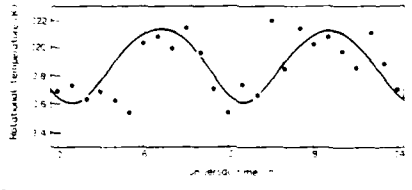

FIG. 5. HOURLY MEAN TEMPERATURES AVERAGED OVER A 19-day PERIOD AROUND WINTER SOLSTICE FROM 9 DECEMBER TO 27 DECEMBER 1982.
Semidiurnal trend is indicated.

A semidiurnal tide curve has been fitted to the data following the method of Petitdidier and Teitelbaum (1977):

$$(\partial T/T) = A \cos[(2\pi/\Lambda)(Z - Z_0) + (2\pi/P)(t - t_T)],$$

where Λ is the vertical wavelength, P is the period, Z_0 is the altitude of OH (8–3) nightglow intensity maximum, t_T is the time of maximum temperature T at Z_0 altitude and A is the amplitude of the relative variation in the temperature. The best fit gives an amplitude of 5 K and the time of maximum temperature at 01 U.T. or local Longyearbyen time 02:00.

Semidiurnal variations in the OH intensity and deduced temperature are reported by a number of authors (Takeuchi *et al.*, 1979; Takahashi *et al.*, 1974, 1977; Petitdidier and Teitelbaum, 1977) but there seem to be no reports based on OH measurements indicating a diurnal (i.e. 24-h) temperature trend.

Spizzichino (1969) and Teitelbaum and Blamont (1975) argue that non-linear interaction with gravity waves is more important for the first diurnal mode than for the semidiurnal. Thus, the effect of averaging over several days (to obtain an adequate signal-to-noise ratio) is to cancel the diurnal mode since it would be far less stable than the semidiurnal mode.

Continuous observations at lower latitudes normally last less than 10 h, which emphasizes a semidiurnal tide over a diurnal one. This selective effect may therefore be present in previous data. The data here are not so limited. A Fourier analysis of periods failed to retrieve any diurnal tide component. If it does occur, the amplitude is less than 1 K.

According to Forbes (1982), model calculations show the diurnal tide to be dominant over the semidiurnal at high latitudes, while according to Beer (1975), the semidiurnal tide dominates over the diurnal at high latitudes. Zonal wind speed data reported by Spizzichino (1970) favor Beer (1975) and the results reported here. Possible dominance of the diurnal tide at high latitudes on a shorter time scale (i.e. a few days) is, however, not ruled out by this result.

Krassovsky and Shefov (1980) have showed that a linear relationship between measured OH temperatures and wind data in the radio meteor region exists. To a first approximation the relation

$$\Delta T/T \sim \pm(\gamma - 1)^{0.5} v/c$$

is found to satisfy the temperature–wind velocity relationship, where T is the temperature, ΔT the temperature increment, i the imaginary unit (i.e. $\sqrt{-1}$) representing the phase shift, γ the ratio of specific heats, v the wind speed and c is the speed of sound. This relation is also theoretically justified for long period waves (Hines, 1965). Applying this relation to our semidiurnal tide result, and taking the speed of sound, c, to be 258 m s^{-1} (USSA, Supplement 1966), $\gamma = 1.4$, $T = 218$ K and $\Delta T = 5$ K, results in a mean semidiurnal wind speed of 9 m s^{-1} which seems to be of the right order of magnitude (Groves, 1980).

4. SUMMARY

Ground-based observations of atmospheric OH emission temperature and intensity have been carried out at 78°N during December and January 1980/81 and 1982/83 (Fig. 2). 3–6 day warm periods were observed both years in December. In 1982/83 this warm period was followed by 1 week of consistently lower temperatures (down to 172 K). Common to both seasons is a higher mean temperature level reached later in January after the cold periods. This is consistent with Quiroz's (1969) idea of a higher mesospheric temperature in January than in early winter, i.e. November and December.

We find evidence of a stratospheric warming (Najoukat *et al.*, 1983) near the cold period which explains the cold mesosphere (Labitzke, 1977).

We suggest that the warm periods of the order of days are due to heat dissipated from gravity waves originating in the troposphere.

The overall average temperature for the data from the 1980/81 and 1982/83 seasons is found to be 220 K. Assuming that the OH emission at high latitudes in winter peaks at or just above the 90 km level, this temperature is slightly higher than the 80°N model from CIRA 1972 at 80 km.

The difference in the mean temperature obtained from OH (9–3) and (5–1) bands, assuming a height difference of 3–4 km (Shagaev, 1980) is used to deduce a mean temperature slope of 1 K km^{-1}. The data further indicate that OH emissions originate at or just above the polar mesopause (i.e. 88–94 km). The size of the gradient (i.e. 1 K km^{-1}) compared to similar gradients obtained at lower latitudes (i.e. ~1.8 K km^{-1} at 55°N, Shefov, 1980; 1.84 K km^{-1} at 60°N (winter), U.S. Standard Atmosphere, Supplement 1966) implies that the polar mesopause in winter is less pronounced.

Superimposed hourly means for a 19-day period around winter solstice reveal a clear semidiurnal trend with an amplitude of 5 K (Fig. 5). This is connected to the solar semidiurnal tide. No effect of solar diurnal tide is apparent. Wind speeds deduced from the observed OH tide temperature component show a mean semidiurnal wind of approx. 9 m s^{-1}.

Acknowledgements—Financial support for this research was provided by National Science Foundation through grants ATM80-12719, ATM82-00114 and ATM82-14642 to the Geophysical Institute of the University of Alaska and from the Royal Norwegian Council for Scientific and Industrial Research through a fellowship grant.

REFERENCES

Baisley, B. B. and Carter D. A. (1982) The spectrum of atmospheric velocity fluctuations at 8 km and 86 km. *Geophys. Res. Lett.* **9**, 465.

Barnett, J. J. (1980) Satellite measurements of middle atmosphere temperature structure. *Phil. Trans. R. Soc. Lond. A* **296**, 41.

Beer, T. (1975) *Atmospheric Waves*. A. Hilger, London.

Brekke, A. (1977) Auroral effects on neutral dynamics, in *Dynamical and Chemical Coupling Between the Neutral and Ionized Atmosphere* (Edited by Grandal, B., and Holtet, J. A.), p. 313. D. Reidel, Dordrecht.

Charters, P. E., Macdonald, R. G. and Polanyi, J. C. (1971) *Appl. Opt.* **10**, 1747.

CIRA (1982) *COSPAR Working Group 4, COSPAR International Reference Atmosphere*. Pergamon Press, Oxford.

Clark, J. H. and Morone, L. T. (1981) Mesospheric heating due to convectively excited gravity waves—a case study. *Mon. Weath. Rev.* **109**, 990.

Deehr, C. S., Sivjee, G. G., Egeland, A., Henriksen, K., Sandholt, P. E., Smith, R., Sweeney, P., Duncan, C. and Gilmer, F. (1980) Ground-based observations of *F*-region associated with the magnetospheric cusp. *J. geophys. Res.* **85**, 2185.

Dick, K. A., Sivjee, G. G. and Crosswhite, H. M. (1970) Aircraft airglow intensity measurements: variations in OH and OI (5577). *Planet. Space Sci.* **18**, 887.

Drummond, F. R., Houghton F. T., Peskett, G. D., Rodgers, C. D., Wale, M. F., Whitney, F. and Williamson, E. J. (1980). The stratospheric and mesospheric sounder on Nimbus 7. *Phil. Trans. R. Soc. Lond. A* **296**, 219.

Forbes, F. M. (1982) Atmospheric tides: the solar and lunar semidiurnal components. *J. geophys. Res.* **87**, 5241.

Frederick, F. E., Rusch, D. W. and Liu S. C. (1978) Nightglow emission of OH ($X^2\pi$): comparison of theory and measurements in the (9–3) band. *J. geophys. Res.* **83**, 2441.

Gattinger, R. L. (1971) Interpretation of airglow in terms of excitation mechanism. in *The Radiating Atmosphere*. (Edited by McCormac, B. M.), p. 51. D. Reidel, Dordrecht.

Gille, F. C., Baily, P. L. and Russell, F. M., III (1980) Temperature and composition measurements from the l.r.i.r. and l.i.m.s. experiments on Nimbus 6 and 7. *Phil. Trans. R. Soc. Lond. A* **296**, 205.

Groves, G. V. (1980) Seasonal and diurnal variations of middle atmospheric winds. *Phil. Trans. R. Soc. Lond. A* **296**, 19.

Hines, C. O. (1965) Dynamical heating of the upper atmosphere. *J. geophys. Res.* **70**, 177.

Krassovsky, V. I. and Shagaev, M. V. (1977) On the nature of hydroxyl airglow. *Planet Space Sci.* **25**, 509.

Krassovsky, V. I. and Shefov, N. N. (1980) Relation between

temperature and circulation in the mesopause region. *Geom. Aeron.* **20**, 531.
Krassovsky, V. I., Potapov, B. P., Semenov, A. I., Sobolev, V. G., Shagaev, M. V. and Shefov, N. N. (1977) On the equilibrium nature of hydroxyl airglow. *Planet. Space Sci.* **25**, 596.
Kvifte, G. (1959) Nightglow observation at Ås during the I.G.Y. Geophysica Norvegica. *Geophys. Publs* **20**, 1.
Kvifte, G. (1960) Temperature measurements from OH bands. *Planet. Space. Sci.* **5**, 153.
Labitzke, K. (1977) Stratospheric–mesospheric midwinter warmings. in *Dynamical and Chemical Coupling between the Neutral and Ionized Atmosphere* (Edited by Grandal, B. and Holtet J. A.), p. 17. D. Reidel, Dordrecht.
Labitzke, K. (1980) Climatology of the stratosphere and mesosphere. *Phil. Trans. R. Soc. Lond.* **A296**, 7.
Meinel, A. B. (1950) OH emission bands in the spectrum of the night sky. *Ap. J.* **111**, 555.
Meriwether, J. W. (1975) High latitude airglow observations of correlated short term fluctuations in the hydroxyl Meinel 8–3 band intensity and rotational temperature. *Planet. Space Sci.* **23**, 1211.
Myrabø, H. K., Deehr, C. S. and Sivjee, G. G. (1983) Large amplitude nightglow OH (8–3) band intensity and rotational temperature variation during a 24-hour period at 78°N. *J. geophys. Res.* (in press).
Noxon, J. F. (1964) The latitude dependence of OH rotational temperature in the night airglow. *J. geophys. Res.* **69**, 4087.
Petitdidier, M. and Teitelbaum, H. (1977) Lower thermosphere emissions and tides. *Planet. Space Sci.* **25**, 711.
Quiroz, R. S. (1969) The warming of the upper stratosphere in February 1966 and the associated structure of the Mesopause. *Mon. Weath. Rev.* **97**, 541.
Rodgers, C. D. (1976) *Rev. Geophys. Space Physics* **14**, 609.
Rodgers, C. D. (1977) Morphology of upper atmosphere temperatures, in *Dynamical and Chemical Coupling between the Neutral and Ionized Atmosphere* (Edited by Grandal, B. and Holtet, J. A.), p. 3. D. Reidel, Dordrecht.
Rodgers, J. W., Murphy, R. E., Stair, Jr., A. T., Ulwick, J. C., Baker, K. D. and Jensen, L. L. (1973) Rocket-borne radiometric measurements of OH in the auroral zone. *J. geophys. Res.* **78**, 7023.
Schoeberl, M. R. (1978) Stratospheric warmings: observations and theory. *Rev. Geophys. Space Phys.* **16**, 521.
Schwalb, A. (1978) The TIROS-N/NOAA A–G satellite Series. *NOAA Tech. Mem. NESS 95*.
Shagaev, M. V. (1980) Vertical temperature gradients and dissipation of internal gravity waves near the mesopause. *Geom. Aeron.* **20**, 529.
Shashun'Kina, V. M. and Yudovich L. A. (1980) Effects of internal gravity waves during the magnetospheric substorm of February 15, 1978. *Geom. Aeron.* **20**, 516.
Shefov, N. N. (1969) Hydroxyl emission of the upper atmosphere. I. The behavior during solar cycle, seasons and geomagnetic disturbances. *Planet. Space Sci.* **17**, 797.
Sissala, J. F. (1975) *The Nimbus 6 Users Guide* Goddard Space Flight Center, Greenbelt, MD.
Sivjee, G. G. and Deehr, C. S. (1980) Differences in polar atmospheric optical emissions between mid-day cusp and night-time auroras. in *Exploration of the Polar Upper Atmosphere* (Edited by Deehr, C. S. and Holtet, J. A.), p. 199. D. Reidel, Dordrecht.
Sivjee, G. G., Dick, K. A. and Feldman, P. D. (1972) Temporal variation in the night time hydroxyl rotational temperature. *Planet. Space Sci.* **20**, 261.
Spizzichino, A. (1969) Étude des interactions entre les différentes composantes du vent dans la haut atmosphère. *Ann. Geophys.* **25**, 93.
Spizzichino, A. (1970) Étude des interactions entre les différentes composantes du vent dans la haut atmosphère. *Ann. Geophys.* **2**, 9.
Takahashi, H. and Batista, P. P. (1981) Simultaneous measurements of OH (9, 4), (8, 3), (7, 2), (6, 2) and (5, 1) bands in the airglow. *J. geophys. Res.* **86**, 5632.
Takahashi, H., Clemesha, B. R. and Sahai, Y. (1974) Nightglow OH (8–3) band intensities and rotational temperatures at 23°S. *Planet. Space Sci.* **22**, 1323.
Takahashi, H., Sahai, Y., Clemesha, B. R., Batista, P. B. and Teixeira, N. R. (1977) Diurnal and seasonal variations of the OH (8–3) airglow band and its correlation with OI 5577 Å. *Planet. Space Sci.* **25**, 541.
Takeuchi, I., Misawa, K., Kato, Y. and Aoyama, I. (1979) Rotational temperatures and intensities of OH (6–2) and OH (8–3) bands in the nightglow. *J. atmos. terr. Phys.* **41**, 387.
Teitelbaum, H. and Blamont, J. E. (1975) Some consequences of non-linear effects on tides and gravity waves. *J. atmos. terr. Phys.* **37**, 697.
Vallance-Jones, A. (1974) *Aurora*. D. Reidel, Dordrecht.
Visconti, G., Congeduti, F. and Fiocco, G. (1971) Fluctuation in the intensity and excitation temperature in the OH airglow (8–3) band. in *The Radiating Atmosphere* (Edited by McCormac, B. M.), p. 82. D. Reidel, Dordrecht.
Wallace, L. (1961) Seasonal variation and interpretation of the OH rotational temperature in the airglow. *J. atmos. terr. Phys.* **20**, 85.
Wiens, R. H. (1974) Diurnal variation of the (8–3)/(5–0) intensity ratio of nightglow OH at Adi U'gri. *Planet. Space Sci.* **22**, 1059.
Wiens, R. H. and Weill, G. (1973) Diurnal, annual and solar cycle variations of hydroxyl and sodium nightglow intensities in the Europe–Africa sector. *Planet. Space Sci.* **21**, 1011.

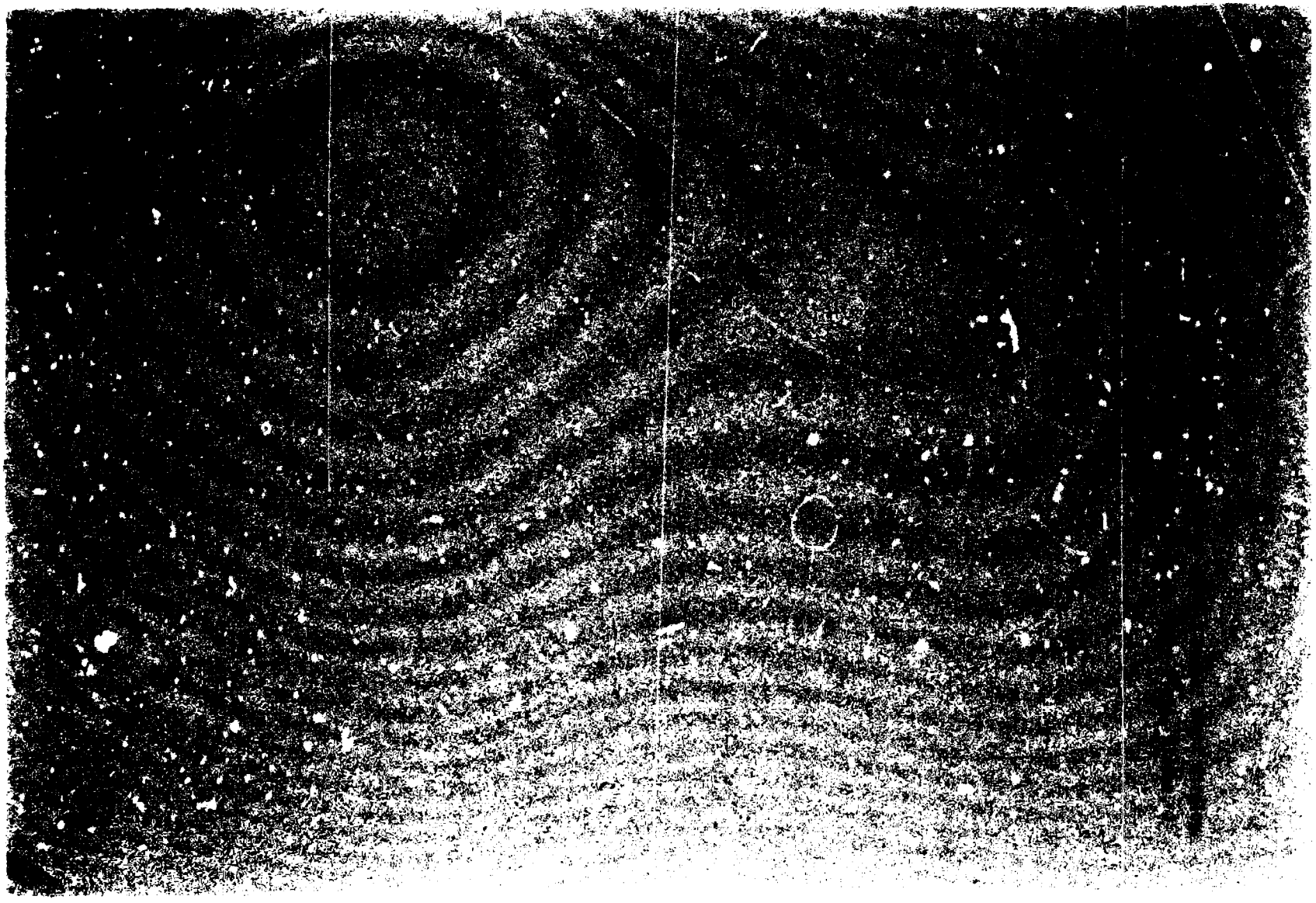

JOURNAL OF GEOPHYSICAL RESEARCH, VOL. 89, NO. A10, PAGES 9153-9156, OCTOBER 1, 1984

NIGHT AIRGLOW OH (8-3) BAND ROTATIONAL TEMPERATURES AT POKER FLAT, ALASKA

H. K. Myrabø[1], G. J. Romick, G. G. Sivjee[2] and C. S. Deehr

Geophysical Institute, University of Alaska, Fairbanks

Abstract. Temperatures of the mesopause region (85-90 km) have been deduced from OH (8-3) molecular band night airglow emission measurements made at Poker Flat (65°N), Alaska. The data cover the first 4 months of each of the years 1976, 1977, and 1978. Mean monthly temperatures of 229, 224, 213 and 193 K were obtained with no significant yearly differences. The mean temperature for each month is about 15 K higher than the respective monthly temperatures in the 85 and 90 km, 60° and 70°N, CIRA (1972) model, and it follows the general decreasing trend shown by the model.

Introduction

Temperatures of the upper atmosphere at the mesopause level (i.e., 80-90 km) are important for studying both the dynamics and the overall circulation pattern of the mesophere and in conjunction with other data can be used to study the interaction between the mesosphere and the thermosphere and stratosphere. Temperature also plays an important part in the local chemistry.

Rocket-borne probes and ground-based remote sensing of the night airglow OH rotational line intensity distribution have been the main methods used to obtain the 80-90 km altitude temperature [Kvifte, 1967; Shefov, 1971; Sivjee et al., 1972; Lenschow and Petzoldt, 1980; Myrabø, 1984].

High-latitude (i.e., above approximately 60°) mesopause region temperatures are very sparse compared to those at lower latitudes. Early spectral measurements yielding OH rotation temperatures at high latitudes were those of Chamberlain and Oliver [1953]; Mironov et al. [1958]; McPherson and Vallance-Jones [1960] and Krassovsky et al. [1962]. However, most of those spectral measurements were of poor quality for accurate temperature estimates and some are even known to be in error [Kvifte, 1961, 1967; Wallace, 1960]. Later and probably more reliable (ground based) spectral data from which OH temperatures were obtained were reported by Kvifte [1967] and Shefov [1969]. Similar data from airborne observations were described by Noxon [1964] and Sivjee et al. [1972]. In situ temperature measurements from rocketsondes were made from Fort Greely (64°N) and Heiss Island (81°N) (CIRA, 1972).

The most recent observations are the OH temperatures reported from Longyearbyen, Spitsbergen (78.4°N) [Myrabø, 1984; Myrabø and Deehr, 1984; Myrabø et al.,1983] and the rocketsonde temperature observations from Heiss Island as part of the Middle Atmosphere Program (MAP) [Naujokat, et al., 1983]. The observations reported in this paper were obtained from Poker Flat, Alaska (65.11°N, 147.46°W, geographic coordinates) during the first 4 months in the years 1976, 1977, and 1978 using a high-throughput Ebert-Fastie spectrometer to resolve the rotational structure of the OH (8-3) vibrational band.

Observations and Data Reduction

A 1-m high-throughput Ebert-Fastie spectrophotometer coupled to a minicomputer was used to obtain the night sky spectra. The instrumentation has been described more fully in the papers by Sivjee et al. [1972] and Romick [1976]. For the measurements reported here, the instrument was normally pointing toward the zenith, operating over the spectral region 7220 to 7450 Å, which covers the OH (8-3) band. The scan time over the band was either 8, 16, or 32, using a slit width of 1 mm, corresponding to a spectral resolution around 2 Å. In the auroral region, aurorally enhanced atomic and molecular emissions can overlap the near-infrared night airglow emissions, making it almost impossible to obtain reliable OH rotational temperatures for long periods of time [Vallance-Jones, 1974; Meriwether, 1975; Myrabø, 1984].

To avoid contamination by auroral emissions, we have used relatively high spectral resolution and have selected magnetically quiet periods mostly during the evening, when the oval is well north of the observing station. Each of the OH spectra have in addition been carefully inspected for any possible auroral contribution. The presence of aurora could easily be detected, as this spectral region contains both the strong $N_2$1P (5,3) and (6,4) bands as well as the OII (^2D-^2P) lines. Spectra showing any sign of these auroral emissions have been rejected from the analysis.

From the selected data set, 30-minute and 60-minute integration periods were used to obtain the individual OH rotational temperatures. The OH $P_1(2)$, $P_1(3)$, $P_1(4)$, $P_1(5)$, and $P_1(6)$ lines and the method of Kvifte [1959] were used to calculate the temperature. The rotational term values used in the plot of $\ln (I/sv^4)$ against $F(J)$ hc/K were calculated using the data taken from Dieke and Crosswhite [1948], Kvifte [1959], Herman and Hornbeck [1953], Bass and Garvin [1962], Chamberlain and Roesler [1955], and Rosen [1970]. The term values for $v = 8$ are almost identical to those listed by Coxon and Foster [1982].

It has been suggested that the temperatures quoted here should be recalculated using the transition probabilities by Mies [1974] [c.f. Meriwether, 1975]. Use of Mies's values lowers the calculated values by approximately 4%, bringing them closer to the CIRA (1972) model. There is disagreement, however, as to the fit of Mies's calculations to the experimental data [cf.

[1]On leave from Norwegian Defense Research Establishment, N-2007, Kjeller, Norway.

[2]On leave at Atmospheric Science Section, National Science Foundation, Washington, D.C.

Paper number 4A0766.
0148-0227/84/004A-0766$02.00

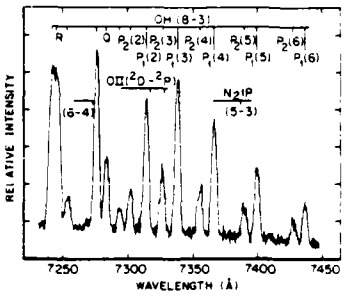

Fig. 1. Example of a spectrum used to deduce the OH rotational temperatures. The spectrum is obtained by summing 112 16-s individual scans over 30 min. In addition to the OH (8-3) lines, the locations of the $N_2$1P band and OII lines originating in the aurora are indicated. The lack of any broadening at the base of the $P_1(2)$ and $P_2(3)$ lines indicates the absence of any auroral emission.

Werner et al., 1983]. It is questionable, however, if the corrections to the lambda-doubling parameters would have any effect on the derived temperatures, especially at the higher vibrational quantum numbers in use here. We have therefore elected to retain the present, traditional method of temperature calculation until we have investigated more thoroughly a comparison between the methods.

An example (Figure 1) of a spectrum obtained using a 30-minute integration time illustrates the lack of auroral features and the typical signal-to-noise ratio for the individual OH lines used to calculate the temperature. The similar shape at the base of the $P_1(2)$ and $P_2(3)$ lines compared to the $P_1(3)$, $P_1(4)$, and $P_1(5)$ lines clearly shows the lack of any auroral contribution. In addition to the OH lines, the wavelengths of the main auroral features are indicated.

The typical uncertainty in each calculated temperature (as given by the standard deviation of the regression line [see Kvifte, 1959] is estimated to be ±5 K. From the individual temperatures, daily means are calculated. Each daily mean covers a minimum observing period of 2 hours, with the average being 4 1/2 hours.

Results and Discussion

Daily mean temperatures deduced as previously described for the years 1976, 1977, and 1978 are plotted in Figure 2. The temperature values for each year are marked with different symbols. A best fit second degree polynomial curve (dashed curve) is drawn through the combined set of individual daily means. The CIRA (1972) temperatures for 60°N at both the 85- and 90-km heights are also plotted in Figure 2 for the appropriate time of the year.

The 3-year means for January, February, March, and April are 229, 224, 213, and 193 K, respectively. The January through April mean is 219 K. In review, the data in Figure 2 show no clear tendency for a yearly trend, thus implying that if there is a solar cycle/ geomagnetic activity effect on the mesopause temperature, it probably has to be of the order of 5 K or less for the particular period represented here (i.e., 1976 through 1978). It should, however, be stressed that the amount of data is too sparse to rule out the possibility of such an effect.

It is obvious from Figure 2 that the measured OH rotational temperatures are higher than the appropriate CIRA (1972) model temperature. The average difference between the 60°N, 90-km height model temperature and the measured mean (dashed curve) is about 15 K during any part of the time period covered. The difference between the CIRA (1972) 60°N and 70°N temperatures for the particular height interval, i.e., 85-90 km, and time of the year is only 1-3 K,and therefore the latitudinal change would little impact on these results. As the lifetime of excited OH molecules is long enough to permit thermalization with the ambient gas at 85-90 km, the OH rotational temperature should be representative of the neutral gas temperature of the emitting region within a degree or so [Krassovksy et al., 1977]. From rocket observations, OH emission is found to peak between 85 and 90 km with a typical half width of 10 km [Evans et al., 1973; Witt et al., 1979; Watanabe et al., 1981. Emissions from the higher vibrational levels peak slightly higher in the atmosphere than do the emissions from the lower vibrational bands [Shagayev, 1980]. Thus there is no reason to believe that the rotational temperatures as deduced from the OH (8-3) band emissions do not represent the neutral gas temperature in the 85-90 km height region. We may therefore conclude that the observed neutral gas temperatures are in agreement with the trend but differ somewhat in magnitude compared with the CIRA (1972) model temperatures for this particular latitude and time of the year.

A similar difference was reported by Sivjee et al. [1972] for the 60°-70°N region, showing a mean temperature for the flights close to 225 K

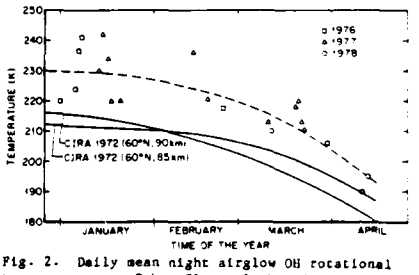

Fig. 2. Daily mean night airglow OH rotational temperatures at Poker Flat, Alaska, during the first 4 months of the years 1976, 1977, and 1978. A best fit second-degree polynomial curve is drawn (dashed curve) through the set of individual daily means. The CIRA (1972), 60°N, 85- and 90-km height temperatures for the respective months are indicated by the solid curves.

during January to March 1968, which is at least 10 K higher than the appropriate CIRA (1972) model temperature. Further differences may also be found in a summary of OH rotational temperatures with latitude by Kvifte [1967]. From these data a 65°N midwinter OH rotational temperature above 240 K may be deduced. The tendency of the CIRA (1972) mesopause midwinter temperature model at high latitudes to be somewhat low is further supported by our recent findings from Longyearbyen, Spitsbergen (78.4°N) during the 1982/1983 season [Myrabø, 1984; Myrabø et al., 1984]. Thus the available winter mesopause temperatures deduced from OH vibration-rotation spectra at high latitudes all show the same tendency; i.e., the measured values are higher than the CIRA (1972) model, but the general decreasing trend is the same. Simultaneous ground-based OH rotational temperature measurements from several high-latitude stations are needed to clarify the mesopause temperature behavior at high latitudes.

Acknowledgements. Financial support for this research was provided by the National Science Foundation through grants ATM8012719, ATM82-14642, and ATM82-00114 to the Geophysical Institute of the University of Alaska. One of us (H.K.M.) is also supported by a fellowship grant from the Royal Norwegian Council for Scientific and Industrial Research.

The Editor thanks E. J. Llewellyn and another referee for their assistance in evaluating this paper.

References

Bass, A. M., and D. Garvin, Analysis of the hydroxyl radical vibration rotation spectrum between 3900Å and 11,500Å, J. Mol. Spectrosc., 9, 114, 1962.

Chamberlain, J. W., and N. J. Oliver, OH in the airglow at high latitudes, Phys. Rev., 90, 1118, 1953.

Chamberlain, J. W., and F. L. Roesler, The OH bands in the infrared airglow, Astrophys. J., 121, 541, 1955.

Coxon, J. A., and S. C. Foster, Rotational analysis of hydroxyl vibration-rotation emission bands: Molecular constants for OH $X^2\pi$, $6 \leq v \leq 10$, Can. J. Phys., 60, 41, 1982.

Dieke, G. H., and H. M. Crosswhite, Bumblebee Series, Rep. 87, Johns Hopkins Univ., Baltimore, Md., 1948.

Evans, W. F. J., E. J. Llewellyn, and A. Vallance-Jones, Altitude distribution of hydroxyl bands of the $\Delta v=2$ sequence in the nightglow, Can. J. Phys., 51, 1288, 1973.

Herman, R. C., and G. A. Hornbeck, Vibration-rotation bands of OH, Astrophys. J., 118, 214, 1951.

Krassovsky, V. I., N. N. Shefov, and V. I. Yarin, Atlas of the airglow spectrum 3000-12400 Å, Planet. Space Sci., 9, 883, 1962.

Krassovsky, V. I., B. P. Potapov, A. I. Semenov, V. G. Sobolev, M. V. Shagaev and N. N. Shefov, On the equilibrium nature of rotational temperature of hydroxyl airglow, Planet. Space Sci., 25, 596, 1977.

Kvifte, G., Night airglow observations at As during the I.G.Y., Geophys. Norv., 12, 1, 1959

Kvifte, G., Temperature measurements from OH bands, Planet. Space Sci., 5, 153, 1961.

Kvifte, G. J., Hydroxyl rotational temperatures and intensities in the nightglow, Planet. Space Sci., 15, 1515, 1967.

Lenschow, R., and K. Petzoldt, Hohenkarten der 2 mbar-Fläche sowie monatliche Mittelkarten für den zeitraum Oktober 1970 bis Dezember 1971, Meteorol. Abh. Berlin, 97, 2, 1980.

McPherson, D. H., and A. Vallance-Jones, A study of the latitude dependence of OH rotational temperatures for Canadian stations, J. Atmos. Terr. Phys., 17, 302, 1960.

Meriwether, J. W., High latitude airglow observations of correlated short term fluctuations in hydroxyl Meinel 8-3 band intensity and rotational temperature, Planet. Space Sci., 23, 1211, 1975.

Mies, F., Calculated vibrational transition probabilities of OH ($X^2\pi$), J. Molec. Spectrosc., 53, 150, 1974.

Mironov, A. V., V. S. Produkina, and N. N. Shefov, Some results of investigations of night airglow and aurora, Ann. Geophys., 14, 365, 1958.

Myrabø, H. K., Temperature variation at mesopause levels during winter solstice at 78°N, Planet. Space Sci., 32, 249, 1984.

Myrabø, H. K., and C. S. Deehr, Mid-winter hydroxyl night airglow emission intensities in the northern polar region, Planet. Space Sci., 32, 263, 1984.

Myrabø, H. K., C. S. Deehr, and G. G. Sivjee, Large-amplitude nightglow OH (8-3) band intensity and rotational temperature variations during a 24-hour period at 78°N, J. Geophys. Res., 88, 9255-9259, 1983.

Naujokat, B., K. Petzoldt, K. Labitzke, and R. Lenschow, Beil. Berl. Wetterkarte, 57/83, 1983.

Noxon, J. F., The latitude dependence of OH rotational temperature in the night airglow, J. Geophys. Res., 69, 4087, 1964.

Romick, G. J., The detection and study of the visible spectrum of the aurora and airglow, Proc. Soc. Photo. Opt. Instrum. Eng., 91, 63-70, 1976.

Rosen, B., in International Tables of Selected Constants, Table 17 Spectroscopic data relative to diatomic molecules, Pergamon, New York, 1970.

Shagayev, M. V., Vertical temperature gradients and dissipation of internal gravity waves near the mesopause, Geom. Aeron., Engl. Transl. 20, 529, 1980.

Shefov, N. N., Hydroxyl emission of the upper atmosphere I, The behavior during solar cycle, seasons and geomagnetic disturbances, Planet. Space Sci., 17, 797, 1969.

Shefov, N. N., Hydroxyl emissions of the upper atmosphere III, Diurnal variations, Planet. Space Sci., 19, 129, 1971.

Sivjee, G. G., K. A. Dick, and P. D. Feldman, Temporal variation in the nighttime hydroxyl rotational temperature, Planet. Space Sci., 20, 261, 1972.

Vallance-Jones, A., Aurora, D. Reidel Hingham, Mass., 1974.

Wallace, L., Note on airglow temperature determinations from OH spectra, J. Geophys. Res., 65, 921, 1960.

Watanabe, T., M. Nakamura, and T. Ogawa, Rocket measurements of O_2 atmospheric and OH Meinel bands in the airglow, J. Geophys. Res., 86, 5768, 1981.

Werner, H.-J., P. Rosmus, and E.-A. Reinsch, Molecular properties from MCSCF-SCEP wave functions, 1, Accurate dipole moment functions of OH, OH^-, and OH^+, J. Chem. Phys., 79(2), 905-916, 1983.

Witt, G., J. Stegman, B. H. Solheim, and E. J. Llewellyn, A measurement of the O_2 ($b^1\Sigma_g^+ - X^3\Sigma_g^-$) atmospheric band and the $OI(^1S)$ green line in the nightglow, Planet. Space Sci., 27, 341, 1979.

C. S. Deehr, G. J. Romick, and G. G. Sivjee, Geophysical Institute, University of Alaska, Fairbanks, AK 99701.

H. K. Myrabø, Norwegian Defense Research Establishment, N-2007, Kjeller, Norway.

(Received June 28, 1983;
revised April 20, 1984;
accepted May 23, 1984.)

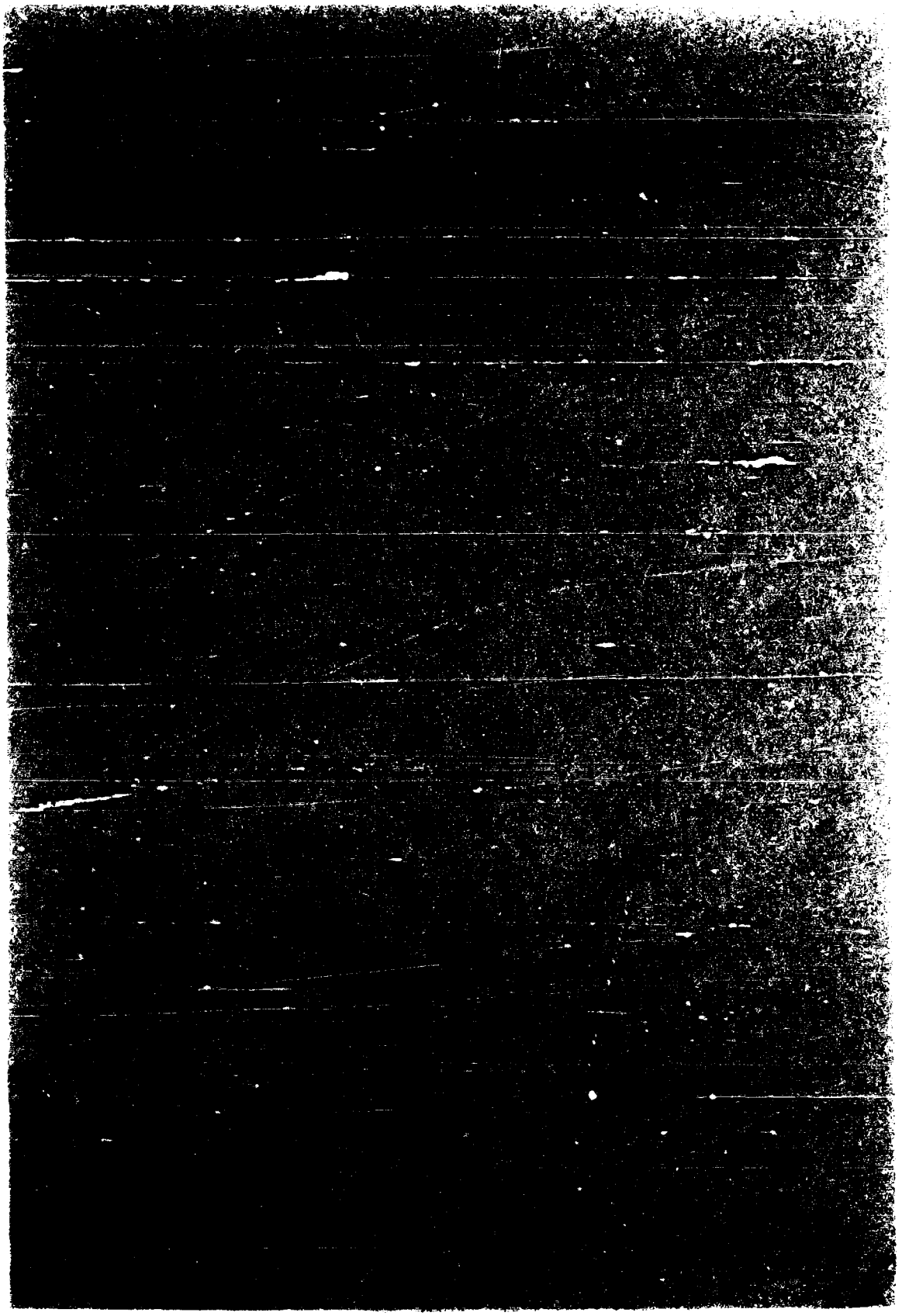

Planet. Space Sci., Vol. 32, No. 7, pp. 853–856, 1984
Printed in Great Britain

0032-0633/84 $3.00 + 0.00

POLAR CAP OH AIRGLOW ROTATIONAL TEMPERATURES AT THE MESOPAUSE DURING A STRATOSPHERIC WARMING EVENT

H. K. MYRABØ* and C. S. DEEHR
Geophysical Institute, University of Alaska, Fairbanks, AK 99701, U.S.A.

and

B. LYBEKK
Institute of Physics, University of Oslo, Oslo, Norway

(*Received in final form* 15 *November* 1983)

Abstract—OH (8-3) band rotational temperature was observed at 78.4°N during a stratospheric warming event. A negative temperature wave of the order of 40 K observed near the mesopause seems to be associated with a corresponding stratospheric warming of the order of 20 K. A 1–2-day delay is observed between the maximum stratospheric warming and the maximum cooling near the mesopause seen in the OH rotational temperature change.

INTRODUCTION

The sudden mid-winter stratospheric warming in the Northern Hemisphere was first discovered by Scherlag (1952). During such a warming, the circulation pattern and temperature profile of the stratosphere and lower mesosphere are changed (Finger and Teweles, 1964). Basically the cold polar vortex existing over the northern winter pole becomes broken and zonal windflow is weakened. Rocket temperature studies and satellite radiance observations show that the mesosphere cools under these conditions. Changes in OH and Na airglow emissions have also been correlated with the stratospheric warmings (Hunten and Godson, 1967; Ruddle and Sullivan, 1972; Shefov, 1973; Reed, 1976; Fishkova, 1978). The cooling in the upper mesosphere (Labitzke, 1977) (at least in the 70–80 km region), should result in decreased airglow emissions (Moreels *et al.*, 1977) contrary to observed results (Reed, 1976; Walker and Reed, 1976). These observed enhanced emission rates are therefore probably mainly due to a mixing and redistribution of the atmospheric constituents associated with the breakdown and reversal of the polar circulation pattern.

The development of the rocketsonde led to *in situ* measurements of temperature with altitude through the mesosphere, and typically a few temperatures were obtained each week from regular observations. Heiss Island (81°N; 58°E) has been the main site for observations in the polar regions. How representative the instantaneous mesopause temperatures at these latitudes are for the daily or weekly averages is highly questionable (Myrabø *et al.*, 1983; Myrabø, 1983; see also Noxon, 1978; Weinstock, 1978). This may also be inferred from the large variations in the temperatures observed (CIRA, 1972). More recently, satellites have provided world coverage of stratospheric and mesospheric temperatures up to approximately 60–70 km altitude. However, the satellite temperature data are not reliable above 60–70 km altitude. Thus, ground-based remote sensing of airglow emissions is necessary to obtain temperatures of the mesopause region (i.e., 85–95 km) with a much better temporal continuity than can be provided by rocket flights.

The purpose of this paper is to report nightglow OH rotational temperatures in the winter polar cap region during a stratospheric warming event. A more extended treatment of mesopause temperature behaviour in the winter polar cap has been given in an earlier paper (Myrabø, 1983).

OBSERVED TEMPERATURES

The OH emission data employed in this work were taken near Longyearbyen on West Spitsbergen (78.4°N; 15°E) during the 1982.83 Multi-National Svalbard Auroral Expedition (Deehr *et al.*, 1980). The spectral region 7280–7410 Å covering the OH (8-3) band was scanned employing a 1 m Ebert–Fastie spectrophotometer operating in the photon counting mode and coupled to an on-line digital data processing

* On leave from Norwegian Defense Research Establishment, N-2007, Kjeller, Norway.

system (Sivjee *et al.*, 1972). A bandwidth of 1.5 Å clearly resolved the OH (8-3) *P* lines from auroral emissions.

The spectrophotometer was normally run for 24 h a day during most of the winter solstice period from 5 December 1982 to 30 January 1983. Individual scans obtained each 8 or 32 s were summed and averaged to obtain hourly mean intensities. The temperatures were then read from the hourly means of the OH P_1 lines using the method of Kvifte (1959). Probable error in a single calculated hourly temperature is estimated to be ± 3 K. The occurrence of aurora is indicated on the high latitude spectra by the appearance of the [OII] 7320-30 multiplet among the lines of the OH (8-3) band. Molecular emissions such as the N_2 1 Pos. bands are only rarely seen from Longyearbyen (Sivjee and Deehr, 1980) and these would tend to increase the deduced rotational temperature by contributing relatively more to the $P_1(5)$ and $P_1(6)$ lines (Meriwether, 1975). Further details on the instrumentation, data taking, and reduction, and examples of the quality of the data are given by Myrabø (1983) and Myrabø *et al.* (1983).

In Fig. 1 is plotted the daily mean OH rotational temperatures, together with atmospheric temperatures deduced from the SSU satellite over the northern polar region at different pressure levels as given by Naujokat *et al.* (1983) for the 1982/83 winter. (The temperature is proportional to the radiance which is given in Fig. 1 for the 1.7 and 4 mbar levels. The exact proportionality depends upon the atmospheric composition, so the authors elected to leave the data in units of radiance.) The temperatures (radiances) are arranged vs height — 30, 10, 4 and 1.7 mbar corresponding to approx. 23, 30, 36 and 42 km altitude. The OH (8-3) rotational temperatures are representative for the 90 km region with an altitude thickness of about 10 km (Watanabe *et al.*, 1981). The first warming event can be seen to occur in the end of December while the second main event seen at the 10 mbar level took place near the end of January. Unfortunately, our data do not include the second event.

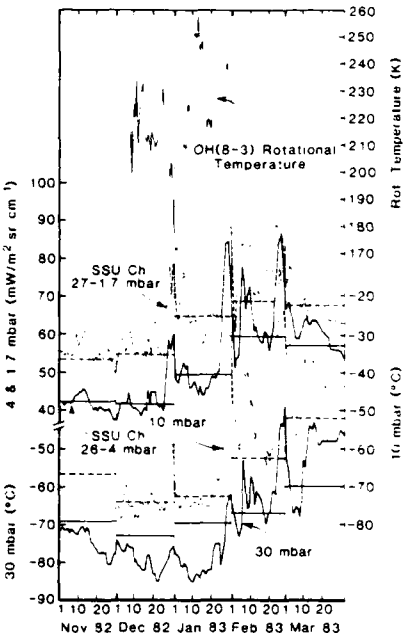

FIG. 1. OH (8-3) BAND ROTATIONAL TEMPERATURES FROM LONGYEARBYEN (78.4 N, 15 E) AND SSU SATELLITE TEMPERATURES AND RADIANCES OVER THE NORTH POLE AT DIFFERENT PRESSURE LEVELS.
The latter are obtained from Beilage zur Berliner Wetterkarte 6.5.1983 (Naujokat *et al.*, 1983).

DISCUSSION

From Fig. 1 it may be seen that the temperatures at all altitudes show irregular fluctuations from day to day. The amplitude of the fluctuations is typically twice as large in the OH data at 90 km as it is in the satellite data from the 30–40 km region, and even smaller fluctuations are normally seen in the 20 km region (i.e., 30 mbar). It is also seen that the different heights show significant deviations and a peak-to-peak correspondence cannot always be found, not even from closely-related curves. The difference in amplitude between the lower levels relative to the higher levels would be expected, if the energy in an upward propagating wave were to remain constant and proportional to ρc^2, then as the density decreases with increasing altitude, the wave velocity has to increase proportionally.

In addition to differences in fluctuation amplitudes, the absolute value of the temperature deduced at Longyearbyen may not be representative of the value averaged over the polar cap, which would correspond to the satellite data for the stratosphere.

The sequence of events reported here is in keeping with a currently accepted theory of stratospheric warming by Matsuno (1971) in which the beginning involves an increase in the amplitude of tropospheric planetary waves. This results in increased poleward heat transport at low levels leading to a rising motion at high latitudes and a sinking motion at low latitudes. The Coriolis force on this rising motion leads to

decreased westerlies at high levels. If these are strong enough to become easterlies, a critical level is reached for stationary planetary waves. The planetary wave energy thus cannot penetrate this critical level resulting in poleward heat transport only below it. This gradient in heat transport with altitude leads to a secondary circulation which includes upward motion in the polar region accompanied by expansion cooling above the critical level nearly balancing the poleward heat transport below that level. This sequence of events has been observed previously but the observations reported here extend to high altitudes and latitudes with a time history which may be important in the further development of the theory (see Geller, 1980).

It is clear from Fig. 1 that the extremely cold mesopause region over Longyearbyen around 1 January 1983 may be associated with a corresponding warm stratospheric region down to below the 10 mbar level. This is in agreement with rocket and satellite observations at the 60–70 km level during stratospheric warmings (Labitzke, 1972, 1977). The result presented here shows that the cooling of the lower mesosphere previously associated with stratospheric warmings extends throughout the mesosphere up to at least 90 km altitude, and also that the central polar cap mesosphere cools in much the same way as the lower latitude mesosphere observed previously during stratospheric warmings.

There seems to be a 1–2-day delay between the mesopause minimum temperature and the corresponding stratospheric temperature maximum. This may be due to the time it takes the secondary circulation system to develop above the critical level or the time required for the mesopause to cool radiatively once the source of heat from the zonal wind has slowed at the mesopause level (2 days, Rodgers, 1977), or it may be the geometrical effect of the limited coverage of the Longyearbyen measurement compared to the satellite measurements integrated over a far larger area.

The initial drop in temperature at the mesopause is followed by a heating which extends at least 20–30 K higher than the average. A corresponding cold stratosphere is not evident. This may be characteristic of the circulation above the critical level, or it might imply that the heating is a local effect.

Unfortunately, our measurements stop just at the beginning of the large stratospheric warming at the end of January 1983. From the data seen in Fig. 1 one may deduce that at least a 1–2-day delay between mesopause minimum temperature and stratosphere maximum may also have been the case for this event.

Future plans include an extended observing period and the establishment of an additional observing site in Alaska.

Acknowledgements—We would like to thank Drs. Nastrokat, Petzoldt, Labitzke and Lenschow for the timely distribution of stratospheric and mesospheric temperature for curves for the 1982/83 winter season. Financial support for this research was provided by the National Science Foundation through grants ATM80-12719, ATM82-14642 and ATM82-00114 to the Geophysical Institute of the University of Alaska. One of us (HKM) is also supported by a fellowship grant from Royal Norwegian Council for Sciences and Industrial Research.

REFERENCES

CIRA, COSPAR Working Group 4. COSPAR International Reference Atmosphere, 1972. Pergamon Press Ltd., Oxford.

Deehr, C. S., Sivjee, G. G., Egeland, A., Henriksen, K., Sandholt, P. E., Smith, R., Sweeney, P., Duncan, C. and Gilmer, F. (1980) Ground-based observations of F-region associated with the magnetospheric cusp. *J. geophys. Res.* **85**, 2185.

Finger, F. G. and Teweles, S. (1964) The mid-winter 1963 stratospheric warming and circulation change. *J. appl. Meteor.* **3**, 1.

Fishkova, L. M. (1978) Intensity fluctuations of the nocturnal emission of the upper atmosphere during stratospheric warmings. *Geomagn. Aeron.* **18**, 375.

Geller, M. A. (1980) Middle atmosphere dynamics and composition, in *Exploration of the Polar Upper Atmosphere* (Edited by Deehr, C. S. and Holtet, J. A.), p. D. Reidel, Dordrecht.

Hunten, D. M. and Godson, W. L. (1967) Upper atmosphere sodium and stratospheric warmings at high latitudes. *J. atmos. Sci.* **24**, 80.

Kvifte, G. (1959) Nightglow observations at As during the I.G.Y. *Geophys. Publ.* **20**, 1.

Labitzke, K. (1972) Temperature changes in the mesosphere and stratosphere connected with circulation changes in winter. *J. atmos. Sci.* **29**, 756.

Labitzke, K. (1977) Stratospheric-mesospheric mid-winter warmings, in *Dynamical and Chemical Coupling between Neutral and Ionized Atmosphere* (Edited by Grandal, B. and Holtet, J. A.), p. 17. D. Reidel, Dordrecht.

Matsuno, T. (1971) A dynamical model of the stratospheric sudden warming. *J. atmos. Sci.* **28**, 1479.

Meriwether, J. W. (1975) High latitude airglow observations of correlated short-term fluctuations in the hydroxyl Meinel 9-3 band intensity and rotational temperature. *Planet. Space Sci.* **23**, 1211.

Moreels, G. G., Megie, G., Vallance-Jones, A. and Gattinger, R. (1977) An oxygen–hydrogen atmospheric model and its application to the OH emission problem. *J. atmos. terr. Phys.* **39**, 551.

Myrabø, H. K., Deehr, C. S. and Sivjee, G. G. (1983) Large amplitude nightglow OH (8-3) band intensity and rotational temperature variations during a 24-hour period at 78°N. *J. geophys. Res.* **88**, 9255.

Myrabø, H. K. (1983) Temperature variation and mesopause levels during winter solstice at 78°N. *Planet. Space Sci.* **32**, 249.

Nastrokat, B., Petzoldt, K., Labitzke, K. and Lenschow, R. (1983) Beilage zur Berliner Wetterkarte, 57/83.

Noxon, J. F. (1978) Effects of internal gravity waves upon night airglow temperatures. *Geophys. Res. Lett.* **5**, 25.

Reed, E. I. (1976) Polar enhancements of nightglow emissions near 6230 Å. *Geophys. Res. Lett.* **3**, 5.

Rodgers, C. D. (1977) Morphology of upper atmosphere temperatures, in *Dynamical and Chemical Coupling Between the Neutral and Ionized Atmosphere* (Edited by Grandal, B. and Holtet, J.). D. Reidel, Dordrecht. (See also p. 84.)

Rundle, H. N. and Sullivan, H. M. (1972) Upper atmospheric sodium and stratospheric warmings. *J. atmos. Sci.* **29**, 977.

Scherlag, R. (1952) Die explosionsartigen Stratosphären-warmungen des Spätwinters, 1951–52. *Ber. Deut. Wetterdienst* **38**, 51.

Shefov, N. N. (1973) Relation between the hydroxyl emission of the upper atmosphere and the stratospheric warmings. *Geriands Beitr. Geophys.* **82**, 111.

Sivjee, G. G., Dick, K. A. and Feldman, P. D. (1972) Temporal variations in the night-time hydroxyl rotational temperature. *Planet. Space Sci.* **20**, 261.

Sivjee, G. G. and Deehr, C. S. (1980) Differences in polar atmospheric optical emissions between mid-day cusp and night-time auroras, in *Exploration of the Polar Upper Atmosphere* (Edited by Deehr, C. S. and Holtet, J.), p. 199. D. Reidel, Dordrecht.

Walker, J. D. and Reed, E. T. (1976) Behavior of the sodium and hydroxyl night-time emissions during a stratospheric warming. *J. atmos. Sci.* **33**, 118.

Watenabe, T., Nakamura, M. and Ogawa, T. (1981) Rocket measurements of O_2 atmospheric and OH Meinel bands in the airglow. *J. geophys. Res.* **86**, 5768.

Weinstock, J. (1978) Theory of interaction of gravity waves with $O_2(^1\Sigma)$ airglow. *J. geophys. Res.* **83**, 5175.

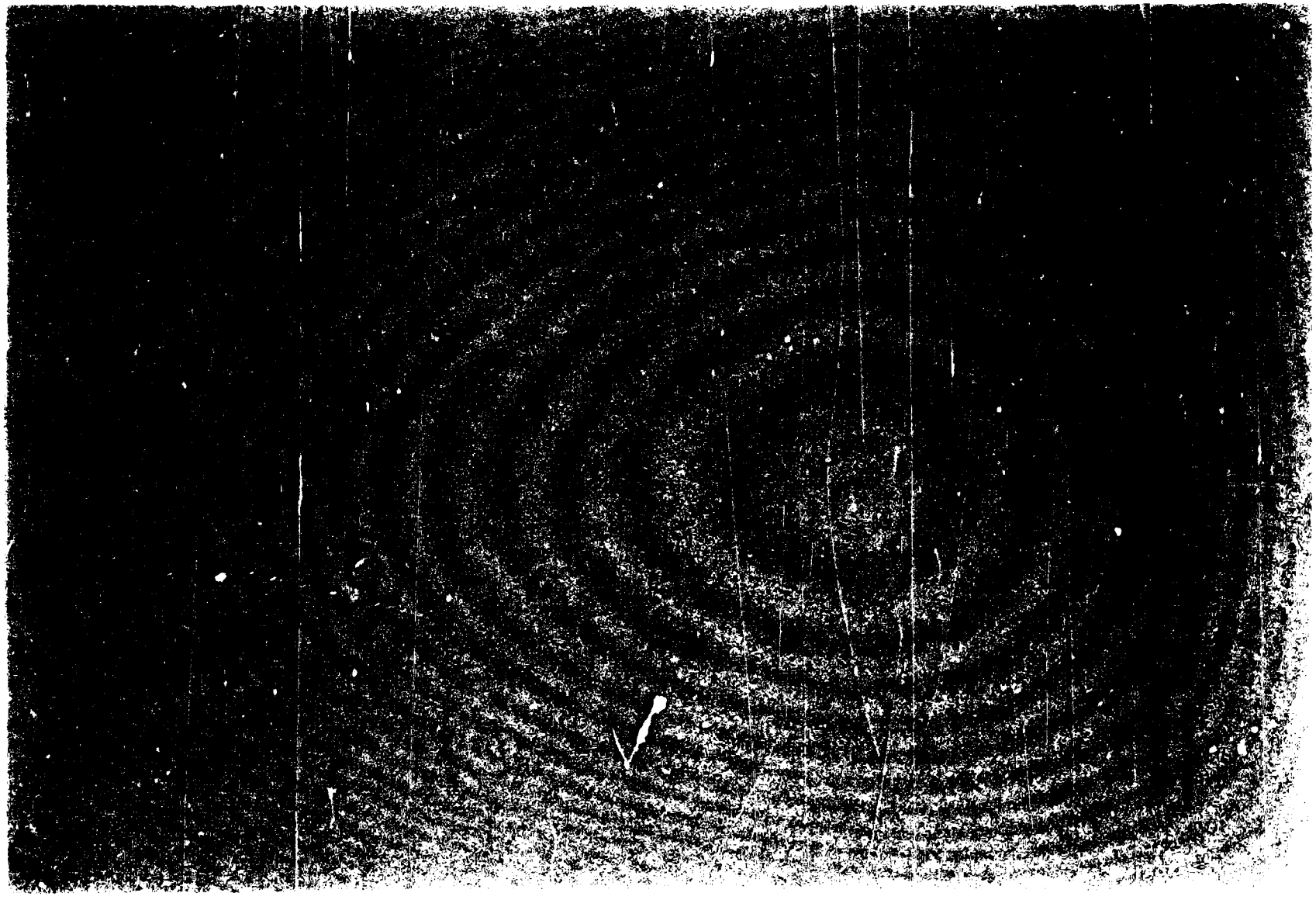

JOURNAL OF GEOPHYSICAL RESEARCH, VOL. 92, NO. A3, PAGES 2527-2534, MARCH 1, 1987

POLAR MESOPAUSE GRAVITY WAVE ACTIVITY IN THE SODIUM AND HYDROXYL NIGHT AIRGLOW

H. K. Myrabø[1], C. S. Deehr, and R. Viereck

Geophysical Institute, University of Alaska, Fairbanks

K. Henriksen

Auroral Observatory, Tromsø, Norway

Abstract. The OH (6-2) band and the Na D lines in the night airglow have been observed from Spitsbergen (78°N latitude) during a 3-day period in the end of November 1983. Regular and quasi-regular variations in temperature and the OH and sodium intensity were observed and are here interpreted in terms of gravity wave theory. In particular, waves with periods in the range 90-120 min having overlying ripple structure, with periods of 5-15 min, were observed. From the phase difference between the waves in the OH and sodium layer a height difference between the centroid of the two emissions of less than 1 km could be deduced. A gravity wave induced vertical eddy diffusion coefficient in the range 8×10^6 to 8×10^7 cm^2/s was estimated from OH-enhanced intensities. No significant net heating or cooling was observed during gravity wave activity. The gravity wave activity was not associated with geomagnetic activity. Mean OH (6-2) band and sodium night airglow intensities were 1.9 kR and 75 R, respectively.

Introduction

The mesopause and lower thermosphere region (i.e., 80-100 km) reflect interactions between the upper, middle, and lower atmosphere and thus hold important keys to the understanding of local and global dynamics of the atmosphere [Holton, 1983; Mohanakumar, 1986; Myrabø et al., 1985].

Gravity waves play an important role in the polar mesopause region [Ebel, 1984; Holton, 1983; Lindzen, 1981; S. Solomon, private communications, 1984). Gravity wave activity in the polar winter atmosphere is reported to be more frequent and violent than at lower latitudes [Tarrago and Chanin, 1982; Juramy et al., 1981; Hirota, 1984; Myrabø et al., 1983]. Juramy et al. [1981] report a 100% occurrence frequency of gravity waves in sodium density profiles obtained with lidar from Heiss Island (81°N) compared to less than 20% [Tarrago and Chanin, 1982] occurrence at Haute Provence (44°N). Thus gravity waves may take a more active part in the circulation, dynamics, and energy balance of the polar atmosphere than is the case for lower latitudes.

The night airglow emissions originating in the 80-100 km region such as the OH emissions, the O_2 (0-1) atmospheric band, the Na D lines, and the 5577Å line are useful for obtaining information on gravity waves. In addition, these emissions might give valuable information on the distribution of minor constituents, odd oxygen and transport processes, and chemistry of the mesopause region.

The main purpose of this paper is to report and discuss recent observations during the polar night of gravity wave activity as manifested by regular and quasi-regular variations in the neutral temperature and the OH (6-2) and Na D night airglow intensities.

Observations and Data Reduction

During a 3-day period with clear weather from November 27 to November 30, 1983, emission spectra of the zenith sky, containing the OH (6-2) P branches, were taken near Longyearbyen on West Spitsbergen (78°N latitude, 15°E longitude, geographic). The night airglow sodium doublet was also recorded for part of this time (i.e., from 0200 UT November 27 to 1700 UT November 28). The measurements were part of the 1983/1984 Multi-National Svalbard Auroral Expedition [Deehr et al., 1980]. Two spectrometers, a 1/2 M and a 1 M Ebert-Fastie, were used to obtain the OH and sodium emissions, respectively. The spectrometers are described in detail in the papers by Sivjee et al. [1972], Romick [1976], and Myrabø et al. [1986].

The 1/2 M instrument recording the OH (6-2) P branches was set up to scan the spectral region from 8370 to 8570Å in 12 s with a bandwidth of 7Å. A sum of 25 individual scans were used to obtain a spectrum, corresponding to one spectrum each 5 min. An example of a typical 5-min integrated spectrum is given in Figure 1. The 1 M instrument was set up to scan the spectral region 5805 to 5965Å in 16 s with a bandwidth corresponding to 4Å. A sum of 10 scans was used to obtain an integrated spectrum in 2 1/2 min. A typical 2 1/2 min spectrum of the Na D lines with the D_1 and D_2 lines well resolved is shown in Figure 2.

One of the main problems with measuring night airglow features in auroral regions is the contamination by aurora. If the emissions are not excited or otherwise directly influenced by auroral particle bombardment, overlying auroral features may normally be filtered out or accounted for given high enough spectral resolution [Myrabø et al., 1983]. In the polar regions, auroral emissions are mainly those of atomic lines [Sivjee and Deehr, 1980; Gault et al., 1981] due to the dominating soft electron precipitation spectrum normally present in the cusp and polar cap area. This makes the night airglow components, such as OH emissions and Na D lines, easy to isolate. The spectral region shown in Figure

[1]On leave from Norwegian Defence Research Establishment, N-2007, Kjeller, Norway.

Paper number 5A8316.
0148-0227/87/005A-8316$05.00

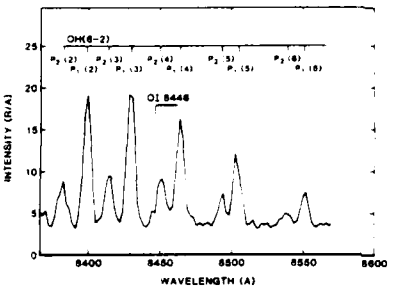

Fig. 1. A typical night airglow spectrum covering the OH (6-2) P branches. The spectrum was obtained during a 5-min integration of 25 individual 12-s scans. The bandwidth was 7Å. The OH (6-2) P lines and the auroral (OI) 8446Å line are indicated.

1 also includes the (OI) 8446Å auroral line as an auroral reference emission. The (OI) 8446Å line is directly excited by electron bombardment [Vallance-Jones, 1973] and thus very sensitive to any auroral particle precipitation in the field of view.

In spite of early reports of aurorally enhanced sodium emissions [Derblom, 1964; Hunten, 1955; Hunten, 1965], the sodium doublet is now believed to be purely chemically excited, mainly through the following reactions [Kirchhoff et al., 1981]:

$$Na + O_3 \rightarrow NaO + O_2 \qquad (1)$$

$$NaO + O \rightarrow Na\ (^2P) + O_2 \qquad (2)$$

which emits the Na D lines through the transition $Na\ (^2P) \rightarrow Na\ (^2S) + h\nu$. Using a large data base, Rees et al. [1975] failed to find any aurorally enhanced sodium emission. Both the OH and sodium emissions may therefore safely be taken to represent only the night airglow.

Spectra with no auroral background contamination have been used for calculating the OH rotational temperature and the absolute intensities of the OH (6-2) band and the Na D lines. The intensities of the lines have been calculated from the area under the lines rather than only the peak values. OH rotational temperatures have been calculated from the intensity distribution of the $P_2(2)$, $P_2(3)$, $P_2(4)$ and $P_1(5)$ lines (see Figure 1), assuming a Boltzmann distribution of the multiplet rotational levels, i.e.,

$$I(J'',i',v''\rightarrow J',i',v') = N_{v'} A(J'',i',v''\rightarrow J',i',v'') \cdot \frac{2(2J'+1)}{Q_{v'}(T_{rot})} \exp\left(\frac{-E_{i'}(J')}{k\,T_{rot}}\right) \qquad (3)$$

where I is the photon intensity in photons sec^{-1} cm^{-3}; $Q_{v'}(T_{rot})$ is the electronic-rotational partition function for the v' level, $N_{v'}$ is the total concentration of molecules in the v' vibrational level, T_{rot} is the derived rotational temperature, and $E_{i'}(J')$ is the upper state term value for the vibrational band $v'' \rightarrow v'$. The other variables have their usual meaning. The Einstein transition probabilities, A, given by Mies [1974] have been used together with energy levels, $E_{i'}(J')$, by Kvifte [1959].

Absolute calibration of the spectra was carried out in the field using a standard source. The total intensities of the OH (6-2) band were calculated from the P_1 line intensities and the rotational temperatures. The uncertainty in the absolute intensities of the OH (6-2) band and the Na D line is estimated to be 20%. The uncertainty in the absolute intensities is mainly due to calibration uncertainties. The relative uncertainty in the emission intensities due to photon noise is less than 2%. The average standard deviation in the temperature is 4K.

Results and Discussion

Figure 3 gives an overview of the sodium D_2 line intensity. The averaged background under the sodium doublet and the solar depression angle

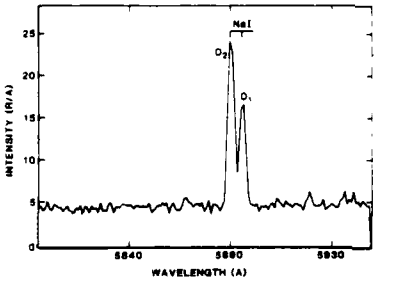

Fig. 2. A typical night airglow emission spectrum of the sodium D(1) and D(2) lines at 5890 and 5896Å, respectively. The spectrum was obtained during a 2 1/2-min integration of 10 individual 16-s scans. The bandwidth was 4Å.

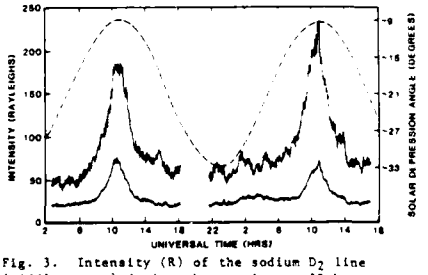

Fig. 3. Intensity (R) of the sodium D_2 line (middle curve) during the continuous 39-hour observing period. The upper curve gives the solar depression angle, while the lower curve shows the average intensity of the background on both sides of the sodium doublet (see Figure 2).

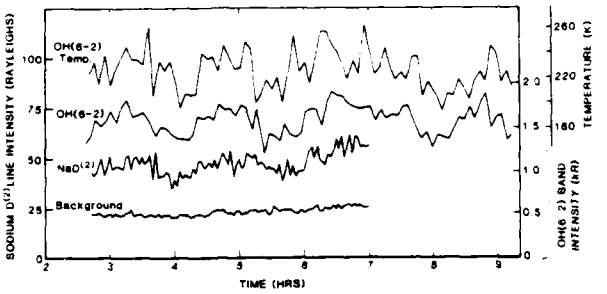

Fig. 4. Intensities of OH (6-2) band, Na D_2 line, and background during the night of November 27, 1983 as taken from Longyearbyen (78°N). The calculated OH (6-2) band rotational temperature is also given (upper curve).

are also plotted for the time period when both OH and sodium emission measurements were obtained. As seen from the figure, measurements were taken on a 24-hour basis for a total of 40 hours. However, OH spectra with daytime Fraunhofer absorption features were not used for obtaining intensities and temperatures. Sodium resonant scattering is obviously present after about 0700 UT (corresponding to approximately 0845 local solar time or solar depression angle ~ 15°). The lack of data between 1900 and 2100 UT was due to computer failure.

3.1 Simultaneous Temperature and Intensity Waves in the OH and Sodium Layers

A closer inspection of Figure 3 reveals wave-like variations in the Na D_2 line intensity not present in the background. Enhancements are also superimposed on the twilight part of the sodium emission, i.e., around 1600 UT, November 27. Expanding the period from 0200 to 0900 UT on November 27 and including the OH temperatures and intensities for the same period, the waves are seen to be present in the sodium emission, the OH emission, and the neutral temperature of the region (Figure 4). The background intensity is indicated at the bottom of Figure 4. The wave pattern, present both in OH temperature and Na and OH intensities, may well be explained by gravity waves passing through the emitting region [Noxon, 1978; Weinstock, 1978; Herse et al., 1980; Myrabø et al., 1983; Takahashi et al., 1985]. Also the power spectra of temperature variations versus frequency, presented in section 3.3, strongly support this interpretation [Smith et al., 1985].

According to linear gravity wave theory, however [Hines, 1960; Holton, 1979], density and temperature fluctuation should be 180° out of phase under conditions when $\rho_0\theta'/\theta_0 \gg p'/c_s^2$, i.e., when density fluctuations due to pressure changes are small compared with those due to temperature changes, then

$$\theta'/\theta^\circ = -\rho'/\rho_0 \qquad (4)$$

where c_s is the speed of sound, p' and θ' are the deviation from the mean values, for the pressure and the potential temperature, respectively, and ρ_0 is the unperturbed density. Assuming that the relative variations in emission intensities are proportional to the relative variations in density (i.e., $\Delta O/O \propto \Delta\rho/\rho$, where O and ρ are the emission and density, respectively), then temperature and intensity fluctuation should be 180° out of phase during the passage of gravity waves. However, the bulk of simultaneous temperature and OH and sodium intensity variations, which are possibly caused by gravity waves, show an in-phase relationship between intensity and temperature [Myrabø et al., 1983; Shagayev, 1974; Krassovsky, 1972; Takeuchi and Misawa, 1981; Takahashi et al., 1985].

The example given in Figure 4 seems to represent a very simple case of gravity wave propagation through the 90 to 95-km region as it mainly shows only a single mode wave with an overlying ripple structure. The period deduced from the figure is in the range 1 1/2-2 hours. Because the wave is continually present throughout this part of the observing period, it probably penetrates the 80 to 95-km region without breaking. The vertical wavelength of the 1 1/2-2 hour wave might be estimated to be in the range 8-15 km [Philbrick et al., 1985; Takahashi et al., 1985]. From the negligible phase difference seen between the OH and sodium emission, a maximum

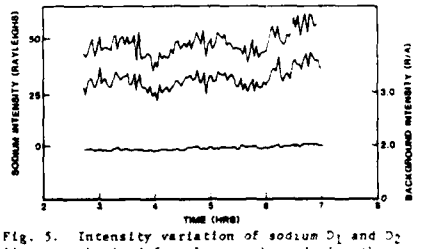

Fig. 5. Intensity variation of sodium D_1 and D_2 lines as obtained from Longyearbyen during the morning hours of November 27, 1983. Background is also shown for comparison.

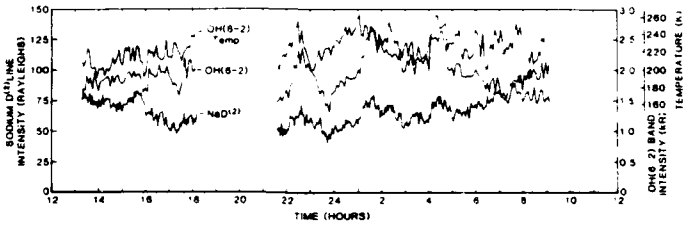

Fig. 6. Traces of the intensities of the OH (6-2) band and the sodium D_2 line. The OH (6-2) rotational temperature is also given (upper curve). The measurement period is from 1200 UT November 27 to 1200 UT November 28, 1983.

height difference between the two emissions of 0-1 km may be deduced. A maximum downward propagating group velocity of 10 km/h is assumed. The maximum probable height difference is somewhat less than that found by Takahashi et al. [1985] for low latitudes, where the phase difference between the OH and sodium intensity clearly could be seen. The bulk of sodium profile measurements, both from low and high latitudes [Chanin, 1984; Juramy et al., 1981] report the centroid of the sodium emission at about 90 km height. Assuming that this is the case for our sodium measurements places the OH-emitting layer at about 90 km, confirming previous findings of the OH emissions peaking at high altitudes in the polar winter mesopause region [Myrabø, 1984].

3.2 Possible Gravity Wave Induced Buoyancy Waves

Figure 4 shows an overlying ripple structure on the 1 1/2 to 2-hour waves, both on the sodium and OH intensity and on the temperature. The amplitude of the ripple structure in the intensities greatly exceeds the photon noise. Atmospheric transmission variations can also be ruled out as the source because the background emissions do not show structures of comparable relative amplitudes. Figure 5, comparing the intensity variations of the D_1 and D_2 lines, confirms that the ripple structures are real, i.e., originate from the emissions at the mesopause. Integration time was only 2 1/2 minutes. The background is also included for comparison. Typical periods are found in the range 5-15 min, with amplitudes 10-15% of the total intensity of the lines. Similar variations in the OI 5577Å night airglow have been reported earlier [Okuda, 1962; Silverman, 1962]. More recently, short-period oscillations, i.e., 5-10 min, have been reported to occur simultaneously in both OH intensity and temperature [Takeuchi and Misawa, 1981]. However, the latter observation was not clearly superimposed on a longer-period wave, and thus might have a different origin. Tuan et al. [1979] have made an effort to explain the ripple oscillation overlying the longer-period waves observed in the OI 5577Å data. They find from theoretical considerations that the short-period oscillations are associated with the buoyancy (Brunt-Vaisala) frequency of the atmosphere and "excited" by the long period waves. The same theoretical considerations also apply to the sodium and OH emissions. The periods of the waves are certainly in the right frequency domain for Brunt-Vaisala oscillations [Hines, 1960]. From Philbrick et al. [1985] one may find that waves with periods in the range 5-10 min should be reflected back into the lower atmosphere from heights of approximately 60-80 km, respectively. Thus at least the main body of the observed "fine structure" waves in Figure 5 originates at altitudes higher than 80 km, which strongly supports that they are localized to the mesopause region and in fact excited by the longer-period waves. From the periods observed, one may estimate vertical and horizontal wavelengths in the range 7-9 km and 12-20 km, respectively [Philbrick et al., 1985].

3.3 Evidence for Breaking Gravity Waves

Figures 6 and 7 show traces of the temperature and the OH and sodium intensities during the remaining parts of the observing period. The missing data between 1830 and 2130 UT November 27 are, as previously stated, due to computer failure, while the data gap in Figure 7 between 0900 and 1130 UT corresponds to spectra with Fraunhofer absorption bands (i.e., twilight).

During the afternoon of November 27 there are still quasi-regular waves present in the OH intensity and temperature. Some correspondence with the sodium intensity is also seen. Then in the evening and night, large simultaneous waves appear both in the OH and sodium intensities and in the temperature. Oscillations in the OH intensity of up to 100% of the minimum intensity accompanied by up to 60 K temperature variation are observed. The intensity of the sodium emission shows similar behavior but with slightly less pronounced variations. After about 0500 UT November 28 the wave pattern disappears and is replaced by irregular variations. After this time the temperature variations become smaller, but the OH intensity starts to show periods of large enhancements (up to 100%) lasting from 3 to 6 hours (see Figure 7). If the gravity waves which were present before this point start to break in the 70-95 km region, one would expect an increased eddy diffusion [Weinstock, 1978; Weinstock, 1985; Ebel, 1984; Walterscheid, 1981].

The result of an increased eddy diffusion in the 70 to 95-km region would be to increase the O_3 concentration in the 85 to 95-km region [Moreels et al., 1977]. An enhanced OH emission would result (assuming O_3 is the limiting factor).

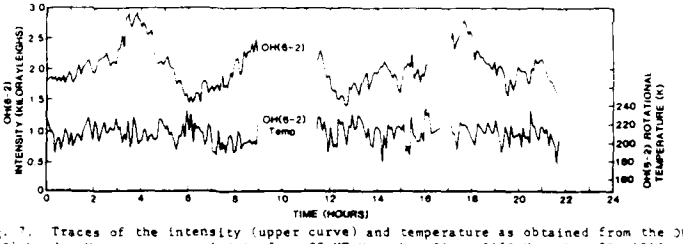

Fig. 7. Traces of the intensity (upper curve) and temperature as obtained from the OH (6-2) band. Measurement period is from 00 UT November 28 to 2130 November 29, 1983.

Further evidence that the gravity wave field is saturated and that the waves really break during this part of the observing period is contained in the power spectrum of the temperature variations. As indicated in Figure 8, on a log/log plot of power against frequency the falloff in the power follows an $N^{-5/3}$ law (N being the frequency). This is a strong indicator of saturated gravity wave fields and breaking waves [Smith et al., 1985; Dewan, 1979; Gage, 1979]. According to some theoretical calculations one should also expect a net heating rate from breaking gravity waves of the order of 5-20 K/hr at the mesopause region [Ebel, 1984]. However, depending upon approach and choice of dissipation parameter [Ebel, 1984], one might also arrive at a net cooling [Walterscheid, 1981]. The rate of heating/cooling is therefore questionable; probably both situations can occur. In view of the above indication we find it reasonable to interpret the variation in intensity and temperature seen in Figure 7 as effects of breaking gravity waves. This places the region of breaking gravity waves in the winter polar middle atmosphere slightly higher (i.e., ~ 10 km) than for the 60-65°N latitudes [Garcia and Solomon, 1985].

The increase in intensity of the OH emission might then be used to estimate the upper limit of enhancement of the eddy diffusion coefficient in connection with the gravity waves [Weinstock, 1978]. The simplified formula

$$D_{zz} = (\Delta z)^2/2\Delta t \qquad (6)$$

will give a first approximation. Δz is the average distance the O_3 or H molecules and atoms need to move in the time interval Δt. Assuming O_3 is the limiting factor [Moreels et al., 1977] and using average number densities of O_3 versus height from Moreels et al. [1977], Δz is approximately 10-15 km for a 70-100% increase in the O_3 density. The 70-100% enhancement in OH intensities takes place typically over 3-6 hours. Applying these numbers to (10) implies a gravity wave induced vertical eddy diffusion coefficient, D_{zz} in the range between 8×10^6 and 8×10^7 cm^2/s. This is a rather large eddy diffusion coefficient as compared to average values [Von Zahn and Herwig, 1977], mainly quoted around 10^6 cm^2/s. It should be noted that part of the intensity variations could be produced by horizontal transport in connection with spatial variation in the breaking or other atmospheric irregularities. Thus our estimate only gives a possible upper limit of the eddy diffusion coefficient. However, it is reasonable to believe that eddy diffusion is highly variable [Weinstock, 1985] and that periods with gravity wave activity represent particularly high levels of D_{zz} in the breaking region.

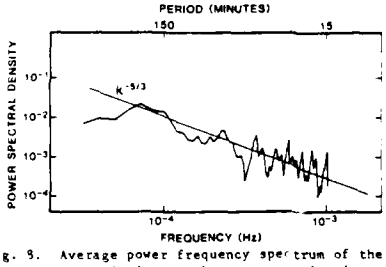

Fig. 8. Average power frequency spectrum of the temperature variation at the mesopause level as obtained from the OH (6-2) rotational lines during the period 1500 UT November 27, to 2130 UT November 29, 1983. A $k^{-5/3}$ (k = frequency) line is indicated.

3.4 OH (6-2) Band and Sodium Night Airglow Absolute Intensities

The average intensity of the OH (6-2) band for the 3-day observing period was found to be 1.9 kR. This value is higher by about 30-70% than values normally reported for low- and mid-latitude stations [Takahashi and Batista, 1981; Llewellyn, 1978; Takeuchi and Misawa, 1981]. A substantial part of this enhancement seems to be related to the enhanced eddy diffusion in connection with breaking gravity waves. Previous results on OH (8-3) band intensity from Longyearbyen have also shown average intensities and intensity variations which are considerably higher than at mid- and low-latitude stations [Myrabø and Deehr, 1984]. Absolute intensities of the OH emission found here seem, therefore, to be in good agreement with previous findings and confirm earlier observations of a rather intense OH night air glow in the polar cap during winter solstice conditions.

The average sodium doublet intensity in the night airglow derived from the measurements was found to be 75 R. Similar intensities have been reported from high-latitude stations [Rees et

al., 1975; Henriksen et al., 1980] and seem also to be typical for lower-latitude [Kirchhoff et al., 1981b] winter conditions. Because both the sodium number density and sodium night airglow emission normally show larger relative variations than is the case for OH emissions, it is difficult to say whether the 75 R sodium emission represents an enhanced level or not. Unfortunately, the sodium emission was not measured during the entire observing period reported here. Whether the sodium emission is enhanced by increased eddy diffusion or not therefore remains to be proven by future measurements.

3.5 Possible Sources of Gravity Waves in the Polar Winter Mesosphere and Lower Thermosphere

Gravity waves are excited in the atmosphere by a variety of mechanisms. Penetrative convection, (i.e., when a rising current suddenly loses its buoyancy as it enters a stable region [Townsend, 1968]), frontal acceleration, and orographic forcing are often quoted as responsible mechanisms. The most important single source might, however, be wind shears in the lower and middle atmosphere [Ebel, 1984; Einaudi, 1979]. In polar regions, speculations of auroral sources launching waves and causing temperature and intensity changes of the airglow in the 85 to 95-km region have also been put forward [Ebel, 1984; Baker et al., 1985; Takahashi et al., 1985]. The idea that OH emission intensity and temperatures of the 85 to 90-km region should be affected by geomagnetic disturbances was first put forward by Krassovsky [1956]. Calculations on Joule heating and ion-drag perturbation upon the 90-km region density and temperature during geomagnetic substorms have, however, given negative results [Brekke, 1977; Maeda and Aikin, 1968]. From earlier observations at Longyearbyen, Myrabø and Deehr [1984] showed that negative, positive, and no correlations could be extracted between OH intensity, temperature, and geomagnetic indices using truncated data sets (i.e., case studies). A clear and simple correlation between mesopause region temperature/temperature variations, nightglow intensity/intensity variations, and geomagnetic activity seems therefore doubtful. In view of the different sources of perturbations (gravity waves from middle and lower atmosphere and possibly from auroral origin, horizontal and vertical transport, chemical reactions) that could act simultaneously, a clear correlation with only one of the possible sources over a longer time interval should perhaps not be expected. The period of observations covered by the measurements reported here are not a particularly disturbed geomagnetic period but rather quiet. Especially the hours before and during the morning of November 27 show no significant auroral perturbation capable of penetrating energy down into the 100-km region. We therefore conclude that the gravity wave activity reported in this paper has its origin in the lower or middle atmosphere and not in the thermosphere in connection with geomagnetic disturbances.

Summary

The OH (6-2) band and the Na D lines in the night airglow have been observed from Longyearbyen, West Spitsbergen (78°N latitude, 15°E longitude, geographic) from 0200 UT November 27 to 1700 UT November 29, 1983. Spectra covering the P_1 lines of the OH band and the D_1 and D_2 lines of Na were obtained with a 1/2 M and a 1 M Ebert spectrophotometer, respectively. Spectral resolution was 7Å and 4Å for the OH and Na D, resolving the P_1 and P_2 lines and the D_1 and D_2 lines. In the first part of the observing period, regular waves were recorded with periods in the range 1 1/2-2 hours and with overlying ripple structures, periods 5-15 min. The waves were present in both the OH and sodium intensity and in the temperature, strongly indicating passing of gravity waves through the emission layers. The ripple structures coincided in both the D_1 and D_2 lines and appeared in the OH intensity and temperature. There is strong indication that the observed buoyant frequency waves (5-15 min) are excited by the larger waves.

From the downward propagating phase difference between the intensity of waves in the OH and sodium layer, a maximum height difference between the centroid of the two emission regions is found to be less than 1 km. Assuming an average height of the Na layer of 90 km then places the OH layer at approximately the same height, confirming previous findings of the OH emission peaking at about 90 km in the polar winter atmosphere [Myrabø et al., 1983].

From the enhancement of the OH emission, using O_3 and H profiles from Moreels et al. [1977], a gravity wave induced eddy diffusion coefficient in the range 8×10^6 to 8×10^7 cm^2/s was found. Mean night airglow intensities of the OH (6-2) band and Na D lines over the observing period were 1.9 kR and 75 R, respectively.

The gravity wave activity observed during this period could not be found to be associated with geomagnetic activity. Since Krassovsky [1956] indicated that upper mesospheric (i.e., 80-95 km) temperatures and night airglow intensities should be modulated by gravity waves launched from geomagnetic disturbances in auroral regions, theoretical and experimental evidence has appeared, both in support of the hypothesis and against it. Most calculations show negligible and unobservable effects [Brekke, 1977] except in very extreme cases. Recently Baker et al. [1985] reported a positive correlation between ΔK_p and Δ (OH) temperatures but simultaneously also a highly positive correlation between Δ (OH) temperatures and the variation in 30-mbar temperatures. The latter results indicate a connection between ΔK_p and the 30-mbar temperature which is even more difficult to explain.

Acknowledgments. Financial support for this research was provided by National Science Foundation through ATM-8313727 to the Geophysical Institute of the University of Alaska and by the Royal Norwegian Council for Scientific and Industrial Research through a fellowship grant to one of us (HKM). The observations on Svalbard are made through a cooperative effort involving the universities in Fairbanks, Tromsø and Oslo, with the help and cooperation of the Great Norwegian Spitsbergen Coal Company and the Norwegian Polar Institute. The authors also want to thank Dan Osborne and Bob Erickson for technical assistance and programming assistance.

The Editor thanks V. W. J. H. Kirchhoff and G. C. Reid for their assistance in evaluating this paper.

References

Baker, D. F., A. F. Steed, G. A. Ware, D. Offermann, G. Lange and H. Lauche, Ground-based atmospheric infrared and visible emission measurements, J. Atmos. Terr. Phys., 47, 133, 1985.

Brekke, A., Auroral effects on neutral dynamics, from Dynamical and chemical coupling between the neutral and ionized atmosphere, ed.. B. Grandal and J. A. Holtet, D. Reidel, Holland, p. 313, 1977.

Chanin, M. L., Review of lidar contributions to the description and understanding of middle atmosphere, J. Atmos. Terr. Phys., 46, 987, 1984.

Daehr, C. S., G. G. Sivjee, A. Egeland, K. Henriksen, P. E. Sandholt, R. Smith, P. Sweeney, C. Duncan and F. Gilmer, Ground-based observations of F-region associated with the magnetospheric cusp, J. Geophys. Res., 85, 2185, 1980.

Derblom, H., Observations of sodium emissions in aurora, J. Atmos. Terr. Phys., 26, 791, 1964.

Dewan, E. M., Stratospheric wave spectra resembling turbulence, Science, 204, 832, 1979.

Ebel, A., Contributions of gravity waves to the momentum, heat and turbulent energy budget of the upper mesosphere and lower thermosphere, J. Atmos. Terr. Phys., 46, 727, 1984.

Einaudi, F., D. P. Lalas and G. E. Perona, The role of gravity waves in tropospheric processes, Pure Appl. Geophys., 117, 627, 1979.

Gage, K. S., Evidence for a $K^{-5/3}$ law internal range in mesoscale two-dimensional turbulence, J. Atmos. Sci., 36, 1950, 1979.

Garcia, R. R. and S. Solomon, The effect of breaking gravity waves on the dynamics and chemical composition of the mesosphere and lower thermosphere, J. Geophys. Res., 90, 3850, 1985.

Gault, W. A., R. A. Koehler, R. Link, and G. G. Shepherd, Observations of the optical spectrum of the dayside magnetospheric cleft aurora, Planet. Space Sci., 29, 321, 1981.

Henriksen, K., G. G. Sivjee, and C. S. Deehr, Winter enhancement of atomic lithium and sodium in the polar upper atmosphere, J. Geophys. Res., 85, 5153, 1980.

Herse, M., G. Moreels, and J. Clairemidi, Waves in the OH emission layer: Photogrammetry and topography, Appl. Opt., 19, 355, 1980.

Hines, C. O., Internal atmospheric gravity waves at ionospheric heights, Can. J. Phys., 38, 1441, 1960.

Hirota, I., Climatology of gravity waves in the middle atmosphere, J. Atmos. Terr. Phys., 46, 767, 1984.

Holton, J. R., An Introduction to Dynamical Meteorology, Academic, Orlando, Fla., 1979.

Holton, F. R., The influence of gravity wave breaking on the general circulation of the middle atmosphere, J. Atmos. Sci., 40, 2497, 1983.

Hunten, D. M., Some photometric observations of auroral spectra, J. Atmos. Terr. Phys., 7, 141, 1955.

Hunten, D. M., Excitation of sodium emission in aurora, J. Atmos. Terr. Phys., 27, 583, 1965.

Juramy, P., M. L. Chanin, G. Megie, G. F. Toulinov, and Y. P. Doudoladov, Lidar sounding of mesospheric sodium layer at high latitude, J. Atmos. Terr. Phys., 43, 209, 1981.

Kirchhoff, V. W. J. H., B. R. Clemesha, and D. M. Simonich, The atmospheric neutral sodium layer, 1, Recent modelling compared to measurements, J. Geophys. Res., 86, 6892, 1981a.

Kirchhoff, V. W. J. H., B. R. Clemesha, and D. M. Simonich, Average nocturnal and seasonal variations of sodium nightglow at 23°S, 46°W, Planet. Space Sci., 29, 765, 1981b.

Krassovsky, V. I., Infrared night airglow as a manifestation of the process of oxygen recombination, in Airglow and Aurora, edited by E. B. Armstrong and A. Dalgarno, p. 193, Pergammon, New York, 1956.

Krassovsky, V. I., Infrasonic variations of OH emission in the upper atmosphere, Ann. Geophys., 28, 739, 1972.

Kvifte, G., Nightglow observations at 4n during the I. G. Y., Geophys. Publ., 20, 1, 1959.

Lindzen, R. S., Turbulence and stress owing to gravity wave and tidal breakdown, J. Geophys. Res., 86, 9707, 1981.

Llewellyn, E. E., B. H. Long, and B. H. Solheim, The quenching of OH^* in the atmosphere, Planet. Space Sci., 26, 525, 1978.

Maeda, K., and A.C. Aikin, Variations of polar mesospheric ozone during events, Planet. Space Sci., 16, 371, 1968.

Mies, F. H., Calculated vibrational transition probabilities of $OH(X^2\pi)$, J. Mol. Spectrosc., 53, 150, 1974.

Mohanakumar, K., An investigation on the influence of solar cycle on mesospheric temperature, Planet. Space. Sci., 33, 795, 1985.

Moreels, G., G. Megie, A. Vallance-Jones, and R. L. Gattinger, An oxygen-hydrogen atmospheric model and its application to the OH emission problem, J. Atmos. Terr. Phys., 39, 551, 1977.

Myrabø, H. K., Temperature variation at mesopause levels during winter solstice at 78°N, Planet. Space Sci., 32, 249, 1984.

Myrabø, H. K., and C. S. Deehr, Mid-winter hydroxyl night airglow emission intensities in the northern polar region, Planet. Space Sci., 32, 263, 1984.

Myrabø, H. K., C. S. Deehr, and G. G. Sivjee, Large-amplitude nightglow OH (8-3) band intensity and rotational temperature variations during a 24-hour period at 78°N, J. Geophys. Res., 88, 9255, 1983.

Myrabø, H. K., C. S. Deehr, G. J. Romick, and K. Henericksen, Mid-winter intensities of the night airglow O_2 (0-1) atmospheric band emission at high latitudes, J. Geophys. Res., 91, 1684, 1986.

Noxon, J. F., Effects of internal gravity waves upon night airglow temperatures, Geophys. Res. Lett., 5, 25, 1978.

Okuda, M., A study of excitation processes in night airglow, Sci. Rep. Tohoken Univ., 14, 9, 1962.

Philbrick, C. R., F. J. Schmidlin, K. V. Grossmann, G. Lange, D. Offermann, K. D. Baker, D. Krankowsky, and V. von Zahn, Density and temperature structure over northern Europe, J. Atmos. Terr. Phys., 47, 159, 1985.

Rees, M. H., G. J. Romick, and A. E. Belon, The

intensity of the sodium D lines in the auroral zone, Ann. Geophys., 31, 311, 1975.
Romick, G. J., The detection and study of visible spectrum of the aurora and airglow, Proc. Soc. Photo. Opt. Instrum. Eng., 91, 63, 1976.
Shagayev, M. V., Fast variations of hydroxyl night airglow emissions, J. Atmos. Terr. Phys., 36, 367, 1974.
Shelton, F. D., C. S. Gardner, and C. F. Sechrist, Jr., Density response of the mesospheric sodium layer to gravity wave perturbations, Geophys. Res. Lett., 7, 1069, 1980.
Silverman, S. M., Unusual fluctuations of 5577 Å OI airglow emission intensity on October 28-29, 1961, Nature, 195, 481, 1962.
Sivjee, G. G., and C. S. Deehr, Differences in polar atmospheric optical emissions between mid-day cusp and night-time auroras, in Exploration of the Polar Upper Atmosphere, edited by C. S. Deehr and J. A. Holtet, p. 199, D. Reidel, Hingham, Mass, 1980.
Sivjee, G. G., K. A. Dick, and P. D. Feldman, Temporal variations in the nighttime hydroxyl rotational temperature, Planet. Space Sci., 20, 261, 1972.
Smith, S. A., D. C. Fritts, and T. E. Van Zandt, Comparison of mesospheric wind spectra with a gravity wave model, Radio Sci., 20(6), 1331-1338, 1985.
Takahashi, H. and P. P. Batista, Simultaneous measurements of OH (9-4), (8-3), (7-2), (6-2), and (5-1) bands in the airglow, J. Geophys. Res., 86, 5632, 1981.
Takahashi, H., P. P. Batista, Y. Sahai, and B. R. Clemesha, Atmospheric wave propagations in the mesopause region observed by the OH (8-3) band, Na D, O_2 A (8645Å) band and OI 5577Å nightglow emissions, Planet. Space Sci., 33, 331, 1985.
Takeuchi, I., and K. Misawa, Short-period oscillations of intensity and rotational temperature of the OH (6-2) band, Ann. Geophys., 37, 315, 1981.
Tarrago, A., and M. L. Chanin, Interpretation in terms of gravity waves of structures observed at the mesopause level by photogrammetry and lidar, Planet. Space. Sci., 30, 611, 1982.
Townsend, A. A., Excitation of internal waves in a stably-stratified atmosphere with considerable wind shear, J. Fluid Mech., 32, 145, 1968.
Tuan, T. F., R. Hedinger, S. M. Silverman, and M. Okuda, On gravity wave induced Brunt-Vaisala oscillations, J. Geophys. Res., 84, 393, 1979.
Vallance-Jones, A., Aurora, Hingham, Mass., D. Reidel, 1973.
Von Zahn, V., and T. Herwig, Inert gas abundance as indicators for the strength of eddy diffusion at turbopause altitudes, in Dynamical and Chemical Coupling Between the Neutral and Ionized Atmosphere, edited by, B. Grandal and J. A. Holtet, p. 49, D. Reidel, Hingham, Mass., 1977.
Walterscheid, R. L., Dynamical cooling induced by dissipating internal gravity waves, Geophys. Res. Lett., 8, 1235, 1981.
Weinstock, J., Theory of the interaction of gravity waves with O_2 ($^1\Sigma$) airglow, J. Geophys. Res., 83, 5175, 1978.
Weinstock, J., Gravity wave saturation and eddy diffusion in the middle atmosphere, J. Atmos. Terr. Phys., 46, 1069, 1985.

C. S. Deehr, H. K. Myrabø, and R. Viereck, Geophysical Institute, University of Alaska, Fairbanks, AK 99775-0800.
K. Henriksen, Auroral Observatory, Tromsø, Norway.

(Received November 21, 1985;
revised October 3, 1986;
accepted October 21, 1986.)

Planet. Space Sci. Vol. 34, No. 11, pp. 1023–1029, 1986
Printed in Great Britain

0032-0633/86 $3.00 + 0.00

WINTER-SEASON MESOPAUSE AND LOWER THERMOSPHERE TEMPERATURES IN THE NORTHERN POLAR REGION

H. K. MYRABØ*
Geophysical Institute, University of Alaska, Fairbanks, AK 99775-0800, U.S.A.

(*Received in final form* 12 May 1986)

Abstract—Mesopause lower thermosphere nocturnal temperatures have been deduced from spectrophotometric observations of the night airglow OH emissions at Longyearbyen, Svalbard (78°N), during four winter seasons (1980–1985). A monthly average temperature maximum of 223 K is found to occur in January with monthly averages of 206, 212, 212 and 198 K respectively for November, December, February and March. A relatively low temperature in late December followed by a very warm mesopause in early January seems to be consistent for all four seasons and might be associated with changes in transmission of gravity waves to the upper mesosphere in connection with stratospheric and lower mesospheric circulation changes.

1. INTRODUCTION

Temperature and temperature variations are basic parameters in the understanding of atmospheric dynamics, chemistry, circulation and energy flux, and in the overall interaction between the upper-middle and lower atmosphere. The 70–100 km region of the atmosphere has been found to hold important keys to the understanding of local and global dynamics of the middle atmosphere (Holton, 1983; Fritts *et al.*, 1984; Myrabø *et al.*, 1985). In spite of this, measurements of the temperature in this part of the middle atmosphere have been sparse. This is mainly due to the relative inaccessibility of this region of the atmosphere to different temperature measuring methods (Myrabø, 1984; Barnett, 1980).

In the polar cap, measurements of the mesopause and lower thermospheric temperatures and their variations are even more sparse. Besides rocketsonde measurements from Heiss Island (81°N), mainly giving a few snapshots in time and space, the only measurements on a regular basis covering a longer time period are those reported by Myrabø (1984). Due to considerable short time-scale variations caused by gravity waves, local transport phenomena, and stratospheric and lower mesospheric circulation changes (i.e. stratwarms) (Myrabø *et al.*, 1983; Myrabø *et al.*, 1984), temperatures must be measured frequently (covering at least 5–8 h) to give reliable daily means. Thus, ground-based methods are the only means of obtaining this temporal coverage, and resolving dynamical phenomena.

In the polar regions, the present ground-based method of obtaining temperatures of the 80–100 km altitude is to extract temperatures from the measured rotational intensity distribution of the different night airglow emissions, such as the OH bands and the O_2 (0–1) Atmospheric bands (Myrabø, 1984). Temperatures obtained from these emissions yield neutral air temperatures at the emitting height because the emitting molecules are in thermodynamic equilibrium with the surrounding atmosphere (Krassovsky *et al.*, 1977). There is no OH emission height profile published for latitudes 75–80°N that could be truly representative of the measurements in this paper. The northernmost obtained profile (ϕ = 68°N; by Witt *et al.*, 1979), however, shows an extremely large half width (15 km), believed not to be typical for the OH layer in polar regions (Myrabø *et al.*, 1986). Therefore, to illustrate the position and shape of the OH layer in the atmosphere, the emission height profile by Rogers *et al.* (1973) has been plotted in Fig. 1 together with the CIRA 1972, 70°N, December, model atmospheric temperature profile. A half width in the range 5–10 km is typical for the emission, and the peak height normally ranges from 82 to 90 km, probably closer to 90 km for winter solstice polar conditions (Myrabø *et al.*, 1983; Myrabø, 1984). Also included in Fig. 1 is the weighting function with height of the *NOAA* 7, Ch. 27 spacecraft radiometer and the CIRA 1972, 70°N, December, model atmospheric temperature profile. The Ch. 27 radiometer reading is proportional to temperature and was used to monitor the lower mesospheric temperatures and circulation changes over the northern polar cap (Labitzke *et al.*, 1985). It has been shown to anticorrelate with larger temperature changes in the 80–100 km region (Myrabø *et al.*, 1984).

*On leave from the Norwegian Defence Research Establishment, N-2007, Kjeller, Norway.

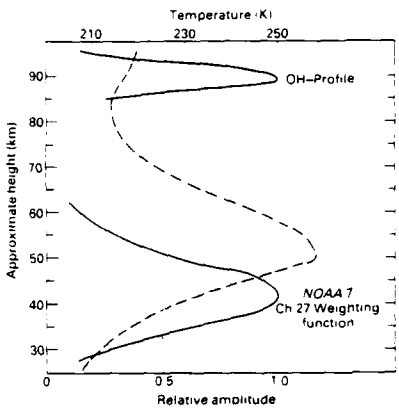

FIG. 1. EXAMPLE OF A TYPICAL OH EMISSION HEIGHT PROFILE AS OBTAINED FROM ROCKET MEASUREMENTS (ROGERS *et al.*, 1973).
The weighting function with height of the *NOAA* 7, Ch. 27 spacecraft radiometer together with the CIRA 1972, 70°N, December, model atmospheric temperature (dashed line) profile are also indicated.

In addition to the measurements reported by Myrabø (1984) from Longyearbyen (78°N), using night airglow OH emissions, earlier sporadic measurements have been reported by Chamberlain and Oliver (1953), Noxon (1964) and Sivjee *et al.* (1972) at latitudes 70–85°N and covering a temperature range of 160 to approximately 300 K. The measurements by Myrabø (1984) yielded a mean winter solstice (i.e. December and January) temperature of 220 K for the 1982/83 season. The purpose of this paper is to extend and generalize these results by including mesopause temperatures obtained from OH observations during the 1983/84 and 1984/85 winter season at Longyearbyen, 78°N.

2. OBSERVATIONS AND DATA REDUCTION

As part of the 1983/84 and 1984/85 Multi-National Svalbard Auroral Expedition (Deehr *et al.*, 1980), spectra of the zenith sky were taken close to Longyearbyen on West Spitsbergen (78°N, Lat., 15°E, Long., geographic). Both winters, measurements covered a 3–4 month period around solstice. Emission spectra were obtained using a 1.2 M Ebert Fastie spectrophotometer coupled to a minicomputer and recording in the photon counting mode. The instrument is further described by Sivjee *et al.* (1972) and Myrabø *et al.* (1985). The spectral region from 8240 to 8740 Å was scanned in 12 s using the spectrometer in the first order with a 0.5 mm slit corresponding to a spectral resolution of 7 Å. Each scan was recorded on magnetic tape. Individual rotational temperatures were calculated from 1 and 2-h integrated scans (300 and 600 scans, respectively) using the OH (6–2) band. An example of a typical 1-h integrated spectrum used to obtain the temperature is given in Fig. 2. The P_1 and P_2 lines of the OH (6–2) band are indicated together with the R and Q

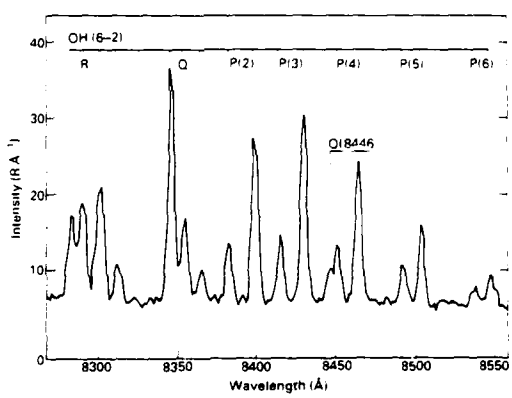

FIG. 2. A TYPICAL 1-h INTEGRATED SPECTRUM USED TO OBTAIN THE TEMPERATURE.
In addition to the different lines and branches of the OH (6–2) band, the auroral emission from atomic oxygen at 8446 Å is also indicated.

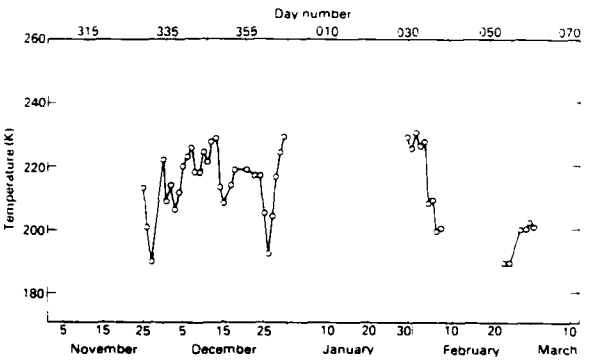

FIG. 3. DAILY MEAN TEMPERATURES FOR THE WINTER SEASON 1983-84 AS OBTAINED FROM OH (6–2) BAND NIGHT AIRGLOW EMISSIONS NEAR LONGYEARBYEN, 78 N
Straight lines are drawn between the daily means. Temperatures are given in degrees Kelvin (K).

branches. Also shown is the auroral permitted emission at 8446 Å from atomic oxygen. The auroral emission is excited from particle bombardment (i.e. mainly electrons) (Vallence-Jones, 1974) and may be used as an indicator of auroral activity. Using spectra with a relatively high resolution as shown in Fig. 2, and containing an auroral reference emission, makes it possible to eliminate spectra with auroral emission features which may contaminate the OH P_1 line measurements. In the polar cap, auroral emissions from molecular species are less frequent than in the auroral oval, due to a lower energy in the precipitating particles (Sivjee and Deehr, 1980). Thus, only spectra void of auroral contamination of the OH P_1 lines were used to obtain temperatures.

The temperatures have been calculated from the intensity distribution of the $P_1(2)$, $P_1(3)$, $P_1(4)$ and $P_1(5)$ lines assuming a Boltzmann distribution of the multiplet rotational levels, i.e.

$$I(J'', i', v'' \leftarrow J', i', v') = N'_{v'} \bar{A}(J'', i', v'' \leftarrow J'', i', v') \times \frac{2(2J'+1)}{Q'_{v'}(T_{\text{rot}})} \exp\left(\frac{-E'_{i,v'}(J')}{kT_{\text{rot}}}\right),$$

where I is the photon intensity in photons s^{-1} cm^{-3}, $Q'_{v'}(T_{\text{rot}})$ the electronic–rotational partition function for the v' level, $N'_{v'}$ the total concentraton of molecules in the v' vibrational level, T_{rot} the derived rotational temperature and $E'_{i,v'}(J')$ the upper state term value for the vibrational band $v'' \leftarrow v'$. The other variables have their usual meaning. The Einstein transition probabilities, $\bar{A}$, given by Mies (1974), have been used together with energy levels, $E_{i,v'}(J')$ by Kvifte (1959). Absolute calibration of the spectra were carried out in the field using a standard lamp. The average uncertainty in an individual temperature as derived from a 1- or 2-h integrated spectrum is ± 3 K, mainly due to uncertainty in defining the background continuum.

3. RESULTS

Nocturnal mean temperatures were obtained by averaging five or more of the 1- or 2-h individual temperatures. The individual temperatures were normally scattered throughout a 20–24 h period, and on the average covered 14 h a night. Although the length of the night possible for OH temperature determination, i.e. $\chi \geq 100°$, lasts only for about 9 h in early March, the correction due to the semidiurnal tide on the nightly average during February–March as compared to winter solstice is found to be less than 1 K (Myrabø, 1984). The nocturnal averages may thus safely be taken as the average for a 12 h period around local midnight over the entire period of observations (i.e. November–March). Because no diurnal variation of temperature amplitude obtained from OH larger than 1 K is found at Svalbard (Myrabø, 1984), the nocturnal averages are equivalent to the daily averages. Thus, no corrections have been made for the semidiurnal or diurnal variation in the temperature (Myrabø, 1984). We therefore use the expression daily averages for the average temperature obtained within each 24-h interval. The resulting daily averages for the 1983-84 winter season are given in Fig. 3. A straight line is drawn between the averages, marked with open circles. In addition to the day and month, the day

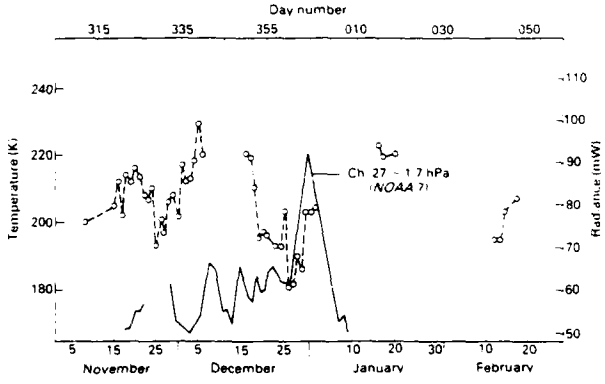

FIG. 4. DAILY MEAN TEMPERATURES FROM THE WINTER SEASON 1984/85 AS OBTAINED FROM OH (6–2) BAND NIGHT AIRGLOW EMISSIONS NEAR LONGYEARBYEN, 78 N.
The radiance level (in nW) from Ch. 27 on the *NOAA* 7 radiometer integrated over the northern polar region is also indicated (stippled line).

number is also marked along the top of the horizontal scale of the figure. The temperature is given in degrees Kelvin (K). In January and the last part of February, the 1.2 m spectrometer was used to obtain auroral spectra, resulting in the data gaps seen in the figure. The temperatures for the 1984/85 winter season are shown in Fig. 4. Figure 4 also includes the radiance level from Ch. 27 on the *NOAA* 7 radiometer (see Fig. 1), as integrated over the northern polar region during the first and mid-part of the winter. As seen from the deflection of the radiometer, a stratospheric warming occurred near the end of December.

Large variations in the temperature may occur within each daily average. An example of this is shown in Fig. 5, depicting the temperature from hour to hour during part of the very intense warming of the lower mesosphere and stratosphere in late December (see Fig. 4). An average trend drawn through the daily means (marked with filled triangles) is indicated.

Due to the large day-to-day and week-to-week

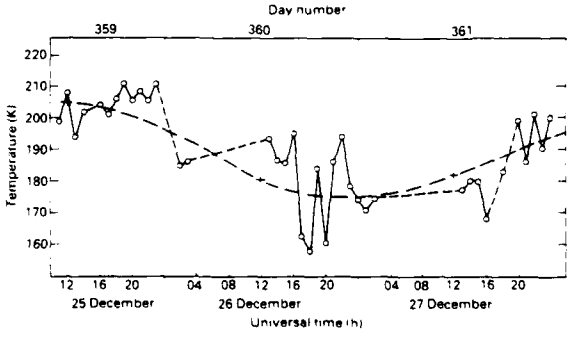

FIG. 5. ONE-HOUR INTEGRATED TEMPERATURES FROM THE OH (6–2) BAND NIGHT AIRGLOW EMISSION DURING PART OF THE INTENSE STRATOSPHERIC WARMING AT THE END OF 1984.
The daily means are marked with open circles. An average trend second degree curve is fitted to the daily means (stippled line).

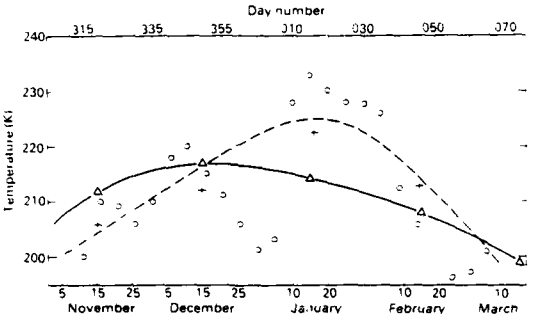

FIG. 6. TEN DAYS RUNNING AVERAGE OF THE DAILY MEAN TEMPERATURES (MARKED WITH CIRCLES) FOR THE 80/81, 82/83, 83/84 AND 84/85 WINTER SEASON AT 78°N
The monthly means are also plotted (crosses) together with the monthly means for the CIRA 1972, 70°N, 90 km, model atmosphere (triangles). A second degree best fit curve is drawn through the means, both for the model atmosphere (solid line) and for the actual monthly mean temperatures from these measurements (stippled curve).

variations in the temperature, data for both seasons have been added to investigate any seasonal trend and for comparison with model atmospheres. The daily temperatures for the 1980/81 and 1982/83 season as obtained by Myrabø (1984) have also been included. The 1980/81 and 82/83 temperatures were obtained using the OH (8–3) band and slightly different molecular constants (Myrabø, 1984). A temperature of 2 K was subtracted from the OH (8–3) band temperatures, because the OH (8–3) band emits mainly from a level 1–2 km higher in the atmosphere than the OH (6–2) band (Charters *et al.*, 1971; Myrabø, 1984; Hamwey, 1985). The temperature gradient obtained by Myrabø (1984) was assumed. Following this adjustment of the 80/81 and 82/83 temperatures, the temperatures were corrected for the differences in molecular constant used. Corrections were normally in the range 3–6 K, to be subtracted from the 80/81 and 82/83 temperatures. Thus, on average, the 80/81 and 82/83 temperatures were lowered by 5–6 K to make the data sets compatible. The maximum error introduced in the average daily means for the four seasons by employing this transformation procedure to the 80/81 and 82/83 temperatures is estimated to be less than 2 K.

Figure 6 shows the 10 day running average of the daily mean temperatures using the temperatures for all four seasons. The 10 day running averages are taken at 5 day intervals, i.e. 50% overlap. The monthly means are also plotted (crosses) together with the monthly means for the CIRA, 1972, 70°N, 90 km model atmosphere (filled triangles). A second degree best fit curve is drawn through the means, both for the model atmosphere (solid line) and for the actual monthly means of these measurements (stippled curve).

4. DISCUSSION

From Figs 3 and 4 it is seen that the day-to-day temperatures show large peak-like variations lasting for a few days to a week or two. This was also seen in the 1980/81 and 82/83 seasons (Myrabø, 1984). A similar pattern was also observed for the OI 5577 Å night airglow intensity variations from Thule (76°N) (Müllen *et al.*, 1977). As seen in Fig. 4, the relatively large and consistent cooling of the OH (6–2) temperature at the mesopause is accompanied by a warming and circulation change (Labitzke *et al.*, 1985) of the lower mesosphere and stratosphere. This was also the case during the stratospheric warming around new year in the 82/83 season (Myrabø *et al.*, 1984). Ismail and Cogger (1982) have also associated large week-to-week changes of the OI 5577 Å night airglow from Thule with minor and major stratospheric warmings. Thus, it seems established that these apparently irregular large scale temperature changes taking place over days and weeks are mainly connected to effects of the changes in the circulation pattern and temperatures in the lower mesosphere and stratosphere. They seem also to be present during seasons with no major stratospheric warmings.

From Fig. 4 it may also be seen that the cold mesopause regions occur before the lower mesosphere and stratosphere start to warm. Simultaneous unpublished mesopause temperatures from Fairbanks (65°N) during the 1984/85 stratospheric warming

seem to indicate the same pattern, i.e. a cooling of the mesopause is seen before the heating of the stratosphere take place (Viereck *et al.*, 1986).

Transmission of gravity waves into the mesosphere is controlled by the propagation in and the interaction with the environment. Phenomena as refraction, reflection and critical-level absorption due to variation in mean zonal wind ($\bar{u}$) and the square of the Brunt–Vaissala frequency (N^2) with height may cause major changes in the waves with height (selective filtering). Spatial inhomogeneities in the transmissivity and or in the gravity-wave sources are thought to be capable of exciting large scale gravity waves or planetary waves (Fritts *et al.*, 1984). Such large scale excited waves may be important in wave–wave interaction in connection with stratospheric warmings (Smith, 1985).

Gravity waves may thus be important both in the warming of the stratosphere and in the cooling of the upper mesosphere.

If the winter mesosphere and mesopause region is kept warm largely from energy deposited by breaking gravity waves originating in the lower atmosphere, a slight change in the circulation pattern of the underlying atmosphere would affect the propagation of these waves (Dunkerton and Butchart, 1984) and the heating rate. Thus, Lindzen (1981) and Holton (1983) have suggested that appearance of easterlies will inhibit propagation of quasi-stationary gravity waves to the mesosphere. This would allow the mesopause and upper mesospheric region to undergo radiative cooling. A 10–20 K per day cooling rate could occur (Chamberlain, 1978; Ebel, 1984), which is in the range of actual average cooling seen. It is also consistent with the observation of the cooling taking place before the heating is observed in the lower part of the atmosphere (Holton, 1983).

The 10 day running average temperature in Fig. 6 (average for all four seasons) also shows a peculiar drop in the temperature during the end of December followed by a very warm period in January. The standard deviation in the 10 days running average is in the range 2–5 K, which means that the December–January dip is real and has a total amplitude of 20–30 K. A closer look at the data for each year shows the tendency for a mesopause cooling to occur around New Year each year, even during 1983/84 which was not a year with a major statospheric warming (Labitzke *et al.*, 1985). No auroral effects seem to have a seasonal pattern that could account for part of the December/January "wave" in the mesopause and lower thermosphere temperature. Thus, we may conclude that this "wave" seems to be entirely associated with changes in the gravity wave activity and in the circulation, temperature or transport in the underlying atmosphere. A further consequence of this seems to be that, on the average, mesopause temperatures in the northern polar cap reach a maximum in January, and not in December as predicted by the CIRA 1972 model atmosphere.

The peculiarity that the mesopause region seems to warm up dramatically just after the cooling accompanied by the stratwarms, and somewhat compensates for the cold period, causing an extremely warm mesopause in January, cannot be explained yet. However, investigations for the coming years are planned which may provide an answer to this.

5. SUMMARY

Mesopause lower thermosphere temperatures have been deduced from spectrophotometric observations of the night airglow OH emissions close to Longyearbyen on West Spitsbergen (78° N, Lat., 15° E, Long., geographic) during the 80/81, 82/83, 83/84 and 84/85 winter seasons. A 1.2 M Ebert–Fastie spectrophotometer has been used to obtain the emission spectra with a spectral resolution of 7 Å, resolving the P_1- and P_2-lines of the OH (6–2) and (8–3) bands. A monthly average temperature maximum of 223 K is found to occur in January with monthly averages of 206, 212, 212 and 198 K, respectively for November, December, February and March. The January monthly average is about 10 K higher than the respective CIRA 1972 model atmosphere temperature at 90 km, 70° N. A relatively low temperature in late December followed by a warm mesopause in early January is seen to be consistent for all four seasons. In the 10-day running average temperature this appears as a 20–30 K amplitude temperature wave around years end. This "wave" might be associated with circulation changes (i.e. stratwarms) in the lower mesosphere and stratosphere, and physically related to the changes in the occurrence of breaking gravity waves at the mesopause caused by interaction with the general flow in the underlying atmosphere. Large hour-to-hour variations in the temperature are regularly seen, indicating the presence of gravity waves. Hourly temperatures as large as 283 K and as low as 158 K have been observed.

Acknowledgements—Financial support for this research was provided by National Science Foundation through Grant ATM-8313727 to the Geophysical Institute of the University of Alaska and by the Royal Norwegian Council for Scientific and Industrial Research through a fellowship grant. The author also wants to thank Mr Rod Viereck, Jim Baldridge and Dan Osborne for programming and technical assistance.

REFERENCES

Barnett, J. J. (1980) Satellite measurements of middle atmosphere temperature structure. *Phil. Trans. R. Soc. Lond* **296A**, 41.

Chamberlain, J. W. (1978) *Theory of Planetary Atmospheres: an Introduction to their Physics and Chemistry*, p. 32. Academic Press, New York.

Chamberlain, J. W. and Oliver, N. J. (1953) OH in the airglow at high latitudes. *Phys. Rev.* **90**, 1118.

Charters, P. E., Macdonald, R. G. and Polanyi, J. C. (1971) *Appl. Optics* **10**, 1747.

CIRA 1972 (1972) *COSPAR working group 4. COSPAR International Reference Atmosphere*. Pergamon Press, Oxford.

Deehr, C. S., Sivjee, G. G., Egeland, A., Henriksen, K., Sandholt, P. E., Smith, R., Sweeney, P., Duncan, C. and Gilmer, F. (1980) Ground-based observations of *F*-region associated with the magnetospheric cusp. *J. geophys. Res.* **85**, 2185.

Dunkerton, T. J. and Butchart, N. (1984) Propagation and selective transmission of internal gravity waves in a sudden warming. *J. atmos. Sci.* **41**, 1443.

Ebel, A. (1984) Contribution of gravity waves to the momentum, heat and turbulent energy budget of the upper mesosphere and lower thermosphere. *J. atmos. terr. Phys.* **46**, 727.

Fritts, D. C., Geller, M. A., Balsley, B. B., Chanin, M. L., Hirota, I., Holton, J. R., Kato, S., Lindzen, R. S., Schoeberl, M. R., Vincent, R. A. and Woodman, R. F. (1984) Research status and recommendation from the Alaska workshop on gravity waves and turbulence in the middle atmosphere, Fairbanks, Alaska, 18–22 July, 1983. *Bull. Am. Met. Soc.* **65**, 149.

Hamwey, R. (1985) Spectroscopy of the night airglow OH *emissions*. M. S. Thesis, Geophysical Institute, Alaska.

Holton, J. R. (1983) The influence of gravity waves breaking on the general circulation of the middle atmosphere. *J. atmos. Sci.* **40**, 2497.

Ismail, S. and Cogger, L.L. (1982) Temporal variations of polar cap OI 5577 Å airglow. *Planet. Space Sci.* **30**, 865.

Krassovsky, V. I., Potapov, B. P., Semenov, A. I., Sobolev, V. G., Shagaev, M. V. and Shefov, N. N. (1977) On the equilibrium nature of rotational temperature of hydroxyl airglow. *Planet. Space Sci.* **25**, 596.

Kvifte, G. (1959) Nightglow observations at Ås during the I.G.Y. *Geophysica norvegica* **20**, 1.

Labitzke, K., Naujokat, B., Lenschow, R., Petzoldt, K., Rajewski, B. and Wohlfart, R. C. (1985) The third winter of MAP*-dynamics, 1984/85: A winter with an extremely intense and early major warming. *Beil. Berliner WettKarte* **67**, 1985.

Lindzen, R. S. (1981) Turbulence and stress due to gravity wave and tidal breakdown. *J. geophys. Res.* **86**, 9707.

Mies, F. H. (1974) Calculated vibrational transition probabilities of OH ($X^2\pi$). *J. molec. Spectrosc.* **53**, 150.

Müllen, E. G., Silverman, S. M. and Korff, D. F. (1977) Nightglow 5577.7 nm of OI) in the central polar cap. *Planet. Space Sci.* **25**, 23.

Myrabø, H. K. (1984) Temperature variation at mesopause levels during winter solstice at 78°N. *Planet. Space Sci.* **32**, 249.

Myrabø, H. K., Deehr, C. S. and Lybekk, B. (1984) Polar cap OH airglow rotational temperatures at the mesopause during a stratospheric warming event. *Planet. Space Sci.* **32**, 853.

Myrabø, H. K., Deehr, C. S., Romick, G. J. and Henriksen, K. (1986) Mid-winter intensities of the night airglow O_2 (0–1) atmospheric band emission at high latitudes. *J. geophys. Res.* **91**, 1684.

Myrabø, H. K., Deehr, C. S. and Sivjee, G. G. (1983) Large-amplitude nightglow OH (8–3) band intensity and rotational temperature variations during a 24-h period at 78°N. *J. geophys. Res.* **88**, 9255.

Noxon, J. F. (1964) The latitude dependence of OH rotational temperature in the night airglow. *J. geophys. Res.* **69**, 4087.

Rogers, J. W., Murphy, R. E., Stair, A. T., Ulwick, J. C., Baker, K. D. and Jensen, L. L. (1973) Rocket-borne radiometric measurements of OH in the auroral zone. *J. geophys. Res.* **78**, 7023.

Sivjee, G. G. and Deehr, C. S. (1980) Differences in polar atmospheric optical emissions between mid-day cusp and night-time auroras. in *Expedition of the Polar Upper Atmosphere* (Edited by Deehr, C. S. and Holtet, J. A.), p. 199. Reidel, Dordrecht.

Sivjee, G. G., Dick, K. A. and Feldman, P. D. (1972) Temporal variations in the night-time hydroxyl rotational temperature. *Planet. Space Sci.* **20**, 261.

Smith, A. K. (1985) Wave transience and wave-mean flow interaction caused by the interference of stationary and traveling waves. *J. atmos. Sci.* **42**, 529.

Vallence-Jones, A. (1974) *Aurora*. Reidel, Dordrecht.

Viereck, R., Myrabø, H. K., Deehr, C. S. and Romick, G. J. (1986) Lower thermosphere and mesopause region temperatures at Fairbanks (65°N) and Longyearbyen (78°N) during the stratospheric warming event around 1 January 1985 (in preparation).

Witt, G., Stegman, J., Solheim, B. and Llewellyn, E. J. (1979) A measurement of the O_2 ($b^1\Sigma_g^+ - X^3\Sigma_g^-$) atmospheric band and the OI(^1S) green line in the nightglow. *Planet. Space Sci.* **27**, 341.

Planet. Space Sci. Vol. 32, No. 3, pp. 263–271, 1984
Printed in Great Britain

0032-0633/84 $3.00 + .00
© 1984 Pergamon Press Ltd.

MID-WINTER HYDROXYL NIGHT AIRGLOW EMISSION INTENSITIES IN THE NORTHERN POLAR REGION

H. K. MYRABØ* and C. S. DEEHR
Geophysical Institute, University of Alaska, Fairbanks, AK 99701, U.S.A.

(*Received in final form* 28 *June* 1983)

Abstract—Ground-based spectrophotometric measurements of night airglow OH (8–3) band absolute intensities in the polar cap region (78.4°N) during winter solstice are reported. A mean value of 425 ± 40 R is found for the absolute intensity of the OH (8–3) band. Maximum and minimum daily mean values were 770 and 320 R respectively with hourly mean values ranging from 180 to 1020 R. Neither a winter solstice minimum or maximum in the intensity is obvious from the data. No consistent correlation was found between the absolute intensity and geomagnetic and solar activity. A mean transport of O and O_3 into the polar cap region corresponding to a meridional wind speed of at least 20 m s^{-1} at 90 km height seems necessary to maintain the observed intensity. A dominant semidiurnal tide component is found in the intensity data, both on a 20-day and a 3-day time scale.

1. INTRODUCTION

The night airglow emissions originating from the $X^2\Pi_i - X^2\Pi_i$ transition of the hydroxyl molecule are confined to the 80–95 km region of the atmosphere. The emissions are a consequence of the ozone reaction (Bates and Nicolet, 1950; Herzberg, 1951):

$$O_3 + H \rightarrow OH(v' \leqslant 9) + O_2. \quad (1)$$

Additional mechanisms have also been proposed (Nicolet, 1970; Krassovsky, 1972) but have not so far been shown to contribute significantly compared to the ozone mechanism (Evans and Llewellyn, 1972; Harrison and Kendall, 1973; Llewellyn and Long, 1978; Takeuchi *et al.*, 1981; Takahashi and Batista, 1981; Myrabø *et al.*, 1983).

Measurements of the OH emission alone or together with other night airglow emissions such as the OI 5577 and 6300 Å lines and the $O_2(^1\Sigma)$ and $(^1\Delta)$ bands may be used as a means of remotely monitoring the spatial and temporal variations of the odd oxygen concentration as well as the dynamical behavior of the atmosphere. Neutral temperatures at the mesopause level may be found by analyzing the rotational line intensity distribution of the emission bands (Kvifte, 1959).

Extensive studies of the OH night airglow have been carried out at low and mid-latitudes in order to clarify the excitation mechanism and behavior of the OH night airglow itself, and also as a means of remotely studying other atmospheric parameters and processes, such as temperature, wind, composition, tides, gravity waves, etc. (Meinel, 1950; Dufay, 1951; Chamberlain and Roesler, 1955; Fedorova, 1959; Kvifte, 1961; Noxon, 1964; Shefov, 1969a, b, 1970; Hunten, 1971; Sivjee *et al.*, 1972; Krassovsky, 1972; Wiens and Weill, 1973; Vallance-Jones, 1973; Good, 1976; Petitdidier and Teitelbaum, 1977; Krassovsky *et al.*, 1977; Moreels *et al.*, 1977; Fishkova, 1978; Shagaev, 1980; Takahashi and Batista, 1981).

By contrast, very little is known regarding airglow emission in the winter polar cap region. Reed (1976) utilized photometric data at 6230 Å (50 Å bandwidth) from the *Ogo 4* spacecraft and found a strongly variable enhanced intensity level during part of the 1967/68 winter at high latitudes that seems not totally explainable by auroral contamination. The enhancements may be explained by an enhanced OH night airglow emission and partly by an increased nightglow continuum from NO_2 (Gadsden and Marovich, 1973). Walker and Reed (1976) showed that the enhanced levels probably were connected with stratospheric warming events. In both these works which are based on photometric data, auroral contribution to the enhancements cannot be ruled out and it seems difficult to attribute the enhancement to a specific emission, i.e. OH or NO_2.

Other airglow measurements in the polar cap region are the OI 5577 Å emission study carried out at the Antarctic station using photographic equipment (Sandford, 1964). Müllen *et al.* (1977) report ground-based measurements of the OI 5577 Å emission from Thule, Greenland. They found the OI 5577 Å night airglow emission in polar cap region to be quite different from that observed at mid- and low latitudes. No significant diurnal variation was found in the data; large amplitude variation, on the time scale minutes to hours are relatively common and for periods of 4–19

*On leave from Norwegian Defense Research Establishment, N-2007, Kjeller, Norway.

days strongly enhanced levels are found to exist. This pattern is similar to that found in the OH intensity reported here, and may point toward a common source. They also show that the intensity distribution is different from lower latitudes (i.e. showing a skewed bimodal distribution for polar region compared to a skewed unimodal at low and mid-latitude) also found by Sandford (1964). A correlation between boundary crossing of the interplanetary field and the sign of the gradient of the airglow intensity (i.e. increasing or decreasing slope) was also found to exist for two of the observing seasons.

Ismail and Cogger (1982) extended the study by Müllen *et al.* (1977) using data from the *ISIS-2* satellite. They attributed the enhanced OI 5577 Å emission periods to increased meridional transport of oxygen into the polar cap and showed that stratospheric warming events might result in an enhanced polar cap OI 5577 Å airglow.

In two recent papers, Myrabø *et al.* (1983) and Myrabø (1983) have reported ground based measurements of OH emissions from Spitsbergen (78.4°N) during winter solstice condition. Large amplitude variation of both intensity and temperature (up to ± 70 K in temperature) is found in the internal gravity wave period range. On a larger time scale, the daily mean temperatures show a wave-like pattern with deviations from the mean, each lasting for about 3–10 days. A semi-diurnal but no diurnal variation in the temperature is also evident.

The purpose of this paper is to continue the study of the OH emission in polar cap region, utilizing the 1982/83 season absolute intensity measurements at winter solstice. From results reported in the previous papers and in this paper, it seems obvious that the OH intensity and temperature pattern in polar cap regions are mainly governed by large and small scale transport and wave phenomena. A disturbed OH intensity and temperature pattern, i.e. strongly fluctuating with time with periods from minutes to days, seems more to be the rule than the exception.

2. OBSERVATIONS AND DATA REDUCTION

The OH emission data employed in this work were part of measurements undertaken during the 1982/83 campaign of the Multi-National Svalbard Auroral Expedition (Deehr *et al.*, 1980) close to Longyearbyen on West Spitsbergen (78.4°N, Lat., 15°E Long. geographic).

OH emissions are normally predominant in the near i.r. part of the night sky spectrum. Contamination by auroral molecular emission as in the auroral zone (Vallance-Jones, 1974; Meriwether, 1975) is most of the time insignificant at Spitsbergen because of a much lower occurrence frequency of auroras (Stringer and Belon, 1967) and because auroras at these latitudes are generally at a higher altitude and emit mainly atomic lines (Sivjee and Deehr, 1980). Thus, a normal, high-responsivity auroral spectrophotometer operated at a resolution of 2000 (4 Å bandwidth) or more may be used to obtain measurement of the OH bands and lines clearly resolved from auroral emissions.

At the Longyearbyen Observatory, a 1 m and a 1.2 m high-throughput Ebert–Fastie spectrometer are coupled to a mini-computer recording in the photon-counting mode. The 1 m instrument, used for the measurements reported here, is further described by Dick *et al.* (1970) and Sivjee *et al.* (1972).

The spectrophotometer was normally operated for 24 h a day from December 1982 to January 1983. For the absolute intensity measurements reported here, only periods with clear sky and stable atmospheric transmission were selected. The transparency of the atmosphere was checked by visually observing a known sequence of non-variable stars. A 10–20% intensity variation of the stars could routinely be detected. Within periods where detectable transparency variation occurred, data were not utilized. Spectra were also rejected when Fraunhofer lines occurred during twilight and full moon periods.

The spectrophotometer was pointed towards the zenith and the OH (8–3) band *P* lines in the 7280–7410 Å region were scanned in 8 or 32 s using the spectrophotometer in the second order with a 1 or 2 mm slit corresponding to a bandwidth of 1.5 and 3 Å respectively. Each scan was recorded on magnetic tape. Individual rotational temperatures were calculated from 1- and 3-h integrated scans, by employing Kvifte's method using the intensity ratio of the $P_1(2)$, $P_1(3)$, $P_1(4)$ and $P_1(5)$ lines (Kvifte, 1959). The total band intensity was calculated using the well-known formula for the variation of the intensity of the lines in a rotational–vibrational band as a function of total angular momentum J (Herzberg, 1950)

$$I_{v'v''} = \sum_{J=J_0}^{N} C \cdot S_{J'J''} (J) \lambda_{J'J''}^{-3} e^{-F_{v'}(J)hc/kT}$$

where $I_{v'v''}$ is the total $v'-v''$ band intensity, C a constant, $S_{J'J''}(J)$ the line strength, $F_{v'}(J)$ the rotational term value in the upper vibrational level v', λ the wavelength of the line, and h, c, k and T have their usual meaning. The total OH (8–3) band intensity was thus calculated (and the constant C determined) using the absolute intensity of the $P_1(3)$ line together with the temperature T calculated from the P_1 lines using Kvifte's method. Summations for the R, Q and P branches up to $N = 9$ were performed. The line strength of Hönl and London

(1925) and the $F(J)$ values as determined from Dieke and Crosswhite (1948) and Kvifte (1959) have been used. Absolute intensity calibration was performed in the field using a standard lamp and a diffusing screen.

Probable error for a single measurement (i.e. 1- or 3-h integration) is estimated to be ± 3 K in the temperature and less than 10% in the relative intensity. The uncertainty of the absolute scale is about 20% mainly due to calibration uncertainty. The absolute intensity given is not corrected for atmospheric extinction. Corrected emission intensity, i.e. at the emission height, may be found by applying an extinction coefficient of 0.2 (Myrabø, 1979) and a ground albedo for snow at the appropriate wavelength of 0.7 (Myrabø *et al.*, 1982).

Example of the quality of the data used is given elsewhere (Myrabø, 1983). Daily mean values are based on 12–24-h averages of the 1- and 3-h values. Auroral activity was monitored by the intensity of the 7320/30 Å OII lines. Additional care was taken to assure that there was no contamination from N_2 1P and other auroral molecular emissions.

3. RESULTS AND DISCUSSION

3.1. *Winter solstice behavior of the intensity*

Absolute intensities of the OH (8–3) band for each day as derived from hourly and three-hourly means are plotted in Fig. 1. The daily means are indicated by filled squares and straight lines are drawn between each mean. Dashed lines indicate that intensities for one or more days are missing. Some of the measurements did not cover 24 h. Where less than a 12-h period of data were missing, interpolation was performed using mean values on each side averaged over the hours of missing data. Daily (24-h) mean values were then calculated from the original and the interpolated data. The OH rotational temperature data for the same period as given by Myrabø (1983) is added to the figure for comparison. In addition, the daily mean value of the planetary geomagnetic activity index K_p is shown together with direction of the interplanetary magnetic field (i.e. +, −). Days with geomagnetic storm sudden commencements are indicated by a ▲ in the lower part of the figure.

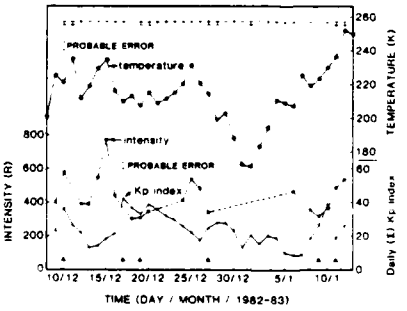

FIG. 1. DAILY MEAN VALUES OF THE OH (8–3) BAND INTENSITY ARE GIVEN WITH STRAIGHT LINES DRAWN BETWEEN THE MEANS. Dashed lines indicate data for one or more days is missing. Planetary geomagnetic disturbance index K_p and OH rotational temperature are also given. Days with geomagnetic storm sudden commencements and the direction of interplanetary magnetic field are indicated by ▲ and +, − respectively.

The dataset consists of absolute intensities from about 150 000 individual spectra recorded during a total time of 402 h covering 20 days. Even though there are several periods with missing data (due to bad weather) Fig. 1 shows neither maximum nor minimum around winter solstice. An irregular intensity fluctuation around the baseline mean of 425 ± 40 R, seems to be a better description of the 1 month winter solstice period covered. This is somewhat in disagreement with the results and suggestions reported by Shefov (1969a). He reports a winter maximum in the OH emission intensity at latitudes poleward of approx. 35° (geographic). Both the data from Yakutsk (62°N, geographic) and Loparskaya (68°N, geographic) shows a very strong intensity maximum around winter solstice. Independent measurements by Visconti *et al.* (1971) at 42°N and by Harrison *et al.* (1971) at 51°N also shows winter intensity maxima in accordance with Shefov (1969a). On the other side, measurements by Kvifte (1967) from Tromsø (70°N, geographic) reveals a clear tendency of a declining intensity during the autumn towards the end of November pointing towards a minima at winter solstice.

Because the main production of O is related to solar photodissociation (Giachardi and Wayne, 1972; Simonaitis *et al.*, 1973; Moreels *et al.*, 1977), by the process

$$O_2 + h\nu \rightarrow O + O, \tag{2}$$

one might expect the diminishing production of O in the 24-h polar night to lead to a decrease in the OH emission, i.e.

$$O + O_2 + M \rightarrow O_3 + M \tag{3}$$

and

$$O_3 + H \rightarrow OH + O_2. \tag{4}$$

The results reported by Kvifte (1967) and the winter solstice minimum of the OI 5577 Å night airglow emission in polar cap regions found by Müllen *et al.* (1977) also suggest that one rather should expect a

winter solstice minimum than a maximum at these latitudes (i.e. > 70°N). However, the one season of data presented here do not rule out a broad (> 1 month) minimum or maximum. The dominance of the wavelike pattern may also partly mask an eventual trend around solstice.

On a planetary scale the absolute intensity of OH emission is found to be at a minimum around 25° (geographic), increasing steadily poleward towards 68°N (Shefov, 1969a). Absolute intensity measurements above 70° latitude have only been recorded from airborne platforms like those by Noxon (1964) and by Sivjee *et al.* (1972) providing data only for a few hours not sufficient to establish any seasonal trend or mean value. The mean winter solstice value of 425 ± 40 R found here for the OH (8–3) band is therefore the first mean value based on a more extensive data set. It is close to the yearly mean found by Krassovsky *et al.* (1956) at 55°N. Compared with more recent measurements, it almost duplicates the 2 yr mean of 408 ± 40 R reported by Takahashi *et al.* (1977) from Brazil (23°S) which is very close to the normalizing latitude employed by Shefov (1969a) in his work, i.e. the latitude of minimum intensity of the OH emission. Thus, using the 2 yr mean Brazilian value to calculate an expected winter solstice maximum at 68°N employing Shefov's (1969a) latitudinal and seasonal variations, an emission intensity of ~950 R is found. Extrapolating this value according to Shefov's results, i.e. a latitudinal increase and a winter solstice maximum, gives an even higher value at ~78°N by 20–30%, i.e. ~1.2 kR. If we instead assume a winter solstice minimum at 80°N, of the same order, i.e. ~30%, an emission intensity of ~530 R is calculated for winter solstice condition at 80°N. The latter value is in much better agreement with the actual value observed.

The data material gathered so far, thus suggest a winter solstice minimum of OH emission rather than a maximum at extreme high latitudes, i.e. > 70°. This is in agreement with the OI 5577 Å nightglow emission minimum in polar cap regions reported by Müllen *et al.* (1977). However, data for more seasons should be gathered before making any firm conclusions on this.

3.2. *Relation to solar and geomagnetic activity*

It was first suggested by Krassovsky (1956) that OH emission intensity should be affected by geomagnetic disturbances. Shefov (1959) reported an intensification of the OH emission intensity during magnetically disturbed periods. Later study by Berg and Shefov (1962) and Saito (1962) failed to show a definite correlation between OH emission intensity and geomagnetic activity.

In a later work Shefov (1969a), using an impressive amount of data, gives experimental evidence for a direct effect on the OH emission intensity and temperature from geomagnetic disturbances. He found a wavelike disturbance in the intensity with an amplitude up to 70% of the OH emission intensity at Zvenigorod (55°N) travelling equatorward from the auroral zone with an apparent speed of 5–10 m s^{-1}. The amplitude decreased as the disturbance moved equatorward.

Theoretical calculations by Maeda (1968) and Maeda and Aikin (1968) concerning the dissociation of O_2 molecules in the case of impact of electrons at the appropriate altitude, show the effects to be very small on the O and O_3 concentration. Dissociation of O_2 associated with auroral substorm directly, seems therefore not sufficient to explain Shefov's data. More recent discussion (Brekke, 1977) concerning effects from Joule heating and ion drag heating on mesospheric and thermospheric temperatures also concludes that the energy present in an auroral substorm seems not sufficient to alter the mean temperature significantly in the 90 km region.

From comparison between the variation in the daily mean OH emission intensity and planetary geomagnetic disturbance index K_p, time of storm sudden commencement and boundary crossing of the interplanetary magnetic field, no consistent correlation can be seen from Fig. 1 between OH emission intensity and the other parameters. Applying 3-h averages instead of daily averages and allowing for time delays, still leaves us with an inconsistent correlation, i.e. positive correlation between one or more peaks may be found while a negative or no correlation applies to the rest of the data. This is very similar to the findings by Saito (1962) and Weill and Christophe-Glaume (1967). While Shefov (1969a) argued that these observations showed negative results because the sites were too far from the auroral regions and/or data only covered a couple of days, this objection cannot be held against our data. Svalbard is far more closely surrounded by the auroral oval than Zvenigorod.

One may, therefore, conclude that the data so far available indicate a very small or no direct correlation between daily mean (or 3-h mean) OH emission intensities and geomagnetic disturbances in polar cap regions. It is evident that this also applies to the OH rotational temperature as given in the upper part of Fig. 1.

3.3. *Relation to transport and wave phenomena*

3.3.1. *Gravity waves.* Figure 1 shows that the behavior of intensity and temperature during December reveals a similar pattern. It may be described as consisting of a relatively stable level with three main

enhanced periods. This is particularly obvious for the temperature. In an earlier paper when only the temperature pattern was available, Myrabø (1983) argued that enhanced temperatures lasting for a few days most likely were due to gravity wave effects, i.e. direct energy deposition as a consequence of the breakdown of the waves (Hines, 1965) and/or turbulent diffusion increased by gravity wave action (Zimmerman and Murphy, 1977) transporting warmer air down from above. The intensity enhancements simultaneous with temperature enhancements further strengthen this suggestion. Increased turbulent diffusion produced by gravity waves may be seen to be a sufficient mechanism to explain both the enhanced intensity and temperature levels by vertical mixing of oxygen and warmer air from above. Increased turbulent diffusion was successfully applied by Moreels *et al.* (1977) in an oxygen–hydrogen atmospheric model to simulate mid- and high latitude observed deviations from a chemical production and loss pattern. Harrison *et al.* (1971) also pointed out a change in the downward transport or height of the oxygen profile as an explanation of observed enhancements in the OH emission intensity.

Unfortunately, due to consistent clouds or mist, only a few days of absolute intensity measurements were available during January. However, both the mean intensity later in January and the behavior of the daily means seem to be not significantly different from December.

3.3.2. *Stratospheric warming.* A stratospheric warming is normally associated with a cooling of the mesosphere (Labitzke, 1977, 1980; Schoeberl, 1978). Connected with such a warming is also a large-scale redistribution and mixing of the upper atmosphere (McInturff, 1978; Labitzke, 1981) that is expected to result in a large increase in the OH emission intensity (Fukuyama, 1977; Walker and Reed, 1976; Fishkova, 1978). The cold mesopause during New Year 1983 does coincide with a stratwarm event (Naujokat *et al.*, 1983), but we can hardly see any large scale enhancement of the OH emission intensity following this event. This is opposite to results reported by Walker and Reed (1976). Thus, it seems that a stratwarm is not necessarily needed to result in a large enhancement of OH emission intensities in the polar regions.

3.3.3. *Meridional transport.* As previously mentioned in Section 3.1, there is no production of odd oxygen compounds by solar photodissociation in the polar cap region during mid-winter. To keep the OH emission intensity at the observed 400 R level for the (8–3) band requires a certain meridional transport from the terminator. An approximate calculation was made assuming

(1) the meridional flux to replace the loss (mainly by equation (1)).

(2) a loss rate of 4×10^5 $[O_3]$ cm^{-3} s^{-1} at the OH emission peak (90 km) (Moreels *et al.*, 1977),

(3) a dark polar cap 650 km radius at 90 km height.

This results in a meridional wind speed of the order of 20 m s^{-1}, which may be compared with the 9 m s^{-1} semidiurnal tide temperature associated wind speed derived from part of the December temperature data presented in Fig. 1 (Myrabø, 1983). Nisbett and Glenar (1977) have analyzed data from a series of high latitude vapor trail experiments and arrived at a meridional transport of 50 m s^{-1} into the polar cap region in the altitude range 100–110 km. Ismail and Cogger (1982) from OI 5577 Å airglow measurements required meridional wind speed into the polar cap of 10–20 m s^{-1} to explain the observed OI 5577 Å intensity and variations.

Assuming that a significant fraction of the O_3 is transported across the polar cap, an even higher wind speed than 20 m s^{-1} would be needed. To explain the intensity gradients of the enhanced periods and the levels reached, a meridional wind speed up to approx. 40 m s^{-1} for some hours is needed. This seems to be rather high for the particular altitude range under consideration (i.e. ~90 km), but Deehr *et al.* (1966) observed the effects at 67°N, 145°W of an Li release from 58°N, 95°W within 12 h implying an average speed of 60 m s^{-1}. Even though the release was near 160 km altitude, the Li was at the mesopause by the time of the observation. Vertical mixing of oxygen from above could be one possible source in addition to meridional transport.

3.4. *Short term behavior—intensity and temperature correlations*

Fluctuations in both OH emission intensity and rotational temperature in the gravity wave period range (i.e. ~5 min or more) with amplitudes from ±20 K in temperature and ±20% intensity are not uncommon for OH measurements generally. These fluctuations appear now and then at all latitudes, but it is not regular behavior (Shefov, 1969a; Wiens and Weill, 1973; Takahashi *et al.*, 1974; Misawa and Takeuchi, 1978).

From OH emission data obtained during the 1980/81 observed season at Longyearbyen, it became clear that very large amplitude regular and irregular oscillations in both intensity and temperature also could occur in the polar cap region. A special event, believed to be due to the passage of gravity waves, with amplitudes up to ±70 K in temperature within a few hours was reported by Myrabø *et al.* (1983).

OH data obtained in 1982.83 further confirm that medium-to-large amplitude oscillations in both temperature and intensity are not exceptional for OH emissions in the polar cap region.

As found from observations at $F2$ region heights (Thome, 1968; Shashun'Kina and Yudovich, 1980) substorms and geomagnetic disturbances are likely to generate internal gravity waves. Internal gravity waves, launched from geomagnetic disturbances and travelling downward into the mesopause region, though not containing enough energy to alter the mean temperature significantly, may cause OH temperature and intensity oscillations around the mean values. Observations by Shagaev (1974) and Krassovsky *et al.* (1977) showed that at least some of the gravity wave events recorded at mid- and high latitudes near the mesopause probably originate in the auroral zone and that they were connected with geomagnetic disturbances.

Figure 2 shows a 75-h (i.e. ~3 days) continuous record of the OH intensity and temperature as obtained from 1-h integrations of emission spectra. This seems to represent a relatively normal behavior, and as can be seen, considerable variations in both temperature and intensity take place.

The correlation between intensity and temperature for the OH emission has been the subject of many papers and widely different and seemingly opposing results have been reported, i.e. both positive, negative and no correlation (Takahashi *et al.*, 1974, 1977; Misawa and Takeuchi, 1978; Visconti *et al.*, 1971; Harrison *et al.*, 1971; Shefov, 1970; Takeuchi *et al.*, 1981).

The 400 h of data, presented in Fig. 2, cover an equivalent time period of about 50 nights of observations at mid- and low latitudes, assuming 8 h as a typical observing night. Choosing separate 8-h periods corresponding to 10–15 nights we are able to produce both positive, slightly negative and insignificant correlation between temperature and intensity. Consideration only of the data between 25 December 1300 U.T. and 27 December 0700 U.T., altogether 39 points, results in a correlation coefficient of 0.81. On the other hand, the data from 26 December 1600 U.T. to 27 December 2200 U.T., consisting of 30 points, gives a negative correlation, i.e. −0.09. The negative correlation is not significant. Figure 3 shows an intensity–temperature plot in the case of a correlation coefficient of 0.81. The above analyses were also performed using 30-min integrated spectra, thus providing twice the number of points, i.e. 78 and 60 respectively. The result was not significantly different.

For limited time intervals, typically less than 12 h, a higher correlation coefficient could sometimes be obtained by shifting the intensity and temperature curves relative to each other. Whether this indicates a real phase shift between intensity and temperature, as reported by some authors (Noxon, 1978; Takahashi *et al.*, 1979) is difficult to justify because applying the same time shift, in other cases results in the opposite effect, i.e. lowers the correlation coefficient.

Mechanisms, such as horizontal transport, vertical transport, turbulent mixing, diffusion, tides and gravity waves act differently on the temperature and the intensity. We believe that the rather confusing patterns observed in both intensity and temperature, resulting in positive, negative and insignificant correlation, and sometimes all three possibilities within a 24-h period, only reflect the dynamical and chemical complexity of the OH-emitting region. From data so far collected,

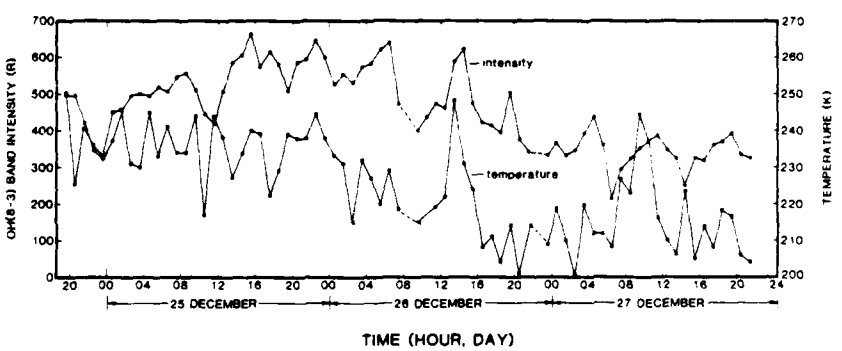

FIG. 2. 1-h AVERAGES OF THE OH(8–3) BAND INTENSITY AND ROTATIONAL TEMPERATURE AS OBTAINED EACH HOUR DURING A 3-DAY PERIOD IN 1982.

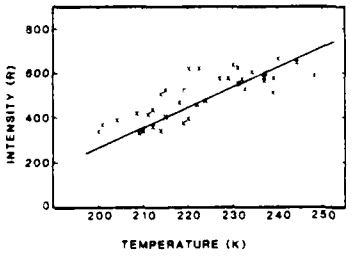

FIG. 3. OH (8–3) BAND INTENSITY–TEMPERATURE PLOT USING THE MEASUREMENTS BETWEEN 25 DECEMBER 1300 U.T. TO 27 DECEMBER 0700 U.T. 1982 (SEE FIG. 2).
The best-fit linear relationship is indicated by the least square regression analysis line. The slope is 11.2 R K.

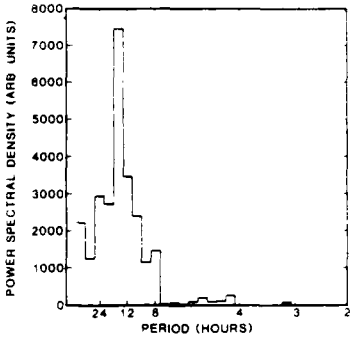

FIG. 4.

it seems that transport and wave phenomena are dominant factors in the overall behavior of the OH emitting layer in polar regions.

3.5. *Tidal components*

In a previous paper Myrabø (1983) reported the presence of a semidiurnal tide in the December 1982 temperature data by applying a superimposed epoch analysis of 19 consecutive days. A diurnal tide component was not evident.

Using Fourier analysis of the intensity data covering the same time interval, a dominant power peak around 12 h is found with far less power around 24 h. According to a model calculation by Forbes (1982) one should expect the diurnal tide mode to be dominant at high latitudes and polar regions. Spizzichino (1969) and Teitelbaum and Blamont (1975) have argued that random interaction with gravity waves has more important affect on the first diurnal mode than on the second. Thus, the effect of averaging over a period of 19 days could be to cancel out the diurnal mode. To check this we have applied Fourier analysis to the three consecutive days of intensity data shown in Fig. 2. As seen from the result presented in Fig. 4, the semidiurnal tide mode is again the dominant mode. The energy seen around 4–5 h and around 3 h are on the limit of what is significant, and may partly be due to side lobes appearing from the Fourier analysis and noise in the intensity data.

The finding of the semidiurnal tide mode also to dominate on a time scale as short as 3 days may be interpreted to be due to a very high occurrence frequency of gravity waves effectively interacting with the diurnal tide mode but not with the semidiurnal. The dominance of the semidiurnal tide in the intensity data also confirms our previous result using the temperature data (Myrabø, 1983).

4. SUMMARY

Ground-based observations of atmospheric OH emission intensity and temperature have been carried out at 78°N during December and January 1982/83. The results from the analysis of the temperature data is reported elsewhere (Myrabø, 1983).

A mean value of 425 ± 40 R is found for the absolute intensity of the OH (8–3) band. Maximum and minimum daily mean values were 770 and 320 R respectively, while the hourly mean values ranged from 180 to 1020 R.

The daily main values of the intensity show large amplitude variations qualitatively very similar to those found in the OI 5577 Å airglow emission in polar cap regions (Müllen *et al.*, 1977). There is, however, no obvious minimum or maximum seen within the 1 month-long period covered around solstice as there was for the OI 5577 Å airglow emission (Müllen *et al.*, 1977). A broad minimum or maximum cannot be ruled out, however the relatively low mean value of 425 ± 40 R rather indicates a minimum than a maximum. The lack of production of O by photodissociation of O_2 in the polar cap region during the polar night also suggest a minimum. The flux of O and O_3 necessary to keep the OH emission at the observed level indicates a meridional transport corresponding to a wind speed of at least 20 m s^{-1} at 90 km height. However, vertical transport induced by gravity waves and mixing would lower the necessary wind speed considerably.

The daily mean OH emission intensity and temperature show no evidence of any consistent correlation with geomagnetic or solar activity.

A dominant semidiurnal tide component in the OH intensity is found and strongly confirms the previous finding of the same variation in the temperature data (Myrabø, 1983). Even on a time scale of three days, the semidiurnal component is dominant. The power spectra appearing from Fourier analysis barely reveals any peak around 24 h, i.e. the diurnal component.

From the OH data gathered so far, it seems that transport and wave phenomena are the dominant mechanisms defining the behavior of both OH intensity and temperature. Further airglow observations are necessary to understand the complex mesopause region dynamics and photochemistry in the polar regions.

Acknowledgements—Financial support for this research was provided by National Science Foundation through grants ATM80-12718 and ATM82-00114 to Geophysical Institute of the University of Alaska. One of us (HKM) was supported by a fellowship grant from Royal Norwegian Council for Scientific and Industrial Research.

REFERENCES

Bates, D. R. and Nicolet, M. (1950) The photochemistry of atmospheric water vapor. *J. geophys Res.* **55**, 301.

Berg, M. A. and Shefov, N. N. (1962) Emissions of the hydroxyl bands and of the (0–2) λ 8645 Å atmospheric band of oxygen in the nightglow. *Planet. Space Sci.* **9**, 1.

Brekke, A. (1977) Auroral effects on neutral dynamics, in *Dynamical and Chemical Coupling Between the Neutral and Ionized Atmosphere*. (Edited by Grandal, B. and Holtet, J. A.), p. 313. Reidel, Dordrecht.

Chamberlain, J. W. and Roesler, F. L. (1955) The OH bands in the infrared airglow. *Ap. J.* **121**, 541.

Deehr, C. S., Romick, G. J. and Belon, A. E. (1966) An observation of artificial lithium twilight emission. *J. Atmos. Sci.* **23**, 362.

Deehr, C. S., Sivjee, G. G., Egeland, A., Henriksen, K., Sandholt, P. E., Smith, R., Sweeney, P., Duncan, C. and Gilmer, F. (1980) Ground-based observations of *F*-region associated with the magnetospheric cusp. *J. geophys. Res.* **85**, 2185.

Dick, K. A., Sivjee, G. G. and Crosswhite, H. M. (1970) Aircraft airglow intensity measurements; variations in OH and OI (5577). *Planet. Space Sci.* **18**, 887.

Dieke, G. H. and Crosswhite, H. M. (1948) Bumblebee Series, John Hopkins Univ. Rep. No. 87.

Dufay, J. (1951) Bandes d'emission des molecules OH et O_2 dans le spectre du ciel nocturne, entre 9000 et 11 000 Å. *Ann. Geophys.* **7**, 1.

Evans, W. F. J. and Llewellyn, E. J. (1972) Excitation rates of the vibrational levels of hydroxyl and nightglow intensities. *Planet. Space Sci.* **20**, 624.

Fedorova, N. I. (1959) Hydroxyl emission in the upper atmosphere (translated title). *Izv. Akad. Nauk. SSSR. Ser. Geofiz.* **6**, 836.

Fishkova, L. M. (1978) Intensity fluctuations of the nocturnal emission of the upper atmosphere during stratospheric warmings. *Geomagn. Aeron.* **18**, 375.

Forbes, F. M. (1982) Atmospheric tides: The solar and lunar semidiurnal components. *J. geophys. Res.* **87**, 5241.

Fukuyama, K. (1977) Airglow variations and dynamics in the lower thermosphere and upper mesosphere—III. Variations during stratospheric warming events. *J. atmos. terr. Phys.* **39**, 317.

Gadsden, M. and Marovich, E. (1973) The nightglow continuum. *J. atmos. terr. Phys.* **35**, 1601.

Giachardi, G. J. and Wayne, R. P. (1972) *Proc. R. Soc. Lond.* **A330**, 331.

Good, R. E. (1976) Determination of atomic oxygen density from rocket borne measurement of hydroxyl airglow. *Planet. Space Sci.* **24**, 389.

Harrison, A. W. and Kendall, D. J. W. (1973) Airglow hydroxyl intensity measurements 0.6–2.3 μm. *Planet. Space Sci.* **21**, 1731.

Harrison, A. W., Evans, W. F. J. and Llewellyn, E. J. (1971) Study of the (4–1) and (5–2) hydroxyl bands in the night airglow. *Can. J. Phys.* **49**, 2509.

Herzberg, G. (1950) *Spectra of Diatomic Molecules*. Van Nostrand, New York.

Herzberg, G. (1951) The atmosphere of planets. *J. R. Astron. Soc. Can.* **45**, 100.

Hines, C. O. (1965) Dynamical heating of the upper atmosphere. *J. geophys. Res.* **70**, 177.

Hönl, H. and London, F. (1925) *Z. Phys.* **33**, 803.

Hunten, D. M. (1971) Airglow-introduction and review, in *The Radiating Atmosphere* (Edited by McCormac, B. M.), p. 3. Reidel, Dordrecht.

Ismail, S. and Cogger, L. L. (1982) Temporal variations of polar cap OI 5577 Å airglow. *Planet. Space Sci.* **30**, 865.

Krassovsky, V. I. (1956) Infrared night airglow as a manifestation of the process of oxygen recombination, in *Airglow and Aurora* (Edited by Armstrong, F. B. and Dalgarno, A.), p. 193. Pergamon Press, Oxford.

Krassovsky, V. I. (1972) Infrasonic variations of OH emission in the upper atmosphere. *A. Geophys.* **28**, 739.

Krassovsky, V. I., Potapov, B. P., Semenov, A. I., Shagaev, M. V., Shefov, N. N., Sobolev, V. G. and Toroschelidze, T. I. (1977) Internal gravity waves near the mesopause and the hydroxyl emission. *A. Geophys.* **33**, 347.

Kvifte, G. (1959) Night glow observations at Ås during the I.G.Y. *Geophys. Norvegica* **20**, 1.

Kvifte, G. (1961) Temperature measurements from OH bands. *Planet. Space Sci.* **5**, 153.

Kvifte, G. I. (1967) Hydroxyl rotational temperatures and intensities in the nightglow. *Planet. Space Sci.* **15**, 1515.

Labitzke, K. (1977) Stratospheric–mesospheric mid-winter warmings, in *Dynamical and Chemical Coupling Between the Neutral and Ionized Atmosphere* (Edited by Grandal, B. and Holtet, J. A.), p. 17. Reidel, Dordrecht.

Labitzke, K. (1980) Climatology of the stratosphere and mesosphere. *Phil. Trans. R. Soc. Lond.* **A296**, 7.

Labitzke, K. (1981) Stratospheric–mesospheric mid-winter disturbances: A summary of observed characteristics. *J. geophys. Res.* **86**, 9665.

Llewellyn, E. J. and Long, B. H. (1978) The OH Meinel bands in the airglow—the radiative lifetime. *Can. J. Phys.* **56**, 581.

Maeda, K. (1968) The auroral O_2-dissociation and the infrared OH emission. *A. Geophys.* **24**, 173.

Maeda, K. and Aikin, A. C. (1968) Variations of polar mesospheric oxygen and ozone during events. *Planet. Space Sci.* **16**, 371.

McInturff, R. M. (1978) Stratospheric warmings: Synoptic, dynamic and general-circulation aspects. *NASA Ref. Publ.* 1017.

Meinel, A. B. (1950) OH emission bands in the spectrum of the night sky. *Ap. J.* **111**, 555.

Meriwether, J. W. (1975) High latitude airglow observations of correlated short term fluctuations in the hydroxyl Meinel 8–

3 band intensity and rotational temperature. *Planet. Space Sci.* **23**, 1211.
Misawa, K. and Takeuchi, I. (1978) Correlations among O_2 (0–1) atmospheric band, OH (8–3) band and [OI] 5577 Å line among $P_1(2)$, $P_1(3)$ and $P_1(4)$ lines of OH (8–3) band. *J. atmos. terr. Phys.* **40**, 421.
Moreels, G., Mege, G., Vallance-Jones, A. and Gattinger, R. (1977) An oxygen–hydrogen atmospheric model and its application to the OH emission problem. *J. atmos. terr. Phys.* **39**, 551.
Müllen, E. G., Silverman, S. M. and Korff, D. I. (1977) Nightglow (557.7 nm of OI) in the central polar cap. *Planet. Space Sci.* **25**, 23.
Myrabø, H. K. (1979) Atmospheric extinction during clear winter nights in the Skiboth Valley, Northern Norway, 1974–1977, Report F-340. Norwegian Defense Research Establishment.
Myrabø, H. K. (1983) Temperature variation at mesopause levels during winter solstice at 78°N. *Planet. Space Sci.*, in press.
Myrabø, H. K., Deehr, C. S. and Sivjee, G. G. (1983) Large amplitude nightglow OH (8–3) band intensity and rotational temperature variations during a 24-h period at 78°N. *J. geophys. Res.*, in press.
Myrabø, H. K., Lilleseter, O. and Høumyr, T. (1982) Portable field spectrometer for reflectance measurements 340–2500 nm. *Appl. Opt.* **21**, 2855.
Naujokat, B., Petzoldt, K., Labitzke, K. and Lenschow, R. (1983) Beilage zur Berliner Wettenkaste, 57 83.
Nicolet, M. (1970) Ozone and hydrogen reactions. *A. Geophys.* **26**, 531.
Nisbett, F. S. and Glenar, D. A. (1977) Thermospheric meridional winds and atomic oxygen depletion at high latitudes. *J. geophys. Res.* **82**, 4685.
Noxon, J. F. (1964) The latitude dependence of OH rotational temperature in the night airglow. *J. geophys. Res.* **69**, 4087.
Petitdidier, M. and Teitelbaum, H. (1977) Lower thermosphere emissions and tides. *Planet. Space Sci.* **25**, 711.
Reed, E. I. (1976) Polar enhancement of nightglow emissions near 6230 Å. *Geophys. Res. Lett.* **3**, 5.
Saito, B. (1962) Unusual enhancement of night airglow intensity at low latitudes on November 13, 1960. *Antarctic Rec.* **14**, 8.
Sandford, B. P. (1964) Aurora and airglow intensity variations with time and magnetic activity at southern high latitudes. *J. atmos. terr. Phys.* **26**, 749.
Schoeberl, M. R. (1978) Stratospheric warmings: Observations and theory. *Rev. Geophys. Space Phys.* **16**, 521.
Shagaev, M. V. (1974) Relation of rapid variations of the rotational temperature of atmospheric hydroxyl to geomagnetic activity. *Geomagn. Aeron.* **14**, 649.
Shagaev, M. V. (1980) Vertical temperature gradients and dissipation of internal gravity waves near the mesopause. *Geomagn. Aeron.* **20**, 529.
Shashun'Kina, V. M. and Yudovich, L. A. (1980) Effects of internal gravity waves during the magnetospheric substorm of February 15, 1978. *Geomagn. Aeron.* **20**, 516.
Shefov, N. N. (1959) Intensities of some twilight and night airglow emissions: spectral, electrophotometrical and radar researches of aurorae and airglow. *U.S.S.R. Acad. Sci.* **1**, 25.
Shefov, N. N. (1969a) Hydroxyl emission of the upper atmosphere—I. The behavior during a solar cycle, seasons and geomagnetic disturbance. *Planet. Space Sci.* **17**, 797.
Shefov, N. N. (1969b) Hydroxyl emission of the upper atmosphere—II. Effects of a sunlit atmosphere. *Planet. Space Sci.* **17**, 1629.
Shefov, N. N. (1970) Hydroxyl emission of the upper atmosphere—III. Diurnal variations. *Planet. Space Sci.* **19**, 129.
Simonaitis, R., Braslavsky, S., Heiklen, J. and Nicolet, M. (1973) *Chem. Phys. Lett.* **19**, 601.
Sivjee, G. G. and Deehr, C. S. (1980) Differences in polar atmospheric optical emissions between mid-day cusp and night-time auroras, in *Exploration of the Polar Upper Atmosphere* (Edited by Deehr, C. S. and Holtet, J. A.), p. 199. Reidel, Dordrecht.
Sivjee, G. G., Dick, K. A. and Feldman, P. D. (1972) Temporal variations in the night-time hydroxyl rotational temperature. *Planet. Space Sci.* **20**, 261.
Spizzichino, A. (1969) Étude des interactions entre les differentes composantes du vent dans la haut atmosphere. *A. Geophys.* **25**, 93.
Stringer, W. J. and Belon, A. E. (1967) The statistical auroral zone during IQSY and its relationship to magnetic activity. *J. geophys. Res.* **72**, 245.
Takahashi, H. and Batista, P. P. (1981) Simultaneous measurement of OH (9, 4), (8, 3), (7, 2), (6, 2) and (5, 1) bands in the airglow. *J. geophys. Res.* **86**, 5632.
Takahashi, H., Batista, P. P., Clemesha, B. R., Simonich, D. M. and Sahai, Y. (1979) Correlation between OH, NaD, and OI 5577 Å emissions in the airglow. *Planet. Space Sci.* **27**, 801.
Takahashi, H., Clemesha, B. R. and Sahai, Y. (1974) Nightglow OH (8–3) band intensities and rotational temperature at 23°S. *Planet. Space Sci.* **22**, 1323.
Takahashi, H., Sahai, Y., Clemesha, B. R., Batista, P. P. and Teixeira, N. R. (1977) Diurnal and seasonal variation of OH (8–3) airglow band and its correlation with OI 5577 Å. *Planet. Space Sci.* **25**, 541.
Takeuchi, I., Misawa, K., Kato, Y. and Aoyama, I. (1981) Seasonal variations of the correlations among nightglow radiations and emission mechanism of OH nightglow emission. *J. atmos. terr. Phys.* **43**, 157.
Teitelbaum, H. and Blamont, J. E. (1975) Some consequences of non-linear effects on tides and gravity waves. *J. atmos. terr. Phys.* **37**, 697.
Thome, G. (1968) Long-period waves generated in the polar ionosphere during the onset of magnetic storms. *J. geophys. Res.* **73**, 6319.
Vallance-Jones, A. (1973) The infrared spectrum of the airglow. *Space Sci. Rev.* **15**, 355.
Vallance-Jones, A. (1974) *Aurora*. Reidel, Dordrecht.
Visconti, G., Congeduti, F. and Fiocco, G. (1971) Fluctuation in the intensity and excitation temperature in the OH airglow (8–3) band, in *The Radiating Atmosphere* (Edited by McCormac, B. M.), p. 82. Reidel, Dordrecht.
Walker, J. D. and Reed, E. I. (1976) Behavior of the sodium and hydroxyl night-time emissions during a stratospheric warming. *J. Atmos. Sci.* **33**, 118.
Weill, G. and Christophe-Gluame, J. (1967) Ciel nocturne et aurores de basse latitude en periode dorange magnetique. *A. Geophys.* **23**, 317.
Wiens, R. H. and Weill, G. (1973) Diurnal, annual and solar cycle variations of hydroxyl and sodium nightglow intensities in the Europe–Africa sector. *Planet. Space Sci.* **21**, 1011.
Zimmerman, S. P. and Murphy, E. A. (1977) Stratospheric and mesospheric turbulence, in *Dynamical and Chemical Coupling Between the Neutral and Ionized Atmosphere* (Edited by Grandal, B. and Holtet, J. A.), p. 17. Reidel, Dordrecht.

O_2 ($b^1\Sigma_g^+ - X^3\Sigma_g^-$) ATMOSPHERIC BAND NIGHT AIRGLOW MEASUREMENTS IN THE NORTHERN POLAR CAP REGION

H. K. Myrabø[1]

Geophysical Institute, University of Alaska, Fairbanks

K. Henriksen

Auroral Observatory, University of Tromsø, Norway

C. S. Deehr and G. J. Romick

Geophysical Institute, University of Alaska, Fairbanks

Abstract. The O_2 atmospheric (0-1) band at 8645 Å has been observed in the airglow during the 1982/1983 winter solstice from the ground at Longyearbyen, West Spitsbergen (78.4°N latitude, 15°E longitude, geographic). The average (0-1) band intensity for the continuous 18-hour period of the observations is found to be 445 R ± 40 R. The mean temperature deduced from the O_2 (0-1) atmospheric band rotational structure is found to be 254 K ± 3 K compared to a mean of 249 K ± 2 K for the OH (8-3) band rotational temperature. This indicates a shallow mesopause with an upper temperature gradient of ~ 1 K/km. Comparison with previous observations shows little or no latitude dependence, although there is considerable scatter in the data indicating that the O_2 airglow is highly variable in time of the order of hours or less.

Introduction

The O_2 ($b^1\Sigma_g^+ - X^3\Sigma_g^-$) atmospheric band system was discovered in the night airglow by Meinel [1950] who observed the (0-1) band emission at 8645 Å. Morphology, diurnal and seasonal intensity variations were extensively studied by Berthier [1956] from Haute-Provence (43.9°N, geographic) using photographic techniques. Early absolute intensity measurements were reported by Barbier [1956] and Dufay [1958]. Mean values of 2000 R and 1500 R were given for the (0-1) band. Later ground-based measurements have showed significantly lower values, giving mean intensities in the range 400-500 R for the (0-1) band [Berg and Shefov, 1962; Broadfoot and Kendall, 1968; Wallace and Hunten, 1968; Shefov, 1971].

The (0-0) band is not observed from the ground due to absorption by O_2 in the lower atmosphere. Observations of the volume emission rate as a function of altitude have been made from rockets [Packer, 1961; Tarasova, 1963; Witt et al., 1979; Watanabe et al., 1981]. The altitudes of the maximum emission from these measurements of the (0-0) band center about 94 ± 3 km except for the results reported by Tarasova [1963] who found a profile maximum at 80 km.

Before the rocket measurements, the (0-0) band emission intensity was estimated using the (0-1) band and a Franck-Condon factor. Fraser et al. [1954] predicted a ratio of 21 for the intensity ratio between the (0-0) and (0-1) bands, ignoring any possible variation in the electronic transition moment. Laboratory measurements by Noxon [1961] gave a value of 20 ± 4 while Nicholls [1965] reported a factor of 20. A measured intensity ratio for the (0-0) to (0-1) bands was found to be 17 ± 2 by Wallace and Hunten [1968] using dayglow measurements. A value close to 20 has thus been commonly accepted [Greer et al., 1981].

Observations of O_2 atmospheric band airglow cover a wide range of latitudes, but both the ground-based and rocket measurements have been made at less than 60° except one recent rocket experiment by Witt et al. [1979] at 68°N. It has been suggested [Deans et al., 1976; Feldmann, 1978] that the atomic oxygen concentration and thus the night airglow atmospheric band emission would decrease toward high latitudes. This has been contradicted by Witt et al. [1979], who found a relatively high O_2 (0-0) band night airglow emission at 68°N.

A low value of the odd oxygen concentration at 95-100 km height should result in a very low 5577 Å green line night airglow and a low O_2 atmospheric band emission. A minimum (100 R) for the 5577 Å green line night airglow during winter solstice in the polar cap region is reported by Mullen et al. [1977] and by Ismail and Cogger [1982]. O_2 atmospheric band night airglow observations have not been reported from the polar cap region. It is the purpose of this paper to report recently obtained spectrophotometric night airglow measurements of the (0-1) band at 78.4°N during winter solstice.

Observations and Data Reduction

The spectra used in this work were part of measurements made during the 1982/1983 campaign of the Multi-National Svalbard Auroral Expedition [Deehr et al., 1980] close to Longyearbyen on West Spitsbergen (78.4°N latitude, 15°E longitude. geographic).

Night airglow OH emission features are normally predominant in the near-infrared spectral region in the polar cap [Gault et al., 1981; Myrabø et al., 1983]. The aurora in the polar cap is usually at a high altitude, and emits mainly atomic lines [Sivjee and Deehr, 1980]. Thus, a high-responsivity auroral spectro-photometer may

[1] On leave from Norwegian Defense Research Establishment, Kjeller.

Paper number 4A0770.
0148-0227/84/004A-0770$02.00

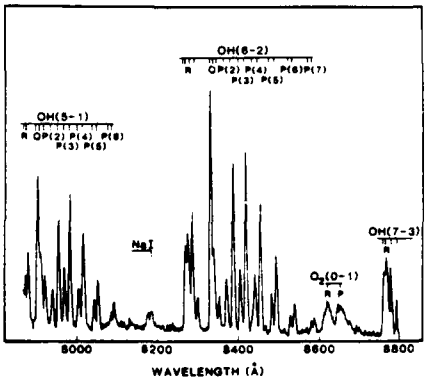

Fig. 1. An airglow spectrum including the spectral region from 7830 to 8800 Å obtained during a 12-min integration of 12-s scans at Longyearbyen. A pressure-broadened sodium line scattered from Longyearbyen during overcast and very hazy weather is indicated. The 1/2-m spectrophotometer with a bandwidth of 7 Å was used to record the spectrum which is uncorrected for instrumental response.

be used to measure the night airglow features clearly resolved from auroral emissions. Figure 1 shows an example of a spectrum which includes the 7800 to 8800 Å region. The bandwidth was approximately 7 Å and the OH and O_2 emissions are indicated.

At the Longyearbyen observatory, 1-m and 1/2-m high-throughput Ebert-Fastie spectrophotometers operate in a photon-counting mode and are coupled to an on-line digital data processing system. The coaligned, steerable instruments are described by Dick et al. [1970] and Sivjee et al. [1972].

During an 18-hour period of clear weather (1900 UT, January 11, to 1300 UT, January 12, 1983), the spectrophotometers were pointing toward the zenith and the spectral regions 7280-7410 Å and 8580-8830 Å covering the OH (8-3) band and the O_2 (0-1) atmospheric band were recorded. The OH (8-3) and O_2 (0-1) atmospheric band were scanned in 32 and 12 s, respectively, with the 1-m and 1/2-m Ebert-Fastie spectrometer instruments at a spectral resolution of 1.5 and 2.5 Å,, respectively. Each scan was recorded on tape and spectra were obtained each 30 min for OH and each hour for O_2 by summing individual scans. Examples of the OH (8-3) band spectrum are given by Myrabø [1984]. Figure 2 shows an example of a 1-hour integration of the O_2 (0-1) atmospheric bands at a resolution of 2.5 Å.

Absolute intensity calibration was performed in the field using a standard lamp and a diffusing screen. The OH rotational temperature has been calculated using the relative intensities P_1 (2), P_1 (3), P_1 (4) and P_1 (5) lines and Kvifte's method [Kvifte, 1959]. The O_2 (0-1) atmospheric band temperature was estimated by comparing with synthetic spectra (Henriksen et al., unpublished manuscript 1983).

Probable error in the rotational temperatures calculated from relative intensity ratios is estimated to be ± 10 K. The error in the absolute intensities is approximately 20%, mainly due to calibration uncertainty.

The incidence of aurora was monitored by the intensity of the 7320/30 Å O II lines, the N I lines and the N_2 1 P (2,1) band. The measurements reported were obtained during a period devoid of aurora except around 0700 UT in the morning of January 12. The relative contribution from aurorally excited O_2 (0-1) emission could thus be estimated together with intensities of other auroral lines and bands. It was observed that an increase of the O_2 (0-1) band of 20% to 33% corresponded to a simultaneous increase of the 7320/30 Å lines by more than a factor of 5. Thus, the observed intensity of the 7320/30 Å [O II] emission served as a monitor of auroral activity and an auroral contribution to the O_2 (0-1) band of less than 1% could easily be detected. The intensity measurements of the O_2 (0-1) band around 0700 UT have been excluded from the data in order to insure that the intensity and temperature data used here contain no auroral components.

Results and Discussion

Absolute Intensity of O_2 Atmospheric Bands (0,0) and (0,1)

Absolute intensity measurements of the O_2 atmospheric (0,1) band taken during a continuous 18-hour period in January 1983 at 78° are shown in Figure 3. The mean intensity during the observational period is 445 R ± 40 R. The data have not been corrected for atmospheric extinction. The OH (8-3) band intensity is given in Figure 3 for comparison. Both the O_2 and OH emission intensities tend to increase during the observing period. The mean OH (8-3) band emission intensity during this 18-hour observing period was 518 R. This may be compared with a mean of 425 R found for the whole 1982/1983 observ-

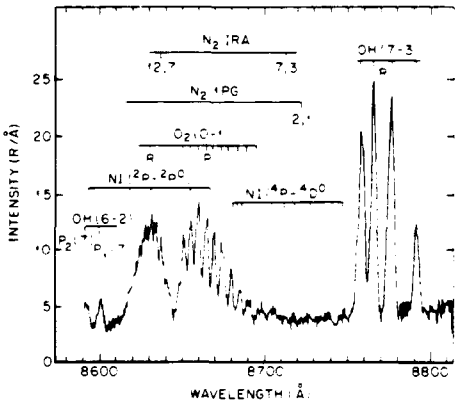

Fig. 2. An airglow emission spectrum typical of the O_2 (0-1) atmospheric band spectra used in the intensity and temperature calculations. The spectrum was obtained from a 1/2-m Ebert-Fastie spectrometer with a bandwidth of 2.5 Å by summing individual 12-s scans for one hour. The location of auroral lines and bands is indicated.

77

ing season [Myrabø and Deehr, 1984]. Thus, the mean value for this 18-hour period was approximately 25% higher than the seasonal mean.

A search for other ground-based observations, unfortunately, yields very few recent measurements giving absolute intensities. Measurements by Misawa and Takeuchi [1978], Misawa et al. [1980] and Takeuchi et al. [1981] are all in arbitrary units. Ground-based absolute measurements available for comparison after 1960 are by Berg and Shefov [1962], Broadfoot and Kendall [1968] and Shefov [1971]. Absolute emission intensities of the (0-1) band were also estimated by Wallace and Hunten [1968] and by Evans and Llewellyn [1970] using Broadfoot and Kendall's spectrum.

From the above measurements, we have calculated the expected (0-0) band emission intensities by applying a Franck-Condon factor of 20. The resulting ground-based calculated (0-0) band intensities are plotted versus latitude in Figure 4 together with available absolute measurements of the (0-0) band emission intensity as obtained from rocket flights. The values calculated from ground-based observations are marked with a G, while the rocket measurements are marked with an R. The rocket measurements are those by Packer [1961], Megill et al. [1970], Witt et al. [1979] and Deans et al. [1976].

Although there seems to be little or no variation with latitude, the (0-0) intensities calculated from the time-averaged ground-based observations of the (0-1) band show a small scatter (20%) at about twice the value of the rocket observations, although the latter are much more scattered. Correction for extinction and reemittance of self-absorbed (0-0) band emission is not included in the ground-based calculations The extinction should be about 10% for the appropriate wavelength region [Allen, 1963], while the correction due to reemittance is found to be about 10% [Wallace and Hunten, 1968]. These effects should, therefore, cancel out.

The scatter in the rocket data may be explained as a result of the short time interval of each measurement of the highly variable airglow compared to the time-averaged ground-based data.

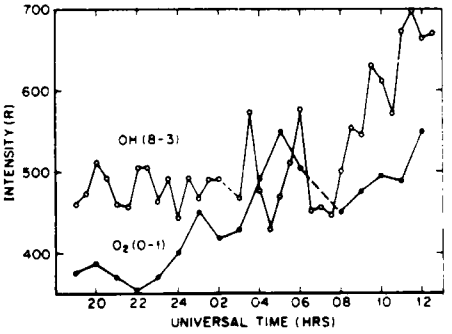

Fig. 3. The hourly and half-hourly mean zenith intensities, at Longyearbyen of the O_2 (0-1) atmospheric band and OH (8-3) intensities plotted as a function of UT for January 11/12, 1983. Straight lines are drawn between each mean and missing data are indicated by a dashed line.

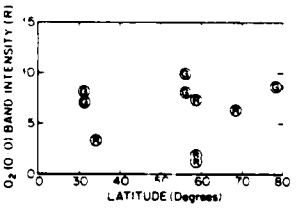

Fig. 4. O_2 (0-0) atmospheric band intensity versus latitude. G signifies the intensity calculated from ground-based observations of the (0-1) band using a Franck-Condon factor of 20 and R signifies rocket-borne observations of the (0-0) band.

(See Figure 3, or Noxon [1978], and Weinstock [1978]). A mean value of 4.1 kR with a standard deviation of 2.7 is found for the rocket measurements while the ground-based estimates have a mean value of 8.4 with a standard deviation of 1.1. It should be mentioned that absolute measurements from the ground of the (0-1) band prior to 1960 have been excluded from these data as it is felt that they may contain a systematic calibration error (Barbier [1956], 2000 R; Dufay [1958], 1500 R) compared to later results (see Figures 4 and 5). The value of 2000 R by Barbier [1956] and 1500 R by Dufay [1958] would only compound the discrepancy between the rocket and ground-based observations. A rocket experiment to observe both the (0-0) and (0-1) bands has been carried out (F. R. Harris, personal communication, 1983) and preliminary results using the generally accepted Franck-Condon factor of 17 to 22 indicate that the differences between the ground-based and rocket data may be reconciled and much higher intensities can occur on a time scale less than that of the time-averaged ground-based data.

O_2 (0-1) Atmospheric Band and OH (8-3) Band Rotational Temperatures

Temperatures deduced from the O_2 (0-1) atmospheric band rotational structure and the OH (8-3) band P_1 lines, are shown in Figure 5. These are 1-hour and 30-min averages for the 18-hour period in the same manner as for the intensity data. The overall temperature difference between the O_2 and OH band temperatures is seen to be small and mean values of 254 K ± 3 K and 249 K ± 2 K are found for the respective emissions. The two temperatures may also be seen to follow a similar trend, which is reasonable since they originate in the same atmospheric height domain; the OH intensity maximum is usually found 3-8 km lower than the O_2 emission [Moreels et al., 1977; Witt et al., 1979; Watanabe et al., 1981]. Although considerable variation in both the O_2 and the OH temperature takes place during the observing period, no wavelike pattern that could be attributed to gravity wave effects as found by Noxon [1978] is seen in this particular data collection. The variations in both the O_2 and OH temperatures may rather be interpreted as being due to transport and mixing phenomena which seem to govern the dynamical behavior of the polar winter atmosphere at mesopause height [Myrabø, 1984; Myrabø and Deehr, 1984].

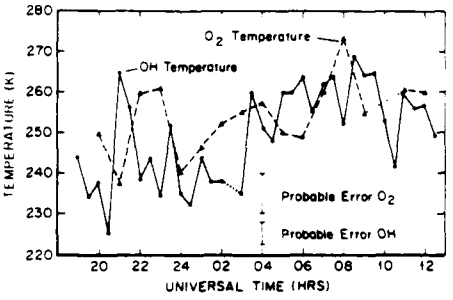

Fig. 5. The hourly and half-hourly mean temperatures from the R and P branches of the O_2 atmospheric (0-1) bands and the OH (83) band P_1 lines observed in the zenith airglow at Longyearbyen on January 11/12, 1983. Straight lines are drawn between each half-hourly and hourly value, respectively.

Assuming a reasonable difference in the peak height of the O_2 atmospheric emissions and the OH (83) band of 5-6 km, the mean temperature difference ΔT of 5 K gives a positive temperature gradient of 1 K/km for the 90 to 95-km region. This confirms previous findings of a shallow polar mesopause with a relatively small positive temperature gradient in the 90 to 95-km region [Myrabø, 1984] for winter solstice conditions.

Summary

The (0-1) atmospheric bands in the night airglow have been observed from Longyearbyen (78°N) during winter solstice conditions using spectrophotometric equipment. The observations reported here were confined to an 18-hour continuous clear-weather observing period from 1900 UT, January 11, to 1300 UT, January 12, 1983. The raw data were recorded with a spectral resolution of 2.5 Å, which resolved the rotational structure of the P branch of the O_2 (0-1) atmospheric band.

A mean O_2 (0-1) atmospheric band intensity of 445 ± 40 R, ranging from 350 R to 5.0 R, is found. The mean temperature deduced from the O_2 (0-1) atmospheric band rotational structure is 254 K ± 3 K compared to a mean of 249 K ± 2 K for simultaneous measured OH (8-3) band rotational temperature. The mean temperature difference between the O_2 (0-1) atmospheric band and the OH (8-3) band yields a positive temperature gradient for the 90 to 95-km region of 1 K/km, assuming a reasonable height difference between the two emissions of 5-6 km.

All available time-averaged ground-based observations of the (0,1) band intensity were used to calculate the intensity of the (0,0) band. These data were plotted together with available rocket observations of the (0,0) band as a function of latitude. No latitude dependence was observed, and although the rocket data were half the intensity of the ground data on the average, the scatter was considerably larger. This indicates that a further correction to the ground-based or the rocket data may be necessary and that the O_2 airglow is highly variable on a time scale of hours.

Acknowledgments. Financial support for this research was provided by National Science Foundation through grants ATM80-12719, ATM82-14642, ATM82-00114 and ATM-8313727 to the Geophysical Institute of the University of Alaska and by the Royal Norwegian Council for Scientific and Industrial Research through a fellowship grant to one of us (H.K.M.). The observations on Svalbard are made through a cooperative effort involving the Universities in Fairbanks, Tromsø and Oslo, with the help and cooperation of the Great Norwegian Spitsbergen Coal Company and the Norwegian Polar Institute.

The Editor thanks the two referees for their assistance in evaluating this paper.

References

Allen, C. W., Astrophysical Quantities, p. 122, Athlone, London, 1963.

Barbier, D., The airglow, in Vistas in Astronomy, edited by A. Beer, p. 929, Pergamon, London, 1956.

Berg, M. A., and N. N. Shefov, Emission of the hydroxyl bands and of the (0,1) λ8645Å atmospheric band of oxygen in the nightglow, Planet. Space Sci., 9, 167, 1962.

Berthier, P., Etude spectrophotometrique de la luminescence nocturne des bandes des molecules OH et O_2 atmospherique, Ann. Geophys., 12, 113, 1956.

Broadfoot, A. L., and K. R. Kendall, The airglow spectrum, 3100-10,000Å, J. Geophys. Res., 73, 426, 1968.

Deans, A. J., G. G. Shepherd, and W. F. J. Evans, A rocket measurement of the O_2 ($b^1\Sigma_g^+ X^3\Sigma_g^-$) atmospheric band nightglow altitude distribution, Geophys. Res. Lett., 3, 441, 1976.

Deehr, C. S., G. G. Sivjee, A. Egeland, K. Henriksen, P. E. Sandholt, R. Smith, P. Sweeney, C. Duncan, and F. Gilmer, Ground-based observations of F region associated with the magnetospheric cusp, J. Geophys. Res., 85, 2185, 1980.

Dick, K. A., G. G. Sivjee, and H. M. Crosswhite, Aircraft airglow intensity measurements: Variations in OH and OI (5577), Planet. Space Sci., 18, 887, 1970.

Dufay, M., Sur les intensities des bandes d'emission du ciel nocturne dans le proche infrarouge, C.R. Hebd. Seances Acad. Sci. Paris, 246, 2281, 1958.

Evans, W. F. J. and E. J. Llewellyn, Molecular oxygen emissions in the airglow, Ann. Geophys., 26, 167-178, 1970.

Feldmann, P., Auroral excitation of optical emissions of atomic and molecular oxygen, J. Geophys. Res., 83, 2511, 1978.

Fraser, P. A., W. R. Jarmain, and R. W. Nicholls, Vibrational transition probabilities of diatomic molecules: Collected results, II, N_2^+, CN, C_2, O_2, TiO, Astrophys. J., 119, 286, 1954.

Gault, W. A., R. A, Koehler, R. Link, and G. G. Shepherd, Observations of the optical spectrum of the dayside magnetospheric cleft aurora, Planet. Space Sci., 29, 321, 1981.

Greer, R. G. H., E. J. Llewellyn, B. H. Solheim, and G. G. Shepherd, Observations of the optical spectrum of the dayside magnetospheric cleft aurora, Planet. Space Sci., 29, 321, 1981.

Henriksen, K., G. G. Sivjee, C. S. Deehr and H.

K. Myrabø, Ground-based observations of O_2 ($b^1\Sigma_g^+ - X^3\Sigma_g^-$) atmospheric bands in high latitude auroras, J. Geophys. Res., has been accepted, in press, 1984.

Ismail, S., and L. L. Cogger, Temporal variations of polar cap OI 5577Å airglow, Planet. Space Sci., 30, 865, 1982.

Kvifte, G., Nightglow observations at Ås during the I.G.Y., Geophys. Publ., 20, 1, 1959.

Megill, L. R., A. M. Despain, D. J. Baker, and K. D. Baker, Oxygen atmospheric and infrared atmospheric bands in the aurora, J. Geophys. Res., 75, 4475, 1970.

Meinel, A. B., O_2 emission bands in the infrared spectrum of the night sky, Astrophys. J., 112, 1464, 1950.

Misawa, K., and I. Takeuchi, Correlation among O_2 0-1) atmospheric band, OH(8-3) band and [OI] 5577Å line and among $P_1(2)$, $P_1(3)$ and $P_1(3)$ and $P_1(4)$ lines of OH (8-3) band, J. Atmos. Terr. Phys., 40, 421, 1978.

Misawa, K., I. Takeuchi, Y. Kato, and I. Aoyama, Correlation between O_2 (0-1) atmospheric band and the NaD lines, J. Atmos. Terr. Phys., 42, 179, 1980.

Moreels, G., G. Megie, A. Vallance-Jones, and R. L. Gattinger, An oxygen-hydrogen atmospheric model and its application to the OH problem, J. Atmos. Terr. Phys., 39, 551, 1977.

Mullen, E. G., S. M. Silverman, and D. F. Korff, Nightglow (557.7 nm of OI) in the central polar cap, Planet. Space Sci., 25, 23, 1977.

Myrabø, H. K., Temperature variation at mesopause levels during winter solstice at 78°N., Planet. Space Sci., 32, 249-255, 1984.

Myrabø, H. K., and C. S. Deehr, Mid-winter hydroxyl night airglow emission intensities in the northern polar region, Planet. Space Sci., 32, 263-271, 1984.

Myrabø, H. K., C. S. Deehr, and G. G. Sivjee, Large-amplitude nightglow OH (8-3) band intensity and rotational temperature variations during a 24-hour period at 78°N, J. Geophys. Res., 88, 9255, 1983.

Nicholls, R. W., Franck-Condon factors to high vibrational quantum numbers, V, O_2 band systems, J. Res. Natl. Bur. Stand., Sect. A, 69, 369, 1965.

Noxon, J. F., Observation of the ($b^1\Sigma_g^+ - a^1\Delta_g$) transition in O_2, Can. J. Phys., 39, 1110, 1961.

Noxon, J. F., Effect of internal gravity waves upon night airglow temperatures, Geophys. Res. Lett., 5, 25, 1978.

Packer, D. M., Altitude of the night airglow radiations, Ann. Geophys., 17, 67, 1961.

Shefov, N. N., Hydroxyl emission of the upper atmosphere, IV, Correlation with the molecular oxygen emission, Planet. Space Sci., 19, 795, 1971.

Sivjee, G. G., and C. S. Deehr, Differences in polar atmospheric optical emissions between mid-day cusp and night-time auroras, in Exploration of the Polar Upper Atmosphere, edited by C. S. Deehr and J. A. Holtet, Hingham, Mass., 1980, p. 199, D. Reidel.

Sivjee, G. G., K. A. Dick, and P. D. Feldman, Temporal variations in the nighttime hydroxyl rotational temperature, Planet. Space Sci., 20, 261, 1972.

Takeuchi, I., K. Misawa, Y. Kato, and I. Aoyama, Seasonal variations of the correlation among nightglow radiations and emission mechanisms of OH nightglow emission, J. Atmos. Terr. Phys., 43, 157, 1981.

Tarasova, T. M., Night-sky emission-line intensity distribution with respect to height, Space Res., 3, 162, 1963.

Wallace, L., and D. M. Hunten, Dayglow of the oxygen A band, J. Geophys. Res., 73, 4813, 1968.

Watanabe, T., M. Nakamura, and T. Ogawa, Rocket measurements of O_2 atmospheric and OH Meinel bands in the airglow, J. Geophys. Res., 86, 5768, 1981.

Weinstock, J., Theory of interaction of gravity waves with O_2 ($^1\Sigma$) airglow, J. Geophys. Res., 83, 5175, 1978.

Witt, G., J. Stegman, B. H. Solheim, and E. J. Llewellyn, A measurement of the $O_2(b^1\Sigma_g^+ - X^3\Sigma_g^-)$ atmospheric band and the $OI(^1S)$ green line in the nightglow, Planet. Space Sci., 27, 341, 1979.

C. S. Deehr and G. J. Romick, Geophysical Institute, University of Alaska, Fairbanks, AK 99701.

K. Henriksen, Auroral Observatory, University of Tromsø, 9000 Tromsø, Norway.

H. K. Myrabø, Norwegian Defense Research Establishment, N-2007, Kjeller, Norway.

(Received June 23, 1983;
revised May 23, 1984;
accepted May 24, 1984.)

4.9 Myrabo H K, C S Deehr, G J Romick and K Henriksen, Mid-winter intensities of the night airglow O_2(0-1) atmospheric band emission at high latitudes, J Geophys Res, 91, 1684 (1986)

JOURNAL OF GEOPHYSICAL RESEARCH, VOL. 91, NO. A2, PAGES 1864-1874, FEBRUARY 1, 1986

MID-WINTER INTENSITIES OF THE NIGHT AIRGLOW O_2 (0-1) ATMOSPHERIC BAND EMISSION AT HIGH LATITUDES

H. K. Myrabø

Norwegian Defence Research Establishment, Kjeller, Norway

C. S. Deehr and G. J. Romick

Geophysical Institute, University of Alaska, Fairbanks

K. Henriksen

Auroral Observatory, University of Tromsø, Norway

Abstract. Absolute intensities of the O_2 (0-1) atmospheric band night airglow emission have been observed from near Longyearbyen on west Spitsbergen (78.4°N latitude, 15°E longitude, geographic) during a 2-month period around winter solstice (1982-1983). Intensities ranging from 110 R to 1590 R with a mean of 570 R ± 60 R are observed. There is no clear maximum or minimum around solstice. A semidiurnal tide component giving rise to a 25-30% intensity variation of the O_2 (0-1) atmospheric emission is present in the data. The maximum and minimum are found to occur at about 0400 and 1000 local time, respectively. No diurnal tide component larger than ±3-4% is present in the data. The day-to-day and short time variations both show a quasi-regular wave pattern which may be associated with gravity waves.

1. Introduction

Night airglow observations provide a powerful and relatively simple means of studying the dynamics and chemistry of the upper atmosphere. Ground-based observations are important for studying smaller-scale dynamical phenomena because rocket measurements only give a snapshot in time and satellite measurements are usually integrated over a large area at widely spaced time intervals.

Ground-based night airglow observations in the polar regions are very sparse compared to lower latitudes. This is also the case for rocket measurements. In some recent papers by Myrabø et al. [1983, 1984a], Myrabø [1984] and Myrabø and Deehr [1984], ground-based measurements of the OH night airglow have been reported. OH emissions originate in the 85-90 km region (i.e., near the mesopause). Measurements of the [OI] 5577 Å line in the lower thermosphere (i.e., ~100 km) have been reported by Sandford [1964], Mullen et al. [1977] and Ismail and Cogger [1982]. No high-latitude, ground-based observations of the night airglow O_2 (0-1) atmospheric band near ~95 km altitude [Deans et al., 1976; Witt et al., 1979] have been published, except for a brief report by Myrabø et al. [1984b].

The O_2 (0-1) atmospheric band is normally found to follow the intensity variations of the [OI] 5577 Å line [Dufay, 1959], and should therefore give an independent measure of odd oxygen variations in the 90-100 km region, which probably reflects the chemical and dynamical behavior of the very lowest part of the thermosphere. Measurements of the O_2 (0-1) atmospheric band emission may also contribute to the understanding of uncertainties in the chemical reactions involved in the atomic and molecular oxygen emission in the night airglow [Wraight, 1982; Bates, 1978; Greer et al., 1981; Ismail and Cogger, 1982].

The purpose of this paper is to report and discuss recent observations of the O_2 (0-1) atmospheric band night airglow emission. These observations were made near Longyearbyen, Svalbard at 78°N during 38 days around the 1982 winter solstice.

2. Observations and Data Reduction

During the 1982/1983 Multi-National Svalbard Auroral Expedition (MNSAE) [Deehr et al., 1983], emission spectra of the zenith sky, containing the O_2 (0-1) atmospheric band emission, were taken near Longyearbyen on West Spitsbergen (78.4°N latitude, 15°E longitude, geographic). From the end of November 1982 throughout January 1983, a 1/2 m Ebert-Fastie spectrophotometer was used to obtain the spectra. Some important parameters for the instrument is given in Table 1. For further reference, a similar 1-m instrument is described more fully in the papers by Sivjee et al. [1972] and Romick [1976]. The spectral region from 8340 to 8870 Å was scanned during 12 s with a bandwidth of 7 Å, except for a brief 18-hour period when the 8580-8830 Å region was recorded with a 1.5 Å bandwidth. The purpose of the high-resolution recordings was mainly to get an accurate rotational temperature for the 95-km level for comparison and check with OH-obtained temperatures. A brief report on this has been given by Myrabø et al. [1984b]. For the 7 Å resolution data, spectra were obtained by averaging 150 individual scans yielding one spectrum every 30 min.

Figure 1 gives an example of two 30-min spectra, one during quiet geomagnetic conditions and one during auroral activity with relatively strong molecular emissions. The difference between the spectra is the presence of auroral emissions in the bottom panel. Most prominent among these are the OI 8446 Å line, the N_2(1P) band, the slightly enhanced O_2 (0-1) atmospheric band and the strongest lines of the NI ($3s^4P - 3p^4D^o$) multiplet.

One of the main problems with measuring night

Paper number 5A8652.
0148-0227/86/005A-8652$05.00

TABLE 1. Characteristics of Spectrometer

Component	Detail
Type of spectrometer	1/2 m Ebert-Fastie
Field of view	6° x 6°
Spectral order used	1 order
Dark count rate	1-3 count/s
Entrance/exit slit height	65 mm
Spectral dispersion (current experiment)	14 Å/mm
Spectral sensitivity (with 7 Å resolution and current experiment)	~15 R/count at 8600 Å
Detector type	Hamamatsu R943-02 Ga As. tube

airglow features in auroral regions is the contamination by aurora. If the emissions are not excited by auroral particle bombardment, overlying auroral features may normally be filtered out or accounted for if a high enough spectral resolution is used. If the airglow emission also occurs in the aurora, as is the case for the [OI] 5577 Å line and the O_2 (0-1) atmospheric band, there is no direct way of knowing if the photons originate in the aurora or airglow. A simultaneous monitoring of pure auroral features, such as the 3914 or 4278 Å N_2^+ 1N1G band, could be used to select time periods devoid of auroral emission features. This method was used by Mullen et al. [1977] and Ismail and Cogger [1982] to isolate the night airglow component of the [OI] 5577 Å line. The problem of establishing a threshold intensity for auroral incidence is alleviated by using a spectrophotometer with a sufficient resolution to record the night airglow and the auroral reference emissions in the same spectra. At very high latitudes, atomic lines dominate the auroral spectrum for most of the time [Sivjee and Deehr, 1980; Gault et al., 1981; Myrabø and Deehr, 1984]. This makes the night airglow component of the O_2 (0-1) atmospheric band much easier to isolate and far less sensitive to auroral emission than the [OI] 5577 Å line.

The spectral region shown in Figure 1 includes the OI 8446 auroral line as an auroral reference emission in addition to the O_2 (0-1) band. An auroral component in the O_2 atm band of 2-3% is indicated by the OI 8446 line rising high above the OH lines, by a factor of 2 or more. For calculating the absolute intensities of the O_2 (0-1) atmospheric band, we have thus only selected spectra with no auroral emissions and only during clear and stable weather conditions. Weather conditions were checked visually by viewing standard stellar sequences. The resulting daily distribution of the spectra is depicted in Figure 2.

Absolute calibration of the spectra were carried out in the field using a standard source. The absolute intensities were calculated by using the area under the band emission and represent only the night airglow component of the O_2 (0-1) atmospheric band. The uncertainty in the band intensity measured from each 30-min spectrum is estimated to be 25%, mainly due to calibration uncertainties. The relative uncertainty due to photon noise and reading off each band intensity is less than 3%.

3. Results and Discussion

3.1. Short Time Variations

The typical short time pattern of the intensity variations of the O_2 (0-1) band emission is somewhat similar to that found for the OH emission in the polar region [Myrabø et al., 1983; Myrabø and Deehr, 1984]. Intensity variations of a factor of 2 or more within a few hours are common. The intensity versus time plots often show wavelike cyclic changes which shift frequently only after a few cycles or are interrupted by peaks or step changes. It is rather unusual to see longer periods (8-12 hours) with low amplitude, smooth variations as is often the case at lower latitudes [Berthier, 1956; Misawa and Takeuchi, 1978].

Figure 3 shows a typical example of the intensity variation with time during a 10-hour period from December 25-26, 1982. It seems reasonable to believe that these variations are associated with gravity waves. Normally, little or no correlation is observed between the intensity

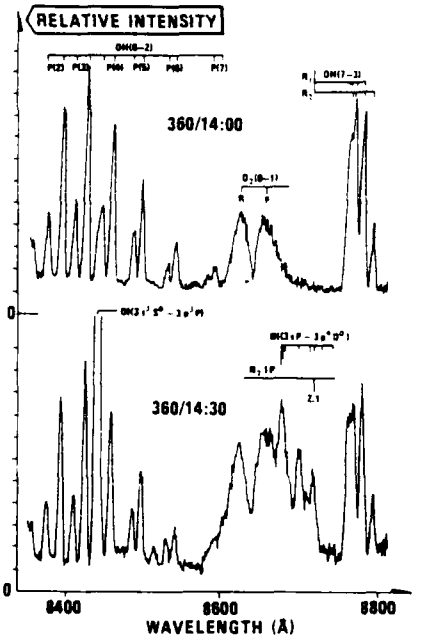

Fig. 1. Examples of spectra averaged for 30 min during quiet conditions (top) and during moderate auroral conditions (bottom).

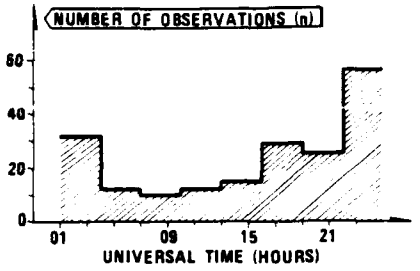

Fig. 2. Histogram showing the distribution in UT of the spectra used in calculating the absolute intensities of the O_2 (0-1) atmospheric band.

variations of the O_2 (0-1) band and those of the OH emissions which are thought to be about 5-10 km lower in the atmosphere (i.e., at the mesopause), even if a time shift is introduced (see also Myrabø et al. [1984b]). An example of two subsequent spectra, including both the O_2 (0-1) band and the OH (6-2) P branches, is shown in Figure 4. A 70-80% decrease is seen in the O_2 (0-1) band intensity, while no change is seen in the OH intensity. Simultaneous observations of the OH (6-2) intensity and temperature and the O_2 (0-1) band intensity are given in Figure 5, showing the lack of correlation between the two emissions.

According to Weinstock [1978], temperature and intensity variations of the O_2 ($b\,^1\Sigma_g^+$) airglow emission need not always correlate during the passage of gravity waves. Observations by Noxon [1978] show examples of this. The intensity variation may be both phase-shifted and have a much smaller amplitude as compared to the temperature fluctuations. A complete correlation between OH temperature or intensity and O_2 ($b\,^1\Sigma_g^+$) intensity should therefore not be expected during passage of gravity waves through both emission layers. However, a higher degree of correspondence than is actually observed should be expected if the intensity variations in the two night airglow emissions largely are caused by the same gravity waves traveling from below throughout the mesopause region to at least above 95 km. The OH temperature and O_2 (0-1) band intensity variations should then show approximately the same active periods and quiet periods. This is normally not seen, which supports the view that the wavelike variations of the two airglow emissions might have two different origins.

If gravity waves were to break in the 85-95 km height region, they would dissipate most of their energy here and cause a very complicated and disturbed density and temperature pattern [Holton, 1979]. Gravity waves due to auroral activity above the 100-km region travel downward and could affect the O_2 (0-1) emission more strongly than the OH emission [Frederick, 1979]. On this basis a hypothesis may be put forward that variations in OH emissions are affected by gravity waves from below, i.e., from lower atmospheric and tropospheric phenomena, while variation in the O_2 (0-1) atmospheric band are affected by gravity waves originating from above, i.e., from auroral-

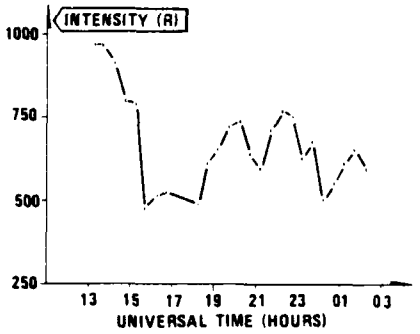

Fig. 3. Typical example of the intensity variation of the O_2 (0-1) atmospheric band as obtained during a 14-hour period from December 25-26, 1982.

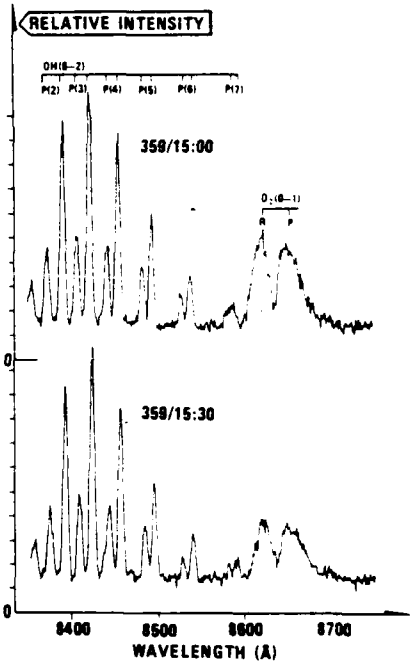

Fig. 4. Two consecutive 30-min spectra of the 8340-8740 Å region showing an almost 100% decrease in the O_2 (0-1) band, while the OH emission is left unchanged.

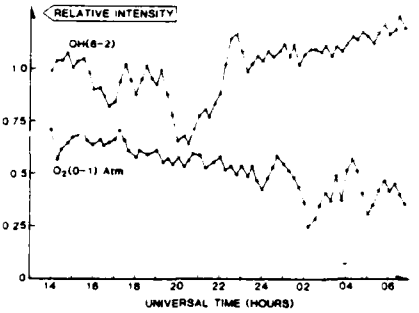

Fig. 5. The 15-min average intensities of the OH (6-2) band and the O_2 (0-1) atm band obtained on December 17, 1982, from Longyearbyen.

ly related phenomena. Seen from a dynamical point of view, chis would divide the polar upper atmosphere in two height regions, i.e., below 85-90 km and above 90-95 km, dominated from below and above respectively, by breaking gravity waves with a turbulent-free mesopause region in between. This picture also fits with rocket measurements from Andøya (69°N) of the turbulence in the 80-100 km region as recorded during the MAPWINE campaign 1983/1984 (T. A. Blix, private communication, 1984).

3.2. Diurnal and Semidiurnal Variations

The large, irregular intensity variations with periods less than 24 hours mask any diurnal or semi diurnal variations in any single 24-hour period. In order to bring out these daily variations we have used a superimposed epoch method, employing all of the absolute intensity data for the 20-day period between December 6 and December 26, 1982. Figure 6 gives the result, showing a semidiurnal intensity variation of the O_2 (0-1) atmospheric band with an amplitude variation of approximately ±15% from the average. A semidiurnal tide curve has been fitted to the data following the method of Petitdidier and Teitelbaum [1977]. The best fit curve gives maximum and minimum of the emission intensity at 1600 UT and 2200 UT. Universal time and local solar time differs only by about 20-30 min, which places the position of the maxima and minima as expressed in local solar time (LST) at approximately 0400 and 1600 LST and 1000 and 2200 LST, respectively.

As seen in Figure 6, there is no sign of a diurnal variation. To test this further, Fourier analysis of the data was undertaken. No diurnal component larger than ±3-4% appeared in the Fourier spectra. Mullen et al. [1977] found no diurnal variation in the OI 5577 Å nightglow at Thule (77°N) larger than ±5%.

Myrabø [1984] and Myrabø and Deehr [1984] found no diurnal variation in the OH rotational temperature and in the OH intensity larger than ±1 K and ±5%, respectively. The absence of a diurnal variation in the O_2 (0-1) atmospheric band intensity is therefore not surprising. A negligible diurnal tide effect in the 80-100 km region at extreme high latitudes seems therefore to be established. This is contrary to the model calculations of Forbes [1982] but agrees with Beer [1975] and Spizzichino [1970]. According to Teitelbaum and Blamont [1975] and Spizzichino [1969], the first diurnal mode effectively interacts with gravity waves. Averaging over several days cancels the diurnal mode. The short time behavior of the intensity variations also (see section 3.1) indicates strong gravity wave activity which, in connection with the above hypothesis, should explain the absence of the first diurnal tide mode.

Mullen et al. [1977] also failed to find any semidiurnal tide component at the 100-km level. However.,recent OH observations from Spitsbergen [Myrabø, 1984; Myrabø and Deehr, 1984] have revealed a dominant semidiurnal tide component both in the rotational temperature and emission intensity data. The semidiurnal variations in the O_2 (0-1) atmospheric band intensity found here confirms the presence of a dominant semidiurnal tide at extreme high latitudes, at least in the 85-95 km region. However, the amplitude of the tidal component is slightly weaker than normally found for the O_2 (0-1) band and the [OI] 5577 Å at mid and high latitudes [Brenton and Silverman, 1970; Petitdidier and Teitelbaum,

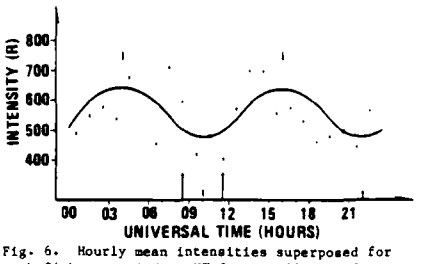

Fig. 6. Hourly mean intensities superposed for each 24-hour period in UT for the 20 days from December 6 to December 26, 1982. The semidiurnal trend is indicated by a solid line with the minima and maxima marked by short arrows. Longer arrows mark local geomagnetic and solar noon.

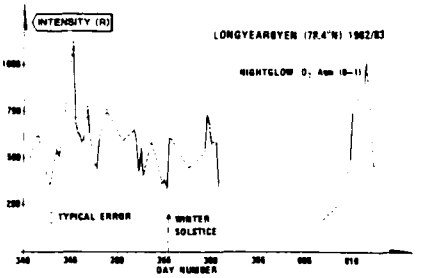

Fig. 7. Six-hour average O_2 (0-1) band absolute intensities at 78°N during the 1982/ 1983 MNSA Expedition. Winter solstice is indicated.

1977]. The time for the maxima and minima fits very well with the calculations of Petitdidier and Teitelbaum [1977], which predicts a maximum intensity of the green line at 100-km height to occur around 0130 local time for winter conditions at 45°N. A shift of the emitting layer of 6-7 km, i.e., around 93-94 km which is a reasonable height for the O_2 (0-1) band [Deans et al., 1976], leads to the maximum occurring 2 to 2 1/2 hours later [Petitdidier and Teitelbaum, 1977]. This is very close to the maximum seen in Figure 6. The calculations of Petitdidier and Teitelbaum also agree very well with experimental [OI] 5577 Å data from mid-latitudes [Brenton and Silverman, 1970].

3.3. Seasonal and Day-to-Day Variation

Six-hour mean intensities have been obtained by averaging 30-min spectra. A minimum of three 30-min spectra were used to calculate each 6-hour mean. Normally, 6 to 12 spectra were used. Figure 7 shows the resulting intensity versus time plots. The pattern in the day-to-day variations is similar to that found for the [OI] 5577 Å line at Thule by Mullen et al. [1977] and that by Ismail and Cogger [1982] from the ISIS 2 data. It is characterized by irregular peaks with intensity variations up to a factor of 5 or more in a few days. The largest 6-hour mean found in the O_2 (0-1) atmospheric band is 1125 R and the lowest value is 165 R with a seasonal average of 570 R ± 60 R. The seasonal average is slightly larger than that reported for a shorter period by Myrabø et al. [1984b].

In the data from Thule of the [OI] 5577 Å line, Mullen et al. [1977] found a correlation between interplanetary magnetic field polarity, i.e., "away" or "toward" sectors corresponding to B_x positive or negative and B_y negative or positive, and increasing and decreasing, respectively, [OI] 5577 Å nightglow trend. Such a correlation is not clear in this data set, as both an increasing and decreasing trend is found for positive interplanetary magnetic field polarity. It might be pointed out that day 344-345 (December 10-11) and January 1-10 were disturbed periods and that both these periods show pronounced maxima in the O_2 (0-1) intensity, although the latter may be partly associated with a stratospheric warming event.

From the ISIS 2 data, Ismail and Cogger [1982] see an enhanced level of polar [OI] 5577 Å nightglow emission during stratospheric warming events. Unfortunately, the time interval covered by our data set only contains one stratospheric warming event around year's end. In the satellite data for the polar area, there is a warming tendency on January 6-8, 1983, that only reaches the 4-mbar level [Naujokat et al., 1983; Myrabø et al., 1984b]. Unfortunately, due to severe storms and full moon conditions, we have a large gap in our data just in this period. However, a very steep increase in the O_2 (0-1) atmospheric band intensity is seen between January 2 and January 10 which may be associated with the stratospheric event of January 6-8.

Ismail and Cogger [1982] found a pronounced minimum in the [OI] 5577 Å line in the southern hemisphere during winter solstice. A similar tendency should be expected for the O_2 (0-1) atmospheric band; however, we do not find a pronounced minimum in the emission of the O_2 (0-1) atmospheric band during winter solstice. But on the other hand, northern [OI] 5577 Å hemisphere night airglow data from Thule (77°N) during three long winter seasons [Mullen et al., 1977] show no clear minimum around winter solstice. Indeed the results by Ismail and Cogger from the northern hemisphere are not conclusive. Thus the result from Ismail and Cogger showing the clear minimum in the southern hemisphere where there is no midwinter sudden stratospheric warming, indicates that the lack of seasonal effect in the northern hemisphere may be due to the effect of the stratospheric warming.

The day-to-day dynamical behavior in our O_2 (0-1) atmospheric data shows the same type of pattern as seen in the [OI] 5577 Å night airglow from the northern polar region [Mullen et al., 1977] during winter solstice, i.e., large irregular variations. This type of behavior therefore seems to be common both for the OH, [OI] 5577 Å line and the O_2 (0-1) atmospheric band night airglow in the northern polar region. It is different from the normal morphological pattern of the night airglow at lower latitudes and is therefore reasonable to connect to the dynamical situation of the polar atmosphere in the 80-110 km region [Myrabø et al., 1983, 1984b; Myrabø and Deehr, 1984].

We think that these irregular variations are partly connected to temporal and spatial variations in the occurrence of gravity waves and their interactions with the zonal winds in the stratosphere and the mesosphere. Model calculations by S. Solomon (private communication, 1984) using a chemical-dynamical model including gravity wave parameterization [Lindzen, 1981; Holton, 1983] have shown how the [OI] 5577 Å night airglow spring maximum at high latitude reported by Cogger et al. [1981] can be reproduced in the model as a direct result of the seasonal variation in the propagation and breaking of gravity waves and the associated diffusion of odd oxygen. Thus the maximum in the [OI] intensity is produced as a result of the final warming of the stratosphere and corresponding cooling of the mesopause region. Similarly, one would expect smaller-scale and local gravity wave blocking by zonal winds to result in shorter periods cooling of the mesopause and possibly enhanced night airglow levels in the altitude regions affected.

Such enhanced levels of the night airglow resulting in gravity wave interaction and sudden stratospheric warmings or minor warmings could also explain the lack of a clear minima during solstice in the northern hemisphere night airglow as compared to southern hemisphere where sudden warmings during midwinter do not occur [Labitzke, 1977].

3.4. O_2 atm (0-1) Intensities

The seasonal mean value of 570 R ± 60 R found here for the O_2 (0-1) atmospheric band also appears rather large as seen from a photochemical point of view; i.e., the polar cap is for most of the winter solstice period without solar irradiance at the 95-km level. This should cause little or no photoexcitation of O_2 into excited states [Moreels et al., 1977]. The presence of a strong O_2 (0-1) atmospheric emission therefore requires other sources for exciting the O_2 mole-

cules. Vertical and horizontal transport of odd oxygen is such a candidate.

One may also compare the observed O_2 (0-1) atmospheric band intensity with oxygen atom density assuming the Chapman reaction to be responsible for the emission [Wallace and Hunten, 1968; Deans et al., 1976], i.e.,

$$O + O + M \rightarrow O_2 (b^1\Sigma_g^+) + M \qquad (1)$$

Different reaction rates have been used. It is well known [Wallace and Hunten, 1968] that the laboratory obtained reaction rate by Young and Black [1965] is not sufficient to account for the observed emission rates. Assuming the reaction rate coefficient given by Barth [1961] or almost equivalent by Campbell and Trush [1967] (taking the neutral temperature to be 220 K at 95 km); one may derive an approximate expression for the average oxygen atom number density over the emission height:

$$[O]^2 = (I\ f/k[M]\ \omega) \qquad (2)$$

For the (0-1) band I is the observed emission rate of the (0-1) band in photons $cm^{-3}\ s^{-1}$, f is the ratio between the total atmospheric bands emission and the (0-1) band, taken to be 20 [Deans et al., 1976]; [M] is the number density of N_2 at 95 km, taken to be 4×10^{13} cm^{-3} (CIRA, 1972); ω is the half width of the (0-1) atmospheric band in centimeters, taken to be 15 km [Deans et al., 1976]; and k is the reaction rate coefficient from Barth [1961], $k = 8 \times 10^{-33}$ $cm^3\ s^{-1}$. Using equation (2) and the above values, one arrives at an average oxygen atom number density of $\sim 1.5 \times 10^{11}$ cm^{-3} for the emission intensity of 570 R. For the emission rate 1590 R the corresponding O number density is 4.2×10^{11} cm^{-2}. Both these numbers are well within observed O number densities for the high-latitude midwinter 90-100 km region [Thomas, 1980; Mullen et al., 1977]. In the above estimation, quenching is not taken into account, but it is reasonable that even if quenching is taken into account, the number density will stay well below 10^{12} cm^{-3}, which is a large but not unreasonably large number density of [O] at 90-100 km for a shorter period of time [Mullen et al., 1977].

4. Summary

The O_2 (0-1) atmospheric band in the night airglow has been observed from near Longyearbyen, Svalbard (78°N) during a 2-month period around winter solstice using spectrophotometric equipment. The raw data were recorded with a spectral resolution of 7 Å which clearly resolved the R and P branches but not the rotational structure within the branches. Absolute intensities have been calculated from 30-min averages of the emission spectra, and a mean O_2 (0-1) atmospheric band intensity of 570 R ± 60 R, ranging from 110 R to 1590 R, is found. No clear intensity maximum or minimum around solstice is observed, but comparison with other data indicates that this may be due to intensity increases associated with mid winter stratospheric warmings. A semidiurnal tide component giving rise to a 25-30% intensity variation of the O_2 (0-1) atmospheric band emission is present in the data. Maxima and minima are found to occur at about 0400 and 1000 local time, respectively. No diurnal tide component larger than ±3-4% is present in the data. The day-to-day and short time variations both show a quasi-irregular wave and peaklike pattern. There seems to be little or no correspondence between variations in the OH and O_2 (0-1) atmospheric band emissions. We believe therefore that the short time variations seen in the O_2 (0-1) band are connected with turbulence and breaking gravity waves directed from above and associated with auroral phenomena. The OH variations seem to be influenced by turbulence connected with breaking gravity waves from the lower atmosphere and troposphere. Further observations of OH and O_2 (0-1) band intensities and temperatures are needed to verify this hypothesis. One should also consider the possibility of using the night airglow [OI] 5577 Å line at about 100 km as an additional indicator of speed and phase of gravity waves.

Acknowledgements. Financial support for this research was provided by the National Science Foundation through grants ATM-8313727, ATM82-14642 and ATM82-00114 to the Geophysical Institute of the University of Alaska and by the Royal Norwegian Council for Scientific and Industrial Research through a fellowship grant to one of us (H.K.M.). The observations on Svalbard are made through a cooperative effort involving the universities in Fairbanks, Tromsø, and Oslo, with the help and cooperation of the Great Norwegian Spitsbergen Coal Company and the Norwegian Polar Institute. The authors also want to thank J. Baldridge for programming assistance in connection with the analysis of the data. The Editor thanks F. Harris and another referee for their assistance in evaluating this paper.

References

Barth, C. A., Nitrogen and oxygen atomic reactions in the chemosphere, in Chemical Reactions in the Lower and Upper Atmosphere, pp. 303-326, Wiley-Interscience, New York, 1961.

Bates, D. R., Forbidden oxygen and nitrogen lines in the nightglow, Planet. Space Sci., 25, 897, 1978.

Beer, T., Atmospheric Waves, A. Hilger, London,

Berthier, P., Etude spectrophotometrique de la luminiscence nocturne des bandes des molecules OH et O_2 atmospherique, Ann. Geophys., 12, 113, 1956.

Brenton, F. G., and S. M. Silverman, A study of diurnal variations of the 5577 Å [OI] airglow emission at selected IGY stations, Planet. Space Sci., 18, 641, 1970.

Campbell, I. M., and B. A. Trush, The association of oxygen atoms and their combination with nitrogen atoms, Proc. R. Soc. London, Ser. A, 296, 222, 1967.

Cogger, L. L., R. D. Elphinstone, and J. S. Murphy, Temporal and latitudinal 5577 Å airglow variations, Can. J. Phys., 59, 1296, 1981.

Deans, A. J., G. G. Shepherd, and W.F.J. Evans, A rocket measurement of the O_2 ($b^1\Sigma_g^+ - X^3\Sigma_g^-$) atmospheric band nightglow altitude distribution, Geophys. Res. Lett., 3, 441, 1976.

Deehr, C. S., G. G. Sivjee, A. Egeland, K. Henriksen, P. E. Sandholt, R. Smith, P. Sweeney, C. Duncan, and F. Gilmer, Ground-

based observations of F region associated with the magnetospheric cusp, J. Geophys. Res., 85, 2185, 1980.
Dufay, M., Etude photoelectrique du spectre du ciel nocturne dans le proche infra-range, Ann. Geophys., 15, 134, 1959.
Forbes, F. M., Atmospheric holes: The solar and lunar semidiurnal components, J. Geophys. Res., 87, 5241, 1982.
Frederick, J. E., Influence of gravity waves activity on power thermospheric photochemistry and comparison, Planet. Space. Sci., 27, 1469, 1979.
Gault, W. A., R. A. Koehler, R. Link and G. G. Shepherd, Observations of the optical spectrum of the dayside magnetospheric cleft aurora, Planet. Space Sci., 29, 321, 1981.
Greer, R.G.H., E. J. Llewellyn, B. H. Solheim, and G. Witt, The excitation of O_2 ($b^1\Sigma_g^+$) in the nightglow, Planet. Space Sci., 29, 383, 1981.
Holton, F. R., An Introduction to Dynamic Meteorology, Academic, Orlando, Fla., 1979.
Holton, F. R., The influence of gravity wave breaking on the general circulation of the middle atmosphere, J. Atmos. Sci., 40, 2497, 1983.
Ismail, S., and L. L. Cogger, Temporal variations of polar cap OI 5577Å airglow, Planet. Space Sci., 30, 865, 1982.
Labitzke, K., Stratospheric-mesospheric mid-winter warmings, Dynamical and Chemical Coupling Between the Neutral and Ionized Atmosphere, edited by B. Grandal and J. A. Holtet, p. 17, D. Reidel, Hingham, Mass., 1977.
Lindzen, R. S., Turbulence and stress owing to gravity wave and tidal breakdown, J. Geophys. Res., 86, 9707, 1981.
Misawa, K., and I. Takeuchi, Correlation among O_2 (0-1) atmospheric band, OH (8-3) band and [OI] 5577Å line and among P_1 (2), P_1(3) and P_1(3) and P_1(4) lines of OH (8-3) band, J. Atmos. Terr. Phys., 40, 421, 1978.
Moreels, G., G. Megie, A. Vallance-Jones, and R.L. Gattinger, An oxygen-hydrogen atmospheric model and its application to the OH problem, J. Atmos. Terr. Phys., 39, 551, 1977.
Mullen, E. G., S. M. Silverman, and D. F. Korff, Nightglow (557.7 nm of OI) in the central polar cap, Planet. Space Sci., 25, 23, 1977.
Myrabø, H. K., Temperature variations at mesopause levels during winter solstice at 78°N, Planet. Space Sci., 32, 249, 1984.
Myrabø, H. K., and C. S. Deehr, Mid-winter hydroxyl night airglow emission intensities in the northern polar region, Planet. Space Sci., 32, 263, 1984.
Myrabø, H. K., C. S. Deehr, and G. G. Sivjee, Large-amplitude nightglow OH (8-3) band intensity and rotational temperature variations during a 24-hour period at 78°N, J. Geophys. Res., 88, 9255, 1983.
Myrabø, H. K., C. S. Deehr, and B. Lybekk, Polar cap OH airglow rotational temperatures at the mesopause during a stratospheric warming event, Planet. Space Sci., 32, 853, 1984a.
Myrabø, H. K., K. Henriksen, C. S. Deehr, and G.J. Romick, O_2 ($b^1\Sigma_g^+ X^3\Sigma_g^-$) atmospheric band night airglow measurements in the northern polar cap region, J. Geophys. Res., 89, 9148, 1984b.
Naujokat, B., K. Petzoldet, K. Labitzke, and R. Lenschow, Beil. Berl. Welterkarte, 37/83, 1983.
Noxon, J. F., Effect of internal gravity waves upon night airglow temperatures, Geophys. Res. Lett., 5, 25, 1978.
Petitdidier, M., and H. Teitelbaum, Lower thermosphere emissions and tides, Planet. Space Sci., 25, 711, 1977.
Romick, G. J., The detection and study of the visible spectrum of the aurora and airglow, Proc. Soc. Photo. Opt. Instrum. Eng., 91, 63, 1976.
Sandford, B. P., Aurora and airglow intensity variations with time and magnetic activity at southern high latitudes, J. Atmos. Terr. Phys., 26, 749, 1964.
Sivjee, G. G., and C. S. Deehr, Differences in polar atmospheric optical emissions between mid-day cusp and nighttime auroras, Exploration of the Polar Upper Atmosphere, edited by C.S. Deehr and J. A. Holtet, p. 199, D. Reidel, Hingham, Mass., 1980.
Sivjee, G. G., K. A. Dick, and P. D. Feldman, Temporal variation in the nighttime hydroxyl rotational temperature, Planet. Space Sci., 20, 261, 1972.
Spizzichino, A., Etude des interactions entre les differentes composantes du vent dans la havt atmosphere, Ann. Geophys., 25, 93, 1969.
Spizzichino, A., Etude des interactions entre les differentes du vent dams la haut atmosphere, Ann. Geophys., 2, 9, 1970.
Teitelbaum, H., and J. E. Blamont, Some consequencies of non-linear effects on tides and gravity waves, J. Atmos. Terr. Phys., 37, 697, 1975.
Thomas, L., The composition of the mesosphere and lower thermosphere, Philos. Trans. R. Soc. London, Ser. A, 296, 243, 1980.
Wallace, L., and D. M. Hunten, Dayglow of the oxygen A band, J. Geophys. Res., 73, 4813, 1968.
Weinstock, J., Theory of interaction of gravity waves with O_2 ($^1\Sigma$) airglow, J. Geophys. Res., 83, 5175, 1978.
Witt, G., J. Stegman, B. H. Soltheim, and E. J. Llewellyn, A measurement of the $O_2(b^1\Sigma_g^+ - X^3\Sigma_g^-)$ atmospheric band and the $OI^1(^1S)^g$ green line in the nightglow, Planet. Space Sci., 27, 341, 1979.
Wraight, P. C., Association of atomic oxygen and airglow excitation mechanics, Planet. Space Sci., 30, 251, 1982.
Young, R. A., and G. Black, Measurements of the rate coefficient of $O_2(a^1\Delta) + O_2(a^1\Delta) + O_2(b^1\Sigma) + O_2(X^3\Sigma)$, J. Chem. Phys., 42, 3740, 1965.

C. S. Deehr and G. J. Romick, Geophysical Institute, University of Alaska, Fairbanks, AK 99775.
K. Henriksen, Auroral Observatory, University of Tromsø, N-9000, Tromsø, Norway.
H. K. Myrabø, Norwegian Defence Research Establishment, N-2007, Kjeller, Norway.

(Received May 3, 1985;
revised August 5, 1985;
accepted August 29, 1985.)

Night airglow O_2 (0-1) atmospheric band emission during the northe·n polar winter

H K Myrabø

Norwegian Defence Research Establishment
P O Box 25, N-2007 Kjeller, Norway

ABSTRACT

The O_2 (0-1) atm band night airglow has been observed from the ground near Longyearbyen (78°N) during the 1983/84 winter solstice period. The 2½ months of observations show no minimum in the emission around winter solstice, but rather large variations with enhancements lasting for days. An average atomic oxygen concentration at the 95 km level of 1.5×10^{11} cm^{-3} is deduced from the average emission intensity of 405R. The absence of a clear minimum in the oxygen concentration during the northern polar winter solstice period, as compared to the southern polar region, is believed to reflect differences in the circulation and transport in the upper mesosphere and lower thermosphere.

1 INTRODUCTION

The height interval 80-120 km is an important region of the upper atmosphere. It contains the transition region between the ionosphere and the lower neutral atmosphere, i e, from conditions of diffusive separation to a well-mixed mesosphere. Gravity waves from below (generated in the troposphere) and from above (in connection with auroral activity) are believed to break in this region and deposit a considerable amount of energy, causing enhanced eddy diffusion flux

and affecting the chemistry (Ebel, 1985; Myrabø et al, 1986). At high latitudes the 80-120 km region is known to undergo large temperature changes (cooling) and disturbances in the circulation associated with stratospheric warming events (Labitzke et al, 1985; Matsuno, 1971; Myrabø et al, 1984). The atmospheric atomic oxygen concentration peaks at this altitude (Murphree et al, 1984).

Night airglow emissions originating from atomic and molecular oxygen have been extensively used to monitor the oxygen concentration and to study transport processes and chemistry of the upper atmosphere (Dufay, 1959; Silverman, 1970; Petitdidier and Teitelbaum, 1977; Cogger et al, 1981). However, most of this work has been concentrated at mid- and low-latitudes. Recently Elphinstone et al (1984) utilized a large data base of ISIS 2 OI 5577Å limb scans to construct a global circulation model of the 80-120 km region consistent with the airglow data. Only latitudes less than 40^{o} were included.

At high latitudes both the OI 5577Å and the O_2 b^1 Σg emissions might be used to monitor the peak oxygen concentration, transport and dynamics of the 80-120 km region (Murphree et al, 1984; Deans et al, 1976, Myrabø et al, 1986). Night airglow measurements of these emissions are sparse in the polar regions. Except for the observations by Myrabø et al, (1986), they are based on photometric data and thus may have a higher risk of auroral contamination (both emissions also occur in the aurora). Ground based photometric observations of the OI 5577Å line from Thule (76^{o}N) have been reported by Müllen et al (1977). Results from Antarctica, utilizing ISIS 2 OI 5577Å limb scans are given by Ismail and Cogger (1982). A clear winter solstice minimum is seen in the Antarctica data, while the Thule observations are characterized by large amplitude irregular variations lasting for periods of days to weeks (Müllen et al, 1977). Recently Myrabø et al (1986) reported similar irregular behaviour of the O_2 (0-1) atm band (i e, O_2 ($b^1 \Sigma^+ g - X^3 \Sigma^- g$)) emission during winter solstice at 78^{o}N. A possible seasonal trend around winter solstice could not be clarified due to a rather short (38 days) observing period. New O_2 (0-1) atm band night airglow emission data from Spitsbergen (78^{o}N) covering a 2½ month period around winter solstice, is consistent with the OI 5577Å Thule observations, clearly

showing that the northern polar region has no winter minimum in the oxygen concentration.

2 OBSERVATIONS

The O_2 (0-1) atm band emission were observed from near Longyearbyen on West Spitsbergen (78.4°N; 15°E) during the 1983/84 Multi-National Svalbard Auroral Expedition (Deehr et al, 1980). The spectral region from 8235 to 8685Å was scanned in 12 seconds employing a ½ M Ebert-Fastie spectrophotometer pointing towards the zenith. A band-width of 7Å clearly resolved the R and P branches of the O_2 (0-1) atm band and the P1 and P2 lines of the OH (6-2) band. Individual scans (300) were summed and averaged to obtain hourly mean spectra. Only spectra during clear weather periods and with no auroral features were used. The aurora was monitored by the OI 8446Å line present in the spectrum (Myrabø et al, 1986). An example of a typical spectrum used for calcuating the O_2 (0-1) atm band intensity is presented in Figure 1. The OH (6-2) P-lines, the OI 8446Å auroral line and the OH (7-3) R branches are indicated in addition to the O_2 (0-1) atm band. The absolute intensities were obtained by calibrating the spectrophotometer in the field, using a standard lamp and a diffusion screen (Hamwey, 1985). For the O_2 (0-1) atm band the area under the R and P branches represent the absolute intensity (see Figure). The uncertainty in the absolute intensity is estimated to be 20%, mainly due to uncertainty in the calibration. The relative uncertainty is mainly due to photon noise and to the uncertainty in the background subtraction. This is less than 5% for a single one hour mean. From the hourly values of the intensities, daily averages were formed. At least 3 hourly values have been used to obtain a daily average. A ± 12-15% bias due to the semi-diurnal variation has been removed, assuming the amplitude and phase found by Myrabø et al (1986). Because the daily averages were obtained from 3-10 hourly values, the average correction was less than 5%. Possible seasonal variations of the amplitude and phase of the tides should therefore not effect the result significantly. Probably the largest uncertainty in the daily values are caused by short time variations of the intensity (Myrabø et

al, 1986). An example of this is given in Figure 2 showing 20 minute averages of intensities during the evening of 25 December.

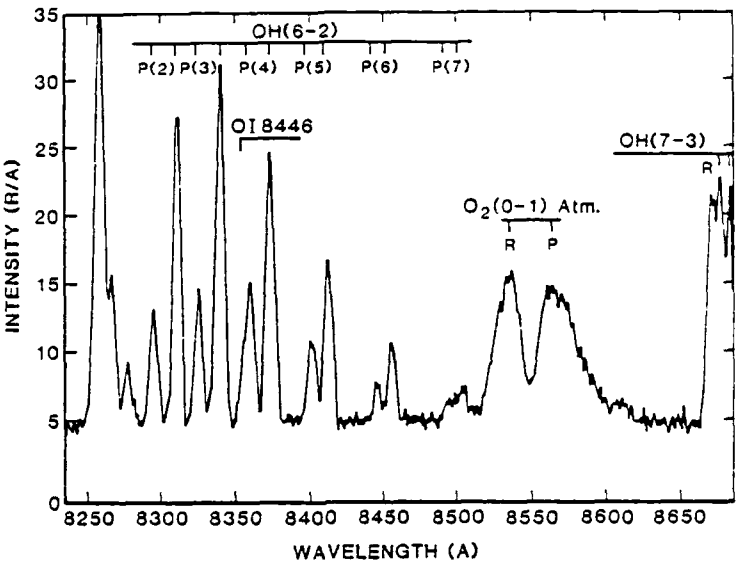

Figure 1 Example of 1 hour of averaged scans used to obtain the absolute intensities for the O_2 (0-1) atm band. The OH (6-2) P-lines, the auroral OI 8446Å and the R branches of the OH (7-3) band are also indicated.

The daily means of the O_2 (0-1) atm band intensities as obtained during the observing period from 25 November 1983 to 6 February 1984 is presented in Figure 3. The result from the 1982/83, 38-days of observations, is given on the same plot (dashed line) for comparison, and as an extension of the data set. Winter solstice is marked with an arrow. Figure 4 compares the O_2 (0-1) band 864.5 nm night airglow data from Spitsbergen to reflect differences in the dynamics of the two regions. The dashed line indicates the seasonal trend in the Antarctica data. Both the OI 5577Å line and the O_2 (0-1) atm band intensities are given with similar relative scales, i e, one unit corresponds to the same relative variation.

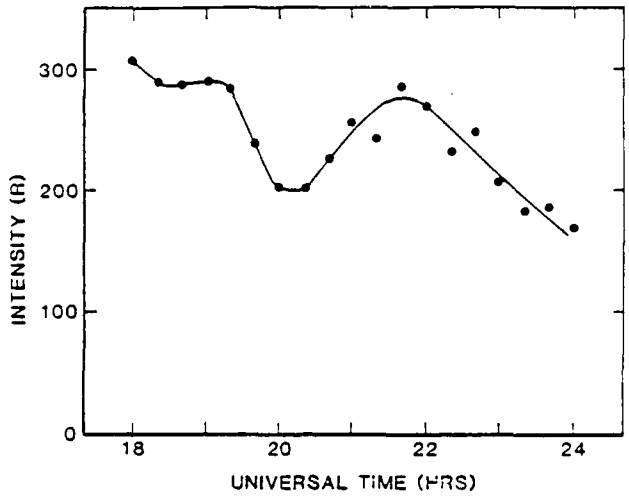

Figure 2 Variation of the O_2 (0-1) atm band intensities in the evening of 25 December. Intensities are obtained from 20 minutes of averaged individual scans. Observed values are marked.

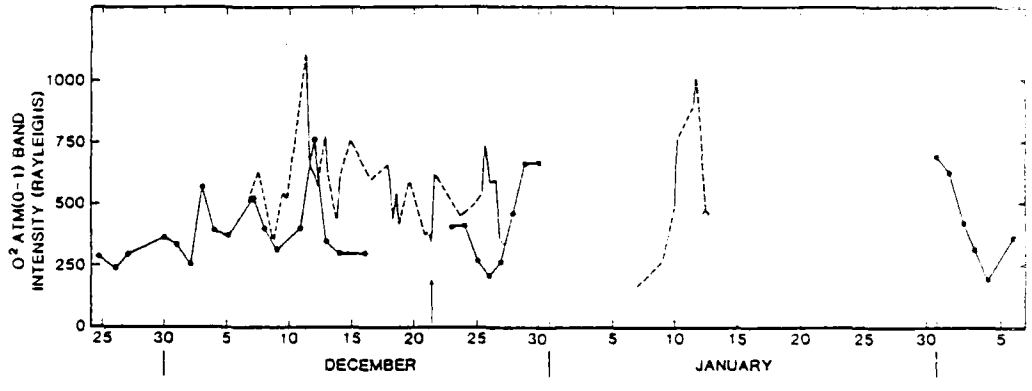

Figure 3 The daily mean intensities of the O_2 (0-1) atm band for the 1983/84 season. The result from the 82/83 season is given on the same plot (dashed line) for comparison.

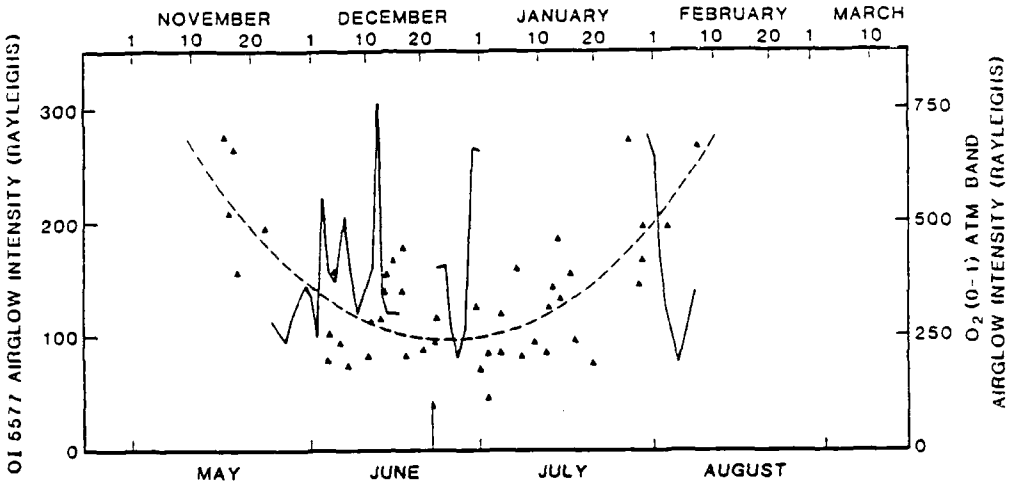

Figure 4 The daily averages of the O_2 (0-1) atm band intensities as obtained from Longyearbyen (78°N) during the 1983/84 season. The intensities of the OI 5577Å line from Antarctica observations (ISIS 2 data) during winter solstice conditions are also plotted (filled triangles). The dashed line indicates the seasonal trend for the Antarctica data. Antarctica data is from Ismail and Cogger (1982)

3 DISCUSSION

3.1 The winter solstice pattern and the differences between the two poles

The OI 5577Å line and the O_2 (0-1) atm band emissions originate at about the same altitude (Greer et al, 1981) and are known to covary (Dufay, 1959). As pointed out in an earlier paper by Myrabø et al (1986) the OI 5577Å line and the O_2 (0-1) atm band emission should show the same seasonal variation and reflect the atomic oxygen concentration in the 85-105 km region.

From Figure 3 it can be seen that both the 1982/83 and 83/84 winter season at 78°N show irregular peaks of enhanced O_2 (0-1) atm band intensity levels, lasting for a few days to a week or more. This

is very similar to the OI 5577Å night airglow observations from Thule (76^{o}N) reported by Müllen et al (1977). It is also seen from Figure 3 that there is no minima around winter solstice in the O_2 (0-1) atm band emission at 78^{o}N. When the O_2 (0-1) atm band data from the 1983/84 season are plotted together with the Antarctica data from Ismail and Cogger (1982) (Figure 4), the differences are easier to see, i e, the O_2 (0-1) atm band from the northern hemisphere show much larger day-to-day variations than do the OI 5577Å emission from Antarctica.

Each of the filled triangles in Figure 4, i e, the Antarctic data, corresponds to averaging of several limb scans during a single pass. From the temporal coverage in the Antarctic data as compared to the ground based observations a relatively larger scatter should be expected in the Antarctic data than in the ground based data. From Figure 4 the opposite is seen. If the day-to-day variation in both the OI 5577Å line and O_2 (0-1) atm band emissions were mainly connected to auroral activity, one would expect both the northern and southern polar regions to show a simlar type of behaviour. Ismail and Cogger (1982) have compared the enhanced OI 5577Å line emission from Thule with 30 mbar temperatures over northern Canada and find a relatively good correlation if a 0 and 14 day delay is allowed for. Myrabø et al (1984) have shown that the mesopause (i e, ~90 km) temperatures are affected by disturbances in the circulation pattern at stratospheric levels (i e, stratwarms). It is therefore reasonable to believe that the main part of the variations are connected to circulation changes in the stratosphere and lower mesosphere, affecting the lower thermospheric oxygen concentration and temperature through vertical mixing and horizontal transport. The differenes between the two poles may then be explained as differences in mid-winter circulation disturbances, i e, the northern winter stratosphere is known to have large disturbances while the southern winter stratosphere has only small scale disturbances (Schoeberl, 1978).

Some of the enhancements may indirectly be connected to auroral activity producing odd oxygen followed by a downward transport of the oxygen from the auroral source. The period 8-12 January 1983 shows a 2-3 times enhancement of the O_2 (0-1) atm band which is closely connected to a period of high auroral average activity around 8-10

January. In order to enhance the O atom concentration by a raio e, i e, ~2.7, during a 24 hour period at the 95 km level, assuming downward diffusion from 110 km, an eddy diffusion coefficient,

1) $k_1 \approx \Delta h^2/T_D \approx 2.6 \times 10^7$ cm²/sec

is needed, Δh being the hight difference and T_D the time over which the diffusion take place. Thus assuming that the mechanism for excitation of the O_2 $b^1\Sigma$ state of O_2 is a two step process (Torr et al, 1985), i e,

2) $O + O + M \rightarrow O_2^{**} + M$

followed by

3) $O_2^{**} + O_2 \rightarrow O_2(b^1\Sigma) + O_2$

Following the photochemical scheme and the model atmosphere given in the paper by Torr et al (1985), an eddy diffusion coefficient of the order of 6×10^7 cm²/sec is needed to account for a 2.5 times enhancement of the intensity over 24 hours. The effect of eventually neglecting the quenching by oxygen and even assuming a direct Chapman mechanism for the excitation of the O_2 $b^1\Sigma$ state is negligible on the deduced oxygen profile below about 97-98 km. This is clearly seen from Mc Deans et al (1976) (Deans et al assumed a direct Chapman excitation mechanism and neglected the quenching by oxygen).

The value 6×10^7 cm²/sec is a rather large eddy diffusion coefficient compared to average values, mainly quoted around 10^6 cm²/sec (Von Zahn and Herwig, 1977). It is not unreasonably large, however, since the eddy diffusion coefficient may be highly variable (Weinstock, 1985; Thrane et al, 1985). We may therefore conclude that parts of the enhancement could be associated with auroraly produced oxygen. However, a further separation of the sources have to await measurements of several emissions at different heights, including probably both OH, Na, O_2 (0-1) and OI 5577Å emissions (Myrabø et al, 1987).

3.2 Absolute intensities of the O_2 (0-1) atm band emission and an estimate of the oxygen concentration and its variation

The mean intensity of the O_2 (0-1) atm band for the 1983/84 season was found to be 405R. Daily averages ranged from 180 to 780 R with lowest and highest hourly value of 160 and 860 R, respectively. This is slightly lower than the 570 R 1982/83 seasonal average, but still a relatively high O_2 (0-1) atm band night airglow intensity as compared to lower latitudes (Packer, 1961; Deans et al, 1976; Megill et al, 1970).

Assuming a two step process (eq (2) and (3)) to be responsible for the emission and using the reaction rates and coefficients given by Torr et al, (1985) one might, to a first approximation, deduce an atmospheric oxygen concentration of 1.5×10^{11} cm^{-3} at 95 km.

The highest and lowest measured intensity corresponds to an oxygen concentration of $\sim 2 \times 10^{11}$ cm^{-3} and $\sim 1 \times 10^{10}$ cm^{-3}, respectively. The neutral temperatures are taken to be 220 K for these estimates (Myrabø, 1984). Thus, the oxygen concentration may vary by more than 1000%. Some of this variation might, however, be related to temperature variation as the excitation of O_2 ($b^1 \Sigma^+ g$) might be temperature dependent (Wraight, 1982). The relatively high oxygen concentration found in the northern polar region during winter solstice must be either transported to the 90-100 km region from outside or produced locally by auroral events and downward diffusion of oxygen. Knowing the differences in the behaviour of the night airglow O_2 (0-1) atm band and the OI 5577Å line in the two polar caps, disturbances in the stratosphere and lower mesosphere causing circulation and eddy diffusion changes in the mesopause and lower thermosphere region could be responsible for the variation in the supply of atomic oxygen. Whether this supply of oxygen comes from aurorally produced oxygen or from photodissociation of O_2 in the sunlit lower latitude atmosphere or both, is not yet known. However, experiments is prepared to clarify these questions.

Acknowledgement

Financial support for this research was provided by National Science Foundation through grant ATM-8313727 to the Geophysical Institute of the University of Alaska and by Royal Norwegian Council for Scientific and Industrial Research through a fellowship grant. The author also wants to thank Mr B Erickson, Mr D Osborne and Ms D L Wilkinson for programming and technical assistance.

References

Cogger, L. L., R. D. Elphinstone and J. S. Murphree, 1981. Temporal and latitudinal 5577Å airglow variations, Can. J. Phys., 59, 1296.

Deans, A. J., G. G. Shepherd and W. F. J. Evans, 1976. A rocket measurement of the O_2 ($b^1 \Sigma^+ g - X^3 \Sigma^{-3}$) atmospheric band nightglow altitude distribution, Geophys. Res. Lett., 8, 441.

Deehr, C. S., G. G. Sivjee, A. Egeland, K. Henriksen, P. E. Sandholt, R. Smith, P. Sweeney, C. Duncan, and F. Gilmer, 1980. Groundbased aobservations of F-region associated with the magnetospheric cusp, J. Geophys. Res, 85, 2185.

Dufay, M., 1959. Etude photoelectrique du spectre du ciel nocturne dans le proche infra-rouge, Ann. Gephys., 15, 134.

Ebel, A., 1985. Contribution of gravity waves to the momentum, heat and turbulent energy budget of the upper mesosphere and lower thermosphere, J. Atm. Terr. Phys., 46, 727.

Elphinstone, R. D., J. S. Murphree and L. L. Cogger, 1984. Dynamics of the lower thermosphere consistent with satellite observations of 5577Å airglow: II. Atomic oxygen, local, turbulence, and global circulation results, Can. J. Phys., 62, 382.

Greer, R. G. H., H. J. Llewellyn, B. H. Solheim and G. Witt, 1981. The exitation of O_2 ($b^1 \Sigma^+ g$) in the nightglow, Plant. Space Sci., 29, 383.

Hamway, R., 1985. Spectroscopy of the night airglow OH emissions, M. S. Thesis, Geophysical Institute, Alaska.

Ismail, S. and L. L. Cogger, 1982. Temporal variation of polar cap OI 5577Å airglow, Planet. Space Sci., 9, 865.

Labitzke, K., B. Naujokat, R. Lenschow, K. Petzoldt, B. Rajewski and R. C. Wohlfart, 1985. The third winter of MAP-dynamics, 1984/85: A winter with an extremely intense and early major warming, beilage zur Berliner Wetterkarte 67/85.

Matsuno, T., 1971. A dynamical model of the stratospheric sudden warming, J. Atmos. Sci., 28, 1479.

Mc Dade, I. C., E. J. Llewellyn and R. R. Harris, 1985. Atomic oxygen concentration in the lower auroral thermosphere, Adv. Space Res., 5, 229.

Megill, L. R., A. M. Despain, D. J. Baker and K. D. Baker, 1970. Oxygen atmospheric and infrared atmospheric bands in aurora, J. Geophys, Res., 75, 4775.

Moreels, G., G. Megie, A. Vallance-Jones and R. L. Gattinger, 1977. An oxygen-hydrogen atmospheric model and its application to the OH problem, J. Atm, Terr. Phys., 39, 551.

Müllen, E. G., S. M. Silverman and D. F. Korff, 1977. Nightglow (555.7 nm of OI) in the central polar cap, Planet. Space Sci., 25, 23.

Murphree, J. S., R. D. Elphinstone and L. L. Cogger, 1984. Dynamics of lower thermosphere consistent with satellite observations of 5577Å airglow: I. Method of analysis, Can. J. Phys., 62, 370.

Myrabø, H. K., C. S. Deehr, B. Lybekk, 1984. Polar cap OH airglow rotational temperatures at the mesopause during a stratospheric warming event, Planet. Space Sci., 32, 853.

Myrabø, H. K., 1984. Temperature variations at mesopause levels during winter solstice at 78^{0}N, Planet. Space Sci., 32, 249.

Myrabø, H. K., C. S. Deehr, G. J. Romick and K. Henriksen, 1986. Midwinter intensities of the night airglow O_2 (0-1) atmospheric band emission at high latitudes, J. Geophys. Res., 91, 1684.

Myrabø, H. K., C. S. Deehr, R. Viereck and K. Henriksen, 1987. Polar mesopause region dynamics deduced from night airglow emissions, J. Geophys. Res., (in press).

Packer, D. M., 1961. Altitudes of the night airglow radiations, Ann. Geophys., 17, 67.

Petitdidier, M. and H. Teitelbaum, 1977. Lower thermosphere emissions and tides, Planet. Space Sci., 25, 711.

Shoebend, M. R., 1977. Stratospheric warmings, observations and theory, Rev. Geophys. Space Phys., 16, 521.

Silverman, S. M., 1970. Night airglow phenomenology, Space Sci. Rev., 11, 331.

Thrane, E. V., Ø. Andreassen, T. Blix, B. Grandal, A. Brekke, C. R. Philbrick, F. J. Schmidlin, H. U. Widdel, U. Van Zahn and F. J. Lübken, 1985. Neutral air turbulence in the upper atmosphere observed during the Energy Budget Campaign, J. Atm. Terr. Phys., 47, 243.

Torr, M. R., D. R. Torr and R. R. Laher, 1985. The O_2 atmospheric 0-0 band and related emissions at night from Spacelab 1, J. Geophys. Res., 90, 8525.

von Zahn, V. and T. Herwig, 1977. Inert gas abundances as indicators for the strength of eddy diffusion at turbopause altitudes, in Dynamical and Chemical Couping between the Neutral and Ionized Atmosphere, editors B. Grandal and J. A. Holtet, p. 49, Dortrecht, D. Reidel.

Weinstock, J., 1985. Gravity wave saturation and eddy diffusion in the middle atmosphere, J. Atm. Terr. Phys., 46, 1069.

Wraight, P. C., 1982. Association of atomic oxygen and airglow excitation mechanism, Planet. Space Sci., 30, 251.

END

DATE
FILMED
10-88

DTIC